COMILLAS
UNIVERSIDAD PONTIFICIA
ICAI

DEGREE IN ENGINEERING IN INDUSTRIAL TECHNOLOGIES

BACHELOR'S FINAL PROJECT

EVALUATION OF AN INDEPENDENT PHOTOVOLTAIC MICROGRID: CASE STUDY IN ANTANAMALAZA, MADAGASCAR

Author: Antonio Martinez Puchol

Supervisor: Amaury Ajasse

Madrid

August 2025

Declaro, bajo mi responsabilidad, que el Proyecto presentado con el título *Evaluation of an Independent Photovoltaic Microgrid:Case Study in Antanamalaza, Madagascar* en la ETS de Ingeniería - ICAI de la Universidad Pontificia Comillas en el curso académico 2024/2025 es de mi autoría, original e inédito y no ha sido presentado con anterioridad a otros efectos. El Proyecto no es plagio de otro, ni total ni parcialmente y la información que ha sido tomada de otros documentos está debidamente referenciada.

Fdo.: Antonio Martínez Puchol   Fecha: 24 / 08 / 2025

Autorizada la entrega del proyecto

EL DIRECTOR DEL PROYECTO

Fdo.: Amaury Ajasse   Fecha: 25 / 08 / 2025

COMILLAS
UNIVERSIDAD PONTIFICIA
ICAI

DEGREE IN ENGINEERING IN INDUSTRIAL TECHNOLOGIES

BACHELOR'S FINAL PROJECT

EVALUATION OF AN INDEPENDENT PHOTOVOLTAIC MICROGRID: CASE STUDY IN ANTANAMALAZA, MADAGASCAR

Author: Antonio Martinez Puchol

Supervisor: Amaury Ajasse

Madrid

August 2025

Acknowledgements

The completion of this work would not have been possible without the support, guidance, and encouragement of many individuals and institutions.

I wish to express my sincere gratitude to my director, Amaury, for his invaluable guidance, constructive feedback, and continuous support throughout the process.

I am grateful to the Universidad Pontificia Comillas and CentraleSupélec for providing the academic environment and resources that made this study possible. I also extend my appreciation to the professors and colleagues who contributed with insightful discussions and suggestions.

I owe a profound debt of gratitude to my family, whose unwavering support and guidance have accompanied me not only throughout this thesis but throughout my entire academic journey. Their encouragement, values, and example have been essential in enabling me to reach this stage. I am equally grateful for the patience and motivation provided by those closest to me, whose presence has been a constant source of strength.

Finally, I would like to acknowledge the community of Antanamalaza, whose situation inspired this study. Their resilience and needs were at the heart of this project, and it is my hope that this work contributes, however modestly, to the broader efforts of improving energy access in Madagascar.

EVALUACIÓN DE UNA MICRORED FOTOVOLTAICA INDEPENDIENTE: ESTUDIO DE CASO EN ANTANAMALAZA, MADAGASCAR

Autor: Martinez Puchol, Antonio.
Director: Ajasse, Amaury.
Entidad Colaboradora: ICAI – Universidad Pontificia Comillas y CentraleSupélec

Resumen

Este trabajo diseña y evalúa una microred fotovoltaica autónoma para Antanamalaza, Madagascar, mediante una metodología reproducible que integra estimación demográfica, modelado de la demanda (modelo descendente y ascendente), y un dimensionamiento tecnoeconómico multi-escenario de generación fotovoltaica, almacenamiento y respaldo diésel. El estudio estima la población y necesidades eléctricas, combinando conteo de edificaciones a partir de satélite, encuestas a hogares y datos de tenencia de electrodomésticos. Se incluyen tanto consumos domésticos como actividades productivas (descascarado de arroz, carpinterías, escuelas y el centro de salud local), con el fin de obtener perfiles de demanda representativos.

La metodología evalúa además las opciones tecnológicas, considerando disponibilidad local, costes de importación y degradación de componentes a lo largo del tiempo. La generación fotovoltaica se simula con datos de irradiancia y temperatura específicos del emplazamiento. Se estima la vida útil de las baterías y sus reemplazos, y los inversores se dimensionan respetando las limitaciones eléctricas reales. A través de simulaciones se explora un conjunto de configuraciones factibles, comparando múltiples escenarios para reflejar los compromisos entre coste, fiabilidad e impacto ambiental.

El enfoque propuesto ofrece un marco estructurado y replicable para la planificación de proyectos de electrificación rural en contextos con escasez de datos.

Palabras clave: Electrificación rural; microred fotovoltaica; microred independiente; Madagascar; estimación de demanda; dimensionamiento de microred

Introducción

La electrificación rural sigue siendo un reto de desarrollo a gran escala. En Madagascar, el acceso nacional a la electricidad pasó del 12,3% al 39,4% entre 2010 y 2023, en gran parte gracias a soluciones fuera de red, aunque el acceso y el consumo en áreas rurales siguen siendo bajos [1]. La extensión de la red a aldeas dispersas resulta con frecuencia antieconómica; en este contexto, los sistemas descentralizados, y en particular las microredes fotovoltaicas, representan una alternativa viable. Antanamalaza, en Vakinankaratra, es representativa de las comunas rurales con base agrícola, limitada

presencia institucional y sin conexión a la red nacional [2, 3]. Existe una pequeña instalación de ESF (Électriciens Sans Frontières) en la localidad, pero con escasa información disponible, lo que hace del emplazamiento un caso adecuado para una evaluación independiente.

Metodología

El estudio se estructura en tres pasos principales: (i) caracterización del emplazamiento y demografía; (ii) estimación de la demanda eléctrica; y (iii) dimensionamiento de la microred bajo múltiples escenarios.

Demografía y representatividad. La población comunal se proyectó a partir de datos de 2001 y 2013 utilizando trayectorias nacionales de crecimiento rural. A nivel de aldea, los datos de Google Open Buildings se combinaron con estadísticas de tamaño de hogar para estimar el número de residentes. El área seleccionada contiene 998 estructuras mayores de 9 m^2, equivalentes a unas 901 viviendas y 3.965 habitantes. Una comparación con otras comunas de Madagascar indica que Antanamalaza no presenta rasgos únicos que hagan el análisis no replicable a otras localidades de Madagascar.

Estimación de la demanda. El enfoque descendente utiliza proporciones de ingresos para generar perfiles horarios de carga doméstica con una herramienta establecida [4], guiado por evidencias de que la asequibilidad condiciona la adopción de microredes, mientras que la fiabilidad y la iluminación nocturna son especialmente valoradas. Como complemento, el enfoque ascendente agrega electrodomésticos en función de tasas de tenencia, potencias típicas y tiempos de uso. Ambos enfoques se comparan y ajustan para obtener un perfil doméstico coherente. Las cargas productivas e institucionales (escuelas, el centro de salud CSB II con frigorífico para vacunas, descascaradoras de arroz y carpinterías) se estiman de forma separada con un método ascendente.

Arquitectura y dimensionamiento del sistema. Se adopta una topología trifásica en CA para cubrir distancias y compatibilidad con motores. El módulo de referencia es un panel de 550 W disponible en la región, acoplado a un inversor híbrido de 10 kVA con doble MPPT. El almacenamiento se basa en baterías LiFePO$_4$ (10,24 kWh), con modelado de coste entregado y rendimiento a lo largo del ciclo de vida a partir de datos de fabricante y estimaciones de transporte. Las cadenas FV se dimensionan de acuerdo con los límites del inversor, por lo tanto, el espacio de diseño se discretiza en incrementos de 11 kWp de paneles y 10 kWh de baterías. La producción fotovoltaica se simula con datos históricos de irradiancia y temperatura, aplicando correcciones NOCT y factores de degradación; la inclinación se obtiene de PVGIS.

Se analizan cuatro escenarios: (1) sin generador, toda la demanda cubierta; (2) sin generador, hasta un 5% de demanda insatisfecha; (3) activación de generador cuando SOC <20%; y (4) activación de generador cuando SOC <20% restringido al horario 18:00–06:00. El indicador de comparación es un coste anualizado de inversión, complementado con las emisiones equivalentes de CO$_2$ para evaluar el desempeño ambiental.

Resultados

Contexto y demanda. La aldea presenta características típicas de zonas rurales malgaches: acceso limitado a servicios públicos, empleo principalmente agrícola y fuerte dependencia de iluminación no eléctrica [2, 5]. La demanda eléctrica doméstica en 2025 se estima entre 151 kWh/día (ascendente) y 194 kWh/día (descendente), con un pico nocturno alrededor de las 20:00 y mínima posesión de electrodomésticos sensibles al clima.

Las cargas productivas e institucionales representan una fracción no despreciable de la demanda total. Entre ellas, destacan las descascaradoras de arroz como principales consumidoras, con variaciones estacionales ligadas a las cosechas. Otras cargas provienen de carpinterías, escuelas y el centro de salud.

Se asume un crecimiento anual del 2% para reflejar tanto el aumento demográfico como la mayor penetración de aparatos eléctricos. La Figura 1 muestra el perfil anual de consumo resultante, donde son visibles las fluctuaciones estacionales, los ciclos semanales y el crecimiento anual.
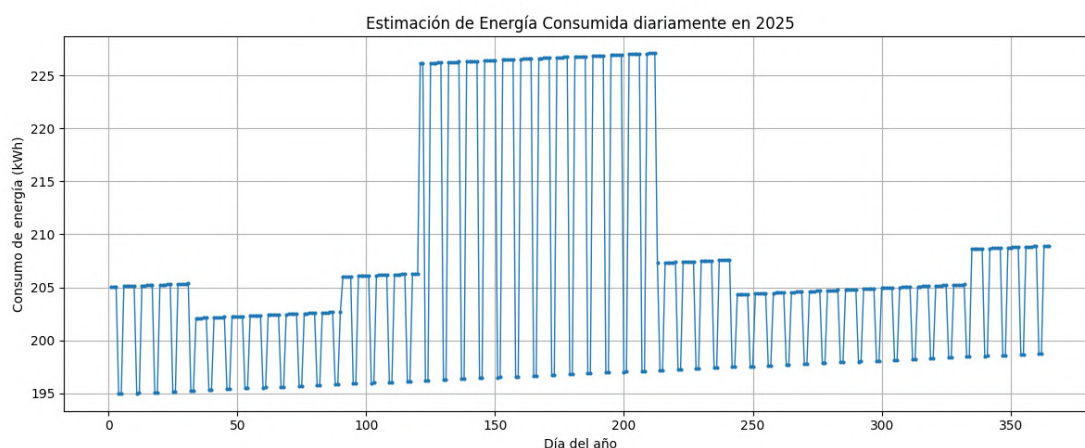

Figure 1: Consumo energético estimado para 2025, incluyendo hogares, actividades productivas y servicios públicos. Nota: el eje y no comienza en cero para visualizar mejor las variaciones estacionales y semanales.

Componentes principales: disponibilidad y costes. La viabilidad de una microred depende no solo del dimensionamiento técnico sino también de la disponibilidad y el coste de sus componentes. En Madagascar, los productos solares de pequeña escala y las baterías de plomo-ácido son relativamente comunes, mientras que los módulos FV de gran tamaño, inversores híbridos de más de 5–10 kVA y las baterías de litio-ferrofosfato (LiFePO$_4$) son escasos. Los proveedores locales atienden principalmente el mercado de sistemas solares a particulares y, por lo general, no divulgan los precios abiertamente.

En este estudio, el panel de referencia (Amerisolar 550 W), el inversor híbrido de 10 kVA con doble MPPT y el generador estaban disponibles en la región, mientras que los bancos de baterías deben importarse. Los costes entregados se estimaron utilizando tarifas de transporte marítimo en grupage (LCL), además de IVA y aranceles.

Esto subraya la necesidad de basar los análisis tecnoeconómicos en precios reales y condiciones de mercado, ya que transporte, impuestos y limitaciones de suministro pueden afectar significativamente la viabilidad y la implementación.

Resultados de escenarios: tecnoeconómicos y ambientales. La Tabla 1 resume los principales resultados de dimensionamiento para 2039 y 2049. En el caso base, sin generador y con cobertura total de demanda (SOC 10–90%), el sistema requiere un sobredimensionamiento sustancial: 264 kWp FV y 0,88 MWh de baterías en 2039, aumentando a 330 kWp y 1,01 MWh en 2049.

Permitir hasta un 5% de demanda insatisfecha reduce la capacidad FV en un 42–47% y el almacenamiento en un 59–63%, disminuyendo casi a la mitad el coste anualizado de inversión. Esto indica que gran parte del gasto de capital se destina a cubrir los últimos porcentajes de demanda bajo condiciones adversas.

Escenario	Año	FV (kWp)	Baterías (kWh)	Diésel (L/año)	Coste de inversión anualizado (€/año)	Emisiones (tCO$_2$-eq)
Toda la demanda, sin generador	2039	264	881	0	19,772	462.04 – 549.22
	2049	330	1,014	0	22,649	
5% de demanda no cubierta	2039	154	328	0	8,760	228.69 – 263.11
	2049	176	420	0	10,718	
Generador con SOC < 20%	2039	110	317	3,541	10,942	517.06 – 549.56
	2049	132	389	4,353	13,329	
Generador con SOC < 20% (noche)	2039	110	317	3,445	10,843	507.94 – 540.44
	2049	132	389	4,218	13,190	

Table 1: Resumen de dimensionamiento por escenario (años 2039 y 2049).

La introducción de un generador diésel reduce aún más las necesidades FV y de almacenamiento (110–132 kWp y 0,32–0,39 MWh). El consumo anual de diésel se estima entre 3.445 y 4.353 L. Restringir su funcionamiento a horas nocturnas no modifica el dimensionamiento y apenas reduce marginalmente el uso de combustible. En conjunto, la inclusión de generación de respaldo disminuye la inversión inicial pero introduce dependencia estructural del combustible importado y exposición a la volatilidad de sus precios.

El análisis de emisiones refuerza estos compromisos. El escenario con 5% de demanda insatisfecha logra la menor huella (229–263 tCO_2-eq), al reducir hardware y evitar consumo de combustible. El caso estricto sin generador casi duplica esta cifra (462–549 tCO_2-eq), dominado por la fabricación FV. Los escenarios con generador superan las 508 tCO_2-eq, con la combustión de diésel eclipsando las emisiones incorporadas en paneles y baterías (Figura 2).

Estos resultados ponen de relieve tres conclusiones clave: (1) la cobertura total de demanda sin generador obliga a un sobredimensionamiento costoso; (2) permitir un pequeño margen de demanda insatisfecha reduce a la mitad los costes y capacidades necesarias; y (3) la inclusión de un generador reduce la inversión inicial pero conlleva costes recurrentes y dependencia en el coste y disponibilidad constante del diésel y elementos de mantenimiento (como aceite).
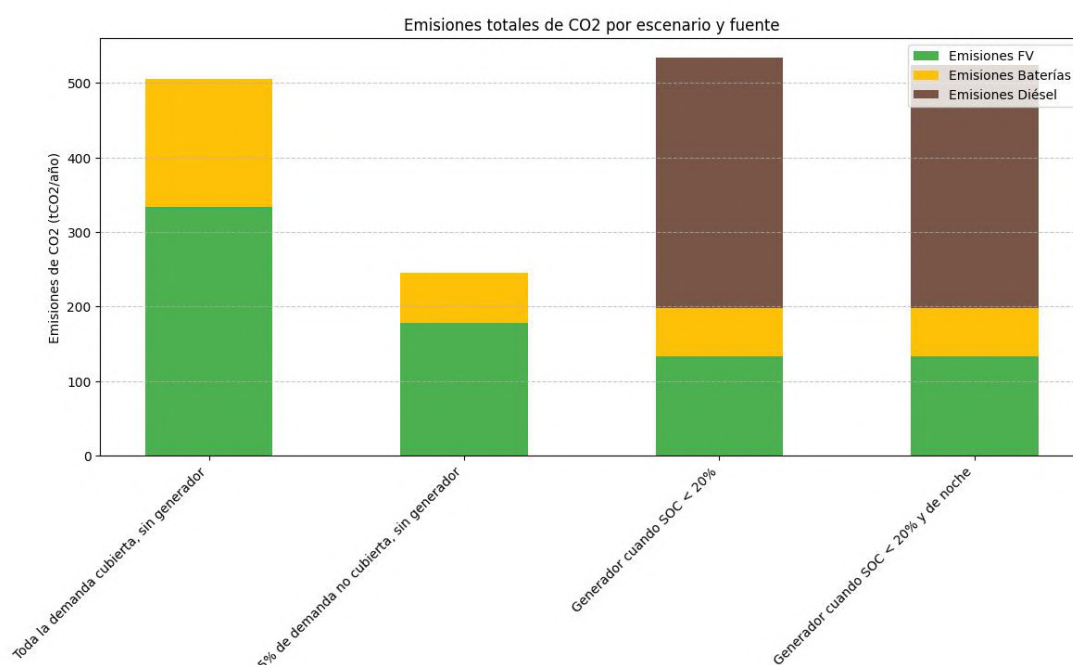
Figure 2: Desglose de emisiones de CO_2-eq por escenario (FV, baterías, diésel).

Discusión y Conclusiones

El análisis de escenarios muestra que la electrificación rural implica equilibrar prioridades en lugar de buscar una única configuración óptima. Garantizar plena fiabilidad solo con FV y baterías exige un fuerte sobredimensionamiento; diseños más flexibles reducen inversión pero toleran déficits ocasionales; y las opciones híbridas con generador

desplazan parte del coste hacia la dependencia de combustibles fósiles.

La principal contribución metodológica de este trabajo es la integración de estimación demográfica a partir de imágenes satelitales, modelado híbrido de la demanda y una optimización del dimensionamiento finita coherente con las limitaciones de inversores y rendimiento FV. Este enfoque ofrece un marco transparente y replicable en aldeas donde las estadísticas oficiales son incompletas y los datos de campo escasos, apoyando la comparación de alternativas en función de condiciones locales.

El estudio también subraya el papel central de la estimación de demanda. Aunque los perfiles de consumo son la base de cualquier dimensionamiento, están sujetos a gran incertidumbre: el comportamiento de los hogares, la adquisición de aparatos y las actividades productivas cambian con el tiempo. Por ello, es esencial realizar revaluaciones periódicas que permitan expansiones modulares y ajustes que mantengan la oferta alineada con las necesidades reales de la comunidad.

En conclusión, el trabajo demuestra que el diseño de microrredes en contextos rurales debe entenderse como un proceso de gestión de compromisos. El análisis de escenarios ayuda a clarificar dichos compromisos y a adaptar los diseños a las prioridades de asequibilidad, fiabilidad y sostenibilidad. Más allá de Antanamalaza, el enfoque destaca la importancia de combinar modelado técnico con supuestos realistas sobre demanda y condiciones de mercado, ofreciendo un método aplicable a la planificación de electrificación rural en contextos de alta incertidumbre.

Referencias

[1] IEA et al. *Tracking SDG 7: The Energy Progress Report 2024*. Some data retrieved from https://data.worldbank.org/indicator/EG.ELC.ACCS.ZS, and EG.ELC.ACCS.UR.ZS and and EG.ELC.ACCS.RU.ZS; Accessed: May 2025. 2024. https://trackingsdg7.esmap.org/downloads.

[2] Ilo Program, Cornell University, FOFIFA, and INSTAT. *Commune Census of Madagascar*. Accessed: May 10, 2025. 2001. https://www.ilo.cornell.edu/ilo/data.html.

[3] Centre de Recherches, d'Études et d'Appui à l'Analyse Économique à Madagascar (CREAM). *Monographie de la Région VAKINANKARATRA*. Accessed: May 10, 2025. 2013. https://www.instat.mg/p/cream-monographie-region-vakinankaratra-fevrier-2013.

[4] Xiangkun Li, James Salasovich, and Tim Reber. *Microgrid Load and LCOE Modelling Results*. https://data.nrel.gov/submissions/79. NREL Data Catalog. Golden, CO. Last updated: December 18, 2024. 2018.

[5] Institut National de la Statistique (INSTAT). *Troisième Recensement Général de la Population et de l'Habitation (RGPH-3)*. Accessed: June 7, 2025. 2018. https://www.instat.mg/autres/rgph-3.

EVALUATION OF AN INDEPENDENT PHOTOVOLTAIC MICROGRID: CASE STUDY IN ANTANAMALAZA, MADAGASCAR

Author: Martinez Puchol, Antonio.
Supervisor: Ajasse, Amaury.
Collaborating Institution: ICAI – Universidad Pontificia Comillas and CentraleSupélec

Abstract

This work designs and evaluates a stand-alone photovoltaic microgrid for Antanamalaza, Madagascar, using a reproducible pipeline that integrates demographic estimation, hybrid (top-down and bottom-up) demand modeling, and multi-scenario techno-economic dimensioning of PV, storage, and diesel backup. The study estimates population and electricity needs, combining satellite-derived building counts, household-size surveys, and appliance ownership data. Both household and productive activities, such as rice dehusking, carpentry, schools, and the local health center, are incorporated to produce representative demand profiles.

The methodology then assesses technological options, taking into account local availability, import costs, and component degradation over time. PV generation is simulated using site-specific irradiance and temperature data. Battery lifetime and replacement are modeled, and inverters are dimensioned following real electrical constraints. A grid of feasible system configurations is explored through simulation, and multiple scenarios are compared to capture the trade-offs between cost, reliability, and environmental impact.

The approach provides a structured and replicable framework for planning rural electrification projects in contexts with scarce data.

Keywords: Rural electrification; photovoltaic microgrid; independent microgrid; stand-alone microgrid; Madagascar; demand estimation; microgrid dimensioning

Introduction

Rural electrification remains a major development challenge. In Madagascar, national access to electricity increased from 12.3% to 39.4% between 2010 and 2023, driven largely by off-grid solutions, yet rural access and consumption levels remain low [1]. Grid extension to dispersed villages is frequently uneconomic; decentralized systems, particularly PV microgrids, offer a practical alternative in such contexts. Antanamalaza, in Vakinankaratra, is representative of rural communes with agricultural livelihoods, modest institutional presence, and no connection to the national grid [2, 3]. A small ESF (Électriciens Sans Frontières) installation exists locally but with scarce usable data, making the site suitable for an independent study.

Methodology

The study is structured around three main steps: (i) site characterization and demographics; (ii) electricity demand estimation; and (iii) microgrid dimensioning under multiple scenarios.

Demographics and representativeness. Commune-level population was projected from 2001 and 2013 baselines using national rural growth trajectories. At the village level, Google Open Buildings footprints were combined with household-size statistics to estimate the number of residents. The selected area contains 998 structures above 9 m^2, corresponding to approximately 901 households and 3,965 residents. A comparison with other communes in Madagascar indicates that Antanamalaza does not present unique features that would make the analysis not generalizable to other geographies in Madagascar .

Demand estimation. A top-down approach uses income shares to generate hourly household load profiles with an established tool [4], guided by evidence that affordability drives microgrid adoption while reliability and evening lighting are particularly valued. A complementary bottom-up approach aggregates appliances based on ownership data, typical power ratings, and usage times. Both approaches are compared and reconciled to obtain a consistent household demand profile. Productive and institutional loads (schools, the CSB II health center with vaccine refrigerator, rice dehuskers, and carpentries) are estimated separately through a bottom-up method.

System architecture and sizing. An AC three-phase topology is adopted to account for distance and motor-compatibility requirements. The reference PV module is a locally available 550 W panel, paired with a 10 kVA hybrid inverter equipped with dual MPPT. Storage relies on LiFePO$_4$ batteries (10.24 kWh units), with delivered-cost modeling and life-cycle performance based on manufacturer data and shipping cost estimates. PV strings are dimensioned according to inverter limits, therefore, the design space is discretized into 11 kWp PV and 10 kWh battery increments. PV output is simulated from historical irradiance and temperature data, applying NOCT-based corrections and degradation factors; optimal tilt is derived from PVGIS.

Four scenarios are analyzed: (1) no generator, full demand met; (2) no generator, up to 5% unmet demand; (3) generator activation when SOC falls below 20%; and (4) generator activation below SOC 20% restricted to 18:00–06:00. The comparison metric is an annualized investment proxy, complemented later by life-cycle CO_2-equivalent emissions used to assess environmental performance across scenarios.

Results

Context and demand. The village exhibits typical rural Malagasy characteristics: limited access to public services, employment largely centered on agriculture, and widespread reliance on non-electric lighting [2, 5]. Household electricity demand in 2025 is esti-

mated between 151 kWh/day (bottom-up) and 194 kWh/day (top-down), with a pronounced evening peak around 20:00 and minimal ownership of climate-sensitive appliances.

Productive and institutional loads represent a non-negligible share of total demand. Among them, rice dehusking workshops stand out as the largest contributors, with consumption that varies seasonally in line with harvest periods. Additional loads arise from carpentries, schools, and the local health center.

An annual growth rate of 2% is assumed to capture both demographic expansion and increasing appliance penetration. Figure 3 illustrates the resulting yearly demand profile, where seasonal fluctuations, weekly cycles, and the imposed annual growth are clearly visible.
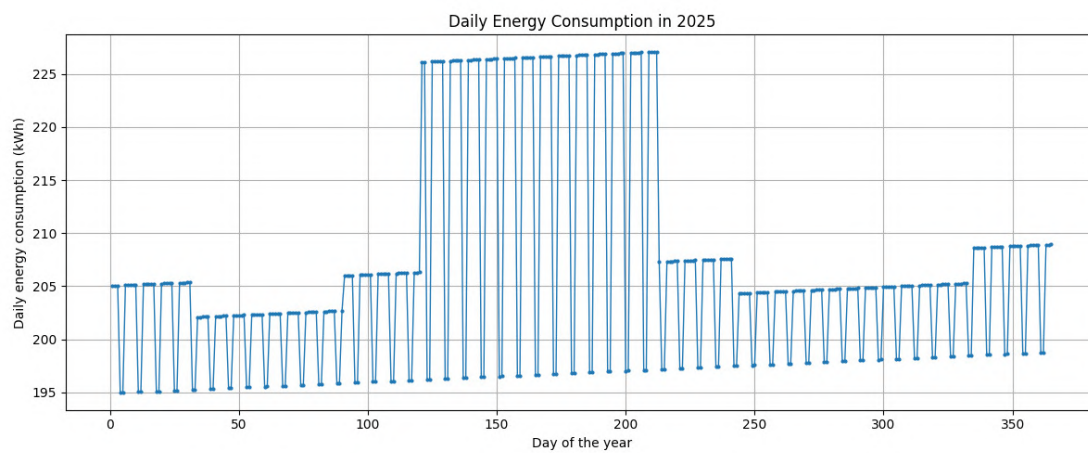
Figure 3: Estimated total energy consumption in 2025, including households, productive activities, and public services. Note: the y-axis does not start at zero to better visualize seasonal and weekly variations.

Main components: availability and costs. The feasibility of a microgrid depends not only on technical sizing but also on the availability and cost of components. In Madagascar, small-scale solar products and lead–acid batteries are relatively common, while utility-scale PV modules, hybrid inverters above 5–10 kVA, and lithium iron phosphate (LiFePO$_4$) batteries remain scarce. Local suppliers primarily serve the solar home system market and generally do not disclose prices openly.

In this study, the reference PV panel (Amerisolar 550 W), a 10 kVA hybrid inverter with dual MPPT and the generator were regionally available, but battery banks must be imported. Delivered costs were estimated using a less-than-container load (LCL) shipping rates, VAT and customs duties.

This underlines the need to base techno-economic analyses on real component prices and market conditions, since shipping, duties, and supplier constraints can significantly affect affordability and implementation.

Scenario outcomes: techno-economic and environmental. Table 2 summarizes the main sizing results for 2039 and 2049. In the baseline case without a generator and requiring full demand satisfaction (SOC 10–90%), the system must be substantially oversized: 264 kWp PV with 0.88 MWh storage in 2039, rising to 330 kWp and 1.01 MWh by 2049.

Relaxing the constraint by allowing up to 5% unmet demand has a striking effect. Required PV capacity falls by 42–47% and batteries by 59–63%, reducing annualized investment costs to nearly half of the strict case. This indicates that a very large share of capital expenditure is devoted to covering the last few percent of demand under adverse conditions.

Scenario	Year	PV (kWp)	Battery (kWh)	Diesel (L/yr)	Annualized investment cost (€/yr)	CO_2 emissions (tCO$_2$-eq)
All demand met, no generator	2039	264	881	0	19,772	462.04 – 549.22
	2049	330	1,014	0	22,649	
5% unmet demand, no generator	2039	154	328	0	8,760	228.69 – 263.11
	2049	176	420	0	10,718	
Generator at SOC < 20%	2039	110	317	3,541	10,942	517.06 – 549.56
	2049	132	389	4,353	13,329	
Generator at SOC < 20% (night)	2039	110	317	3,445	10,843	507.94 – 540.44
	2049	132	389	4,218	13,190	

Table 2: Dimensioning summary by scenario (target years 2039 and 2049).

Introducing a diesel generator further reduces the required PV and storage capacities to 110–132 kWp and 0.32–0.39 MWh, respectively. Annual diesel consumption is estimated at 3,445–4,353 L. Restricting generator operation to night-time hours results in identical system sizing, with only marginal reductions in fuel use. Overall, while the inclusion of backup generation lowers upfront investment needs, it introduces a structural dependence on imported fuel and exposes the system to volatility in fuel prices, which could significantly affect long-term costs.

The emissions analysis reinforces these trade-offs. The 5% unmet-demand scenario achieves the lowest footprint, between 229 and 263 tCO$_2$-eq, reflecting its reduced hardware requirements and absence of fuel use. The strict no-generator case nearly doubles this range (462–549 tCO$_2$-eq), with PV manufacturing as the dominant source. Both generator scenarios exceed 508 tCO$_2$-eq, where diesel combustion overshadows embodied emissions from PV and batteries (Figure 4).

These results highlight three central findings. First, enforcing 100% demand satisfaction without a generator drives substantial oversizing to cover prolonged cloudy spells, producing frequent curtailment and high annualized costs. Second, allowing a limited 5% unmet-demand margin cuts PV and battery capacities by roughly half while preserving reliability for essential uses, in line with stated user preferences for affordability and evening supply. Third, introducing a generator lowers capital needs but locks the system into recurring fuel expenditures, maintenance cycles, and a slightly higher carbon footprint, even when operation is restricted to night-time.
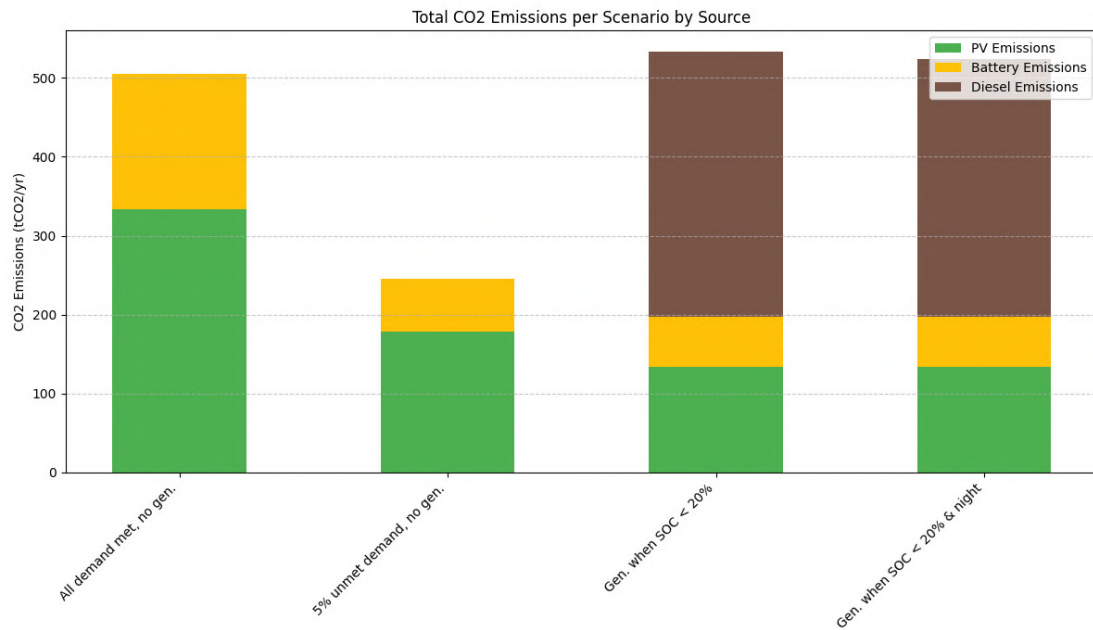
Figure 4: Breakdown of life-cycle CO_2-eq emissions by scenario (PV, batteries, diesel).

Discussion and Conclusions

The scenario-based approach shows that rural electrification involves balancing competing priorities rather than identifying a single optimal configuration. Guaranteeing full reliability with only PV and batteries requires costly oversizing; more flexible designs reduce investment but allow occasional shortages; and hybrid options lower upfront costs while introducing fuel dependence.

An important contribution of this work is methodological. The proposed pipeline integrates demographic estimation from satellite building data, hybrid top-down and bottom-up demand modeling, and discrete system sizing consistent with inverter constraints and PV performance. This combination provides a transparent and replicable framework for villages where official statistics are incomplete or outdated, and where field data are dif-

ficult to obtain. Such an approach can support planners and practitioners in comparing alternatives under local conditions rather than relying solely on generic benchmarks.

The analysis also underscores the central role of demand estimation. While consumption profiles are the foundation of any dimensioning exercise, they are also subject to considerable uncertainty: household behavior, appliance acquisition, and productive activities evolve over time. Initial projections therefore risk under- or over-estimation. Continuous monitoring and re-assessment of demand during the lifetime of the system are essential, enabling modular expansions and adjustments that keep supply aligned with actual community needs.

In conclusion, this study illustrates how microgrid design in rural contexts must be understood as a process of navigating trade-offs rather than identifying a single optimal solution. Scenario analysis helps to clarify these trade-offs and to adapt designs to the priorities of affordability, reliability, and sustainability. More broadly, the approach highlights the value of combining technical modeling with realistic assumptions about demand and market conditions. Such methods can inform rural electrification planning well beyond Madagascar, supporting the design of energy systems that remain adaptable under uncertainty.

References

[1] IEA et al. *Tracking SDG 7: The Energy Progress Report 2024*. Some data retrieved from https://data.worldbank.org/indicator/EG.ELC.ACCS.ZS, and EG.ELC.ACCS.UR.ZS and and EG.ELC.ACCS.RU.ZS; Accessed: May 2025. 2024. https://trackingsdg7.esmap.org/downloads.

[2] Ilo Program, Cornell University, FOFIFA, and INSTAT. *Commune Census of Madagascar*. Accessed: May 10, 2025. 2001. https://www.ilo.cornell.edu/ilo/data.html.

[3] Centre de Recherches, d'Études et d'Appui à l'Analyse Économique à Madagascar (CREAM). *Monographie de la Région VAKINANKARATRA*. Accessed: May 10, 2025. 2013. https://www.instat.mg/p/cream-monographie-region-vakinankaratra-fevrier-2013.

[4] Xiangkun Li, James Salasovich, and Tim Reber. *Microgrid Load and LCOE Modelling Results*. https://data.nrel.gov/submissions/79. NREL Data Catalog. Golden, CO. Last updated: December 18, 2024. 2018.

[5] Institut National de la Statistique (INSTAT). *Troisième Recensement Général de la Population et de l'Habitation (RGPH-3)*. Accessed: June 7, 2025. 2018. https://www.instat.mg/autres/rgph-3.

Contents

List of Figures

List of Tables

Chapter 1

Introduction

1.1 Objectives of the Study

The main objective of this work is to determine the optimal configuration of a solar-powered minigrid, in terms of the type, technology, and number of its main components, to provide electricity to a rural community in Madagascar. Although the study focuses on the specific case of Antanamalaza, the aim is to design and apply a general methodology that can be replicated in similar rural contexts across Madagascar and other sub-Saharan regions.

A central aspect of the analysis is to evaluate whether a minigrid powered solely by photovoltaic energy can adequately meet the community's electricity demand, or whether it would be technically and economically preferable to include an auxiliary diesel generator for backup or peak demand periods.

In this context, the specific objectives of the project are as follows:

- To analyse the key characteristics of the village and estimate its population in order to better understand its electricity needs

- To estimate the expected electricity consumption of the community using two complementary approaches

- To select the model and supplier of the main components of the minigrid (solar panels, batteries, etc.), considering local availability, cost, technology, maintenance, and ecological impact

- To dimension the system under different constraints on energy supply and to assess the inclusion of a diesel generator

- To conduct a preliminary economic and ecological analysis of the proposed system

- To contribute to the broader understanding of minigrids as a decentralised electrification strategy in low-income rural environments, providing a decision-support framework for future development initiatives

Ultimately, this work seeks to assess the practical relevance of solar minigrids as a tool for inclusive and sustainable rural development.

1.2 Motivation

Access to electricity is widely recognized as a fundamental enabler of social and economic development. In rural communities, particularly in low-income countries, electrification plays a pivotal role in enhancing safety, improving health outcomes, increasing productivity, and enabling access to education. Lighting reduces risks associated with darkness, enables evening study, and enhances personal security, especially for women and children. Electricity also allows the use of refrigeration to preserve food and medicine, reduces reliance on biomass fuels that cause indoor air pollution, and facilitates the use of digital technologies that are increasingly essential for education and communication. In short, electricity is not only a basic utility but a driver of opportunity and transformation.

Yet millions of rural households in sub-Saharan Africa remain disconnected from national grids due to high infrastructure costs and dispersed populations. In such contexts, minigrids powered by renewable sources, especially solar, offer a decentralized, scalable, and potentially cost-effective alternative. While these systems are relatively uncommon in developed regions like Europe, where national grids are mature and highly interconnected, they represent a promising solution for energy access in the Global South.

The motivation for this project lies in the opportunity to apply technical engineering skills to a socially relevant challenge. As an engineering student, I saw in this work a chance to align my competencies in energy system design and quantitative analysis with a project that could deliver positive social impact. The goal was not only to produce a technically sound study, but also to contribute, however modestly, to the discussion and development of sustainable solutions for rural electrification.

Choosing Madagascar as the case study was deliberate. Its socio-economic context and energy access challenges are very different from those in Europe, making it an ideal setting to explore innovative approaches to electrification. Furthermore, many of the relevant data sources and government publications are available primarily in French. My fluency in both French and English, languages widely used in scientific literature and international development reports, proved particularly helpful in gathering and understanding this information.

Finally, the focus on solar energy reflects my strong interest in renewable technologies. Solar energy is evolving rapidly, and it remains a central topic in energy research

and policy. Through this project, I aimed to deepen my understanding of energy engineering while engaging with a global effort to make clean and reliable electricity accessible to all.

1.3 Link to the Sustainable Development Goals

This project is aligned with the United Nations 2030 Agenda and contributes directly to the advancement of several Sustainable Development Goals (SDGs). While the primary focus is on Goal 7, *Affordable and Clean Energy*, the nature of rural electrification and its cross-cutting benefits means that several other SDGs are also positively impacted.

1.3.1 Primary SDG: Goal 7 – Affordable and Clean Energy

The most direct contribution of this work is to SDG 7, which aims to "ensure access to affordable, reliable, sustainable and modern energy for all" [1]. The design and analysis of a solar minigrid tailored to the needs of a rural community in Madagascar represent a concrete step toward decentralised energy access in underserved regions. The study promotes renewable energy and energy storage systems to reduce dependence on fossil fuels and to lower greenhouse gas emissions, thereby supporting sustainability and long-term energy resilience.

The project also considers hybridisation options (such as solar combined with diesel generation) when necessary to ensure reliability, particularly under variable weather conditions or in the early phases of deployment. This approach aligns with SDG target 7.1: "By 2030, ensure universal access to affordable, reliable and modern energy services" [1]. Moreover, by focusing primarily on solar energy, the project contributes to SDG target 7.2: "By 2030, increase substantially the share of renewable energy in the global energy mix" [1].

Figure 1.1: SDG 7 – Affordable and Clean Energy [2]

1.3.2 Secondary SDGs

SDG 3 – Good Health and Well-being. Electricity contributes to improved health through better lighting in clinics, refrigeration for vaccines and medicines, and the reduction of indoor air pollution from traditional biomass cooking methods. Access to clean energy supports health infrastructure and reduces risks associated with the use of kerosene lamps and open fires.

SDG 4 – Quality Education. Reliable electricity enables evening study, the use of digital tools, and the operation of electronic devices in schools. This contributes to enhanced learning environments and improved educational outcomes.

SDG 8 – Decent Work and Economic Growth. Electrification stimulates local entrepreneurship by enabling the use of electrical machinery, tools, and communications. It allows longer business hours and improves agricultural productivity through water pumping, cold storage, and post-harvest processing. These factors support job creation and rural economic development.

SDG 9 – Industry, Innovation and Infrastructure. The deployment of decentralised energy infrastructure through solar minigrids fosters innovation and strengthens the resilience of rural infrastructure. This aligns with target 9.1: "Develop quality, reliable, sustainable and resilient infrastructure."

(a) SDG 3 – Good Health and Well-being

(b) SDG 4 – Quality Education
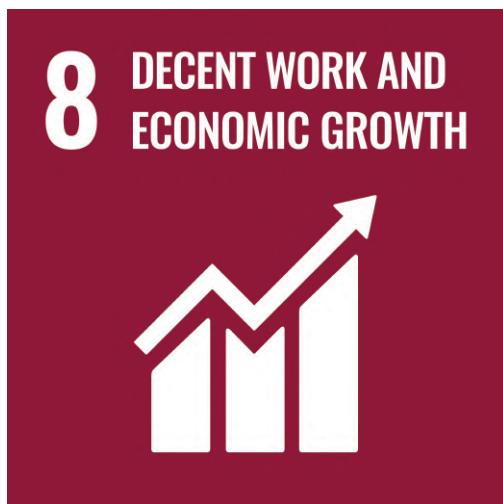
(c) SDG 8 – Decent Work and Economic Growth

(d) SDG 9 – Industry, Innovation and Infrastructure

Figure 1.2: Sustainable Development Goals influenced by the project

1.3.3 Broader Perspective

This project seeks not only to provide a technical solution to a specific energy challenge but also to highlight the role of energy as a vector for development. By addressing multiple SDGs, it positions minigrids as powerful tools in the fight against poverty, inequality, and climate change. The systemic impact of decentralised electrification makes it a crucial element for achieving sustainable and inclusive development in remote areas.

1.4   Methodology

This study follows a structured, multi-step methodology designed to ensure both the technical feasibility and contextual relevance of a solar minigrid installation in a rural village of Madagascar. The approach integrates qualitative insights with quantitative analysis, combining global data sources, local realities, and engineering considerations. The main stages of the methodology are outlined below:

1. **Understanding the Global Context of Energy Access**
   The study begins by situating the analysis within the broader global challenge of energy access. This includes a review of international electrification trends, the persistence of rural energy poverty, and the role that decentralized solutions such as minigrids can play in accelerating universal access to electricity. This step provides the foundation that frames the rest of the project.

2. **Reviewing Other minigrid Projects**
   The second step consists of analyzing other minigrid projects for which public information is available. These case studies provide valuable insights into load curves, installed capacity per household, and potential seasonal variations. Lessons drawn from these projects help to refine demand estimation and inform technology choices for the proposed system.

3. **Characterizing a Typical Rural Village in Madagascar: The Case of Antanamalaza**
   The third step involves a detailed exploration of the local context, focusing on the village of Antanamalaza. Publicly available demographic and socio-economic data are collected to characterize the community. Particular attention is given to population size and density, the number and types of buildings (homes, schools, health centers, small businesses), and the common appliances or electrical loads in use. These data are crucial for estimating current and future electricity demand in a realistic and context-sensitive manner. Antanamalaza is also compared to other rural communities to ensure that it represents a typical case rather than one with exceptional characteristics, which would limit the replicability of the methodology.

4. **Estimating the Electricity Demand of the Village**
   Once the village context is established, electricity demand is estimated under the assumption that a minigrid is installed. Two complementary approaches are employed:

   • A *top-down method*, which applies consumption benchmarks from similar rural electrification projects in Madagascar or comparable contexts. This

approach incorporates the economic level of the inhabitants as a determinant of demand.

- A *bottom-up method*, which identifies the typical appliances expected to be used in the village and estimates their usage patterns (daily operating hours, seasonal variations, etc.) to calculate the total demand.

5. **Component Selection**
Based on the estimated demand, appropriate components are selected for the minigrid. This includes photovoltaic (PV) panels, batteries, inverters, and auxiliary generators. The analysis takes into account availability and costs in Madagascar, environmental impact (CO_2 footprint), and expected lifespan. Consideration is also given to long-term sustainability, including equipment degradation, maintenance requirements, and ease of replacement.

6. **Dimensioning and Scenario Comparison**
Finally, the system is dimensioned for different scenarios of demand coverage, with or without a generator. For each scenario, the optimal combination of components is determined. These scenarios are then compared in terms of cost, CO_2-equivalent impact, and the percentage of energy demand met, in order to identify the most appropriate solution.

1. Understanding the Global Context of Energy Access
Trends in electrification, rural energy poverty, decentralized solutions.

2. Reviewing Other minigrid Projects
Case studies with load curves, per-household capacity, seasonal variation.

3. Characterizing the Case Study (Antanamalaza)
Demography, buildings, appliances, comparison with similar villages.

4. Estimating Electricity Demand
Top-down: benchmarks and income levels.
Bottom-up: appliances and usage patterns.

5. Component Selection
PV panels, batteries, inverters, generators. Availability and costs in Madagascar, CO_2 footprint, lifespan, maintenance.

6. Dimensioning and Scenario Comparison
Optimal configurations for different demand-coverage constraints (with/without generator). Compare cost, CO_2 impact, demand coverage.

Figure 1.3: Methodological roadmap of the study

Chapter 2

Global Challenge of Electrification

2.1 Global Energy Access and Consumption

Access to electricity is a fundamental pillar of sustainable development, serving as a critical enabler of nearly every aspect of modern life. It supports a wide array of essential services, including education, healthcare, clean water provision, food preservation, nutrition, digital connectivity, and the functioning of public institutions. Moreover, it facilitates the development of human capital by enabling learning environments and medical care, while simultaneously creating opportunities for employment, skill development, and entrepreneurship. Access to reliable and modern energy directly contributes to socioeconomic advancement by improving quality of life, supporting income generation, enhancing agricultural and industrial productivity, and increasing community resilience. As highlighted in the SDG 7 progress report, electrification is strongly interlinked with multiple development goals, particularly SDGs 3 (health), 4 (education), 6 (water and sanitation), 8 (decent work), 9 (industry), and 12 (sustainable production), underscoring its centrality to inclusive and long-term development [3]. For instance, the electrification of schools and clinics is directly linked to better health and education outcomes, while electricity access boosts agricultural productivity and enables small-scale industries to thrive.

The definition of "access to electricity" used in SDG 7 monitoring adopts a multidimensional and inclusive approach. It encompasses not only connections to centralized grids, but also decentralized solutions such as mini-grids and stand-alone solar home systems. Even minimal access, classified as Tier 1, is considered, provided that users can power basic services such as lighting and mobile phone charging for at least four hours per day [3].

This framework reflects a more flexible understanding of energy access, adapted to the reality of many communities in the Global South. It contrasts with the expectations prevalent in high-income countries, where access is typically equated with Tier 5 service:

continuous, high-capacity electricity suitable for all residential and productive needs. To better illustrate the range of service levels considered, the Multi-Tier Framework (MTF) is presented in Figure 2.1, detailing the attributes and minimum requirements for each tier.

Multi-tier Matrix for Measuring Access to Household Electricity Supply

ATTRIBUTES			TIER 0	TIER 1	TIER 2	TIER 3	TIER 4	TIER 5
1. Peak Capacity	Power capacity ratings[28] (in W or daily Wh)			Min 3 W	Min 50 W	Min 200 W	Min 800 W	Min 2 kW
				Min 12 Wh	Min 200 Wh	Min 1.0 kWh	Min 3.4 kWh	Min 8.2 kWh
	OR Services			Lighting of 1,000 lmhr/day	Electrical lighting, air circulation, television, and phone charging are possible			
2. Availability (Duration)	Hours per day			Min 4 hrs	Min 4 hrs	Min 8 hrs	Min 16 hrs	Min 23 hrs
	Hours per evening			Min 1 hr	Min 2 hrs	Min 3 hrs	Min 4 hrs	Min 4 hrs
3. Reliability							Max 14 disruptions per week	Max 3 disruptions per week of total duration <2 hrs
4. Quality							Voltage problems do not affect the use of desired appliances	
5. Affordability						Cost of a standard consumption package of 365 kWh/year < 5% of household income		
6. Legality							Bill is paid to the utility, pre-paid card seller, or authorized representative	
7. Health & Safety							Absence of past accidents and perception of high risk in the future	

Figure 2.1: Multi-Tier Framework (MTF) for measuring access to household electricity supply. Source: Bhatia and Angelou (2015) [4].

The United Nations has established universal access to electricity by 2030 as a core objective of Sustainable Development Goal 7 (SDG 7), recognizing energy access as

a prerequisite for development and well-being. Yet, as of 2022, an estimated 685 million people remained without access to electricity, 10 million more than the year before, marking the first increase in over a decade [3]. This reversal, largely attributed to the lingering effects of the COVID-19 pandemic, inflationary pressures, and rising energy prices, illustrates the fragility of progress when global efforts are disrupted.

Although significant advances have been made in past years, the recent setback reveals that continued progress is not guaranteed. Without sustained commitment, investment, and coordination, the goal of achieving universal electricity access may remain out of reach. In this context, maintaining momentum is not only desirable but also essential, to ensure that previously unserved populations are not left further behind.

The 685 million people who still lack access to electricity are not evenly distributed across the globe. As shown in Figure 2.2, electricity access rates vary dramatically between countries and regions. While many upper-middle- and high-income countries have already achieved near-universal coverage, large gaps remain in Sub-Saharan Africa, where electrification rates remain below 50% in several cases.

Figure 2.2: Share of the population with access to electricity by country (2022). Source: Data compiled from multiple sources by World Bank, with minor processing by Our World in Data [5].

Access to electricity is significantly lower in rural areas compared to urban regions, particularly in low-income countries. While urban electrification rates often exceed 90%, rural areas lag behind due to factors such as dispersed populations, challenging terrains, and limited infrastructure. This urban-rural divide underscores the need for targeted interventions to achieve universal electrification.

Table 2.1 presents 20 countries with the lowest overall electrification rates, highlighting the stark contrast between urban and rural access. In all listed countries, rural access is lower than urban access, emphasizing the urgency of addressing rural energy access.

Country	Total Access (%)	Urban Access (%)	Rural Access (%)
South Sudan	5.4	19.1	1.8
Burundi	11.6	65.0	2.3
Chad	12.0	48.1	0.4
Malawi	15.6	57.8	6.1
Central African Republic	17.6	37.4	2.3
Niger	20.1	67.4	10.4
Papua New Guinea	20.5	65.2	13.4
Burkina Faso	21.7	60.5 (2022)	3.4 (2022)
Dem. Rep. of Congo	22.1	55.6	1.0
Liberia	32.5	56.4	9.3
Sierra Leone	35.5	56.3	19.0
Mozambique	36.0	78.9	8.9
Madagascar	**39.4**	**75.6**	**14.6**
Guinea-Bissau	40.5	64.3	20.7
Tanzania	48.3	82.4	27.9
Somalia	50.3	79.0	23.9
Mauritania	50.3	91.6 (2022)	0.8 (2012)
Guinea	51.1	92.5	25.7
Zambia	51.1	89.9	17.6
Angola	51.1	76.2 (2022)	7.3 (2018)

Table 2.1: Access to electricity in urban and rural areas for the 20 least electrified countries by access percentage. Unless otherwise indicated, data corresponds to 2023. Table prepared by the author using World Bank Open Data on total, urban and rural access to electricity [3].

This disparity highlights a key challenge in achieving universal access: progress must be concentrated in communities that are the most underserved. These regions often face structural barriers such as low population density, weak infrastructure, and limited financial and institutional capacity.

2.2 Electricity Landscape in Madagascar

2.2.1 Current electricity situation in Madagascar

According to estimates from the World Bank, more than 18 million individuals in Madagascar remain without electricity access, positioning the country among the top fifteen globally in terms of unelectrified population [6]. As of 2023, only 39.4% of the population had access to electricity, a figure that places Madagascar within the bottom twenty countries worldwide regarding electrification rates. This limited access highlights pronounced geographic and socioeconomic disparities, particularly between urban and rural areas.

Rural electrification rates remain significantly lower than those observed in urban centers, a pattern commonly observed in developing contexts. As illustrated in Table 2.1, just 14.6% of the rural population in Madagascar has access to electricity, in contrast to 75.6% in urban areas. The underlying causes include elevated logistical and financial barriers to infrastructure deployment in low-density regions. These barriers typically manifest in longer transmission distances, higher per-connection costs, and greater energy losses, complicating efforts to extend the national grid to remote areas.

Electricity provision in Madagascar relies on a mixed system comprising both centralized and decentralized approaches. The centralized segment is dominated by JIRAMA (Jiro sy Rano Malagasy), the state-owned utility, which manages three separate, non-interconnected grids, RIA (serving Antananarivo), RIT (Toamasina), and RIF (Fianarantsoa), along with 94 additional isolated networks supplying smaller municipalities [7]. Collectively, these systems serve approximately 620,839 customers, the majority of whom are residential users, as detailed in Table 2.2.

Modality	Estimated 2023 connections	Share (%)
JIRAMA clients	620,839	32.1%
Mini-grids	50,882	2.6%
Solar Home Systems (SHS)	1,260,000	65.3%
Total	1,931,721	100%

Table 2.2: Estimated electricity connections in Madagascar by modality (2023). Source: PEI Madagascar Report (2024) [7].

Despite the existence of grid infrastructure, substantial portions of the country, especially in rural and remote regions, remain without any physical connection to the electrical network. Challenges to grid extension include complex topography, low population densities, and significant capital investment requirements. Figure 2.3 illustrates the

current coverage of medium- and high-voltage infrastructure managed by JIRAMA, including several isolated lines. The map indicates that large areas of the territory remain unserved, as current infrastructure is concentrated in a small geographical area.
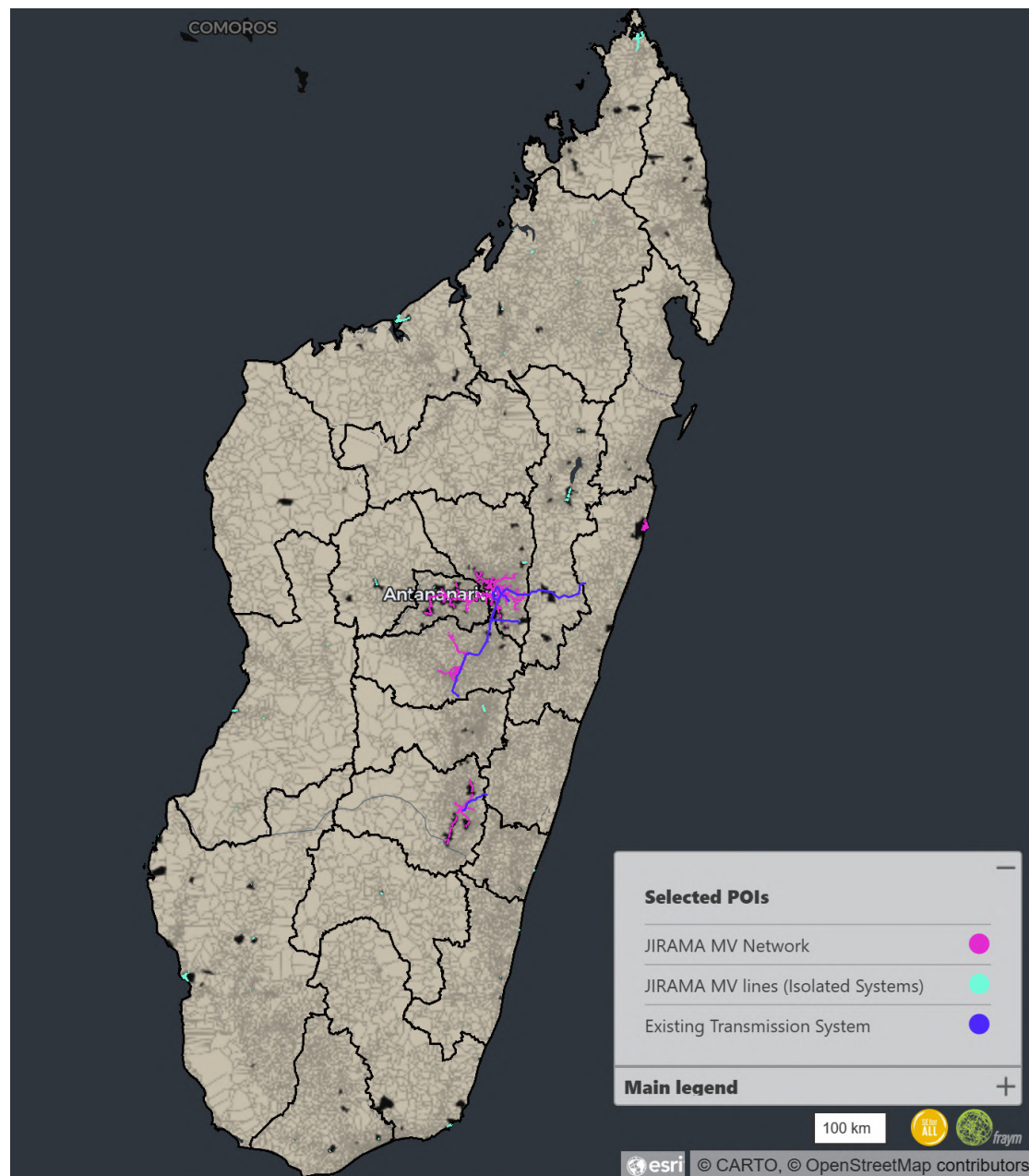
Figure 2.3: Existing medium- and high-voltage electricity grid in Madagascar. Source: Map generated by the author using data from the Madagascar SDG7 Energy Planning Dashboard [8].

14

Given these structural constraints, the national electrification strategy has increasingly prioritized decentralized energy solutions. Off-grid systems have emerged as a key component in efforts to expand energy access, particularly in underserved rural regions. By 2023, solar home systems (SHS) accounted for over 1.26 million household connections, while privately operated mini-grids provided electricity to an additional 50,882 users (Table 2.2). These technologies offer a practical alternative where conventional grid expansion proves technically or economically infeasible, and are now integral to Madagascar's rural electrification agenda.

2.2.2 Future outlook of electricity in Madagascar

Expanding access to electricity remains a fundamental development priority in Madagascar. With access levels still below 40% and marked disparities between rural and urban populations, there is widespread consensus on the urgency of scaling up electrification efforts. In response, national planning frameworks, particularly the Planification Énergétique Intégrée (PEI), have outlined structured pathways to increase national access to 70% by 2030. The PEI sets forth four principal electrification modalities, each tailored to specific geographic and demographic conditions. These are summarised in Table 2.3.

Modality	Target context and features
Grid densification	Unconnected households located near existing low-voltage lines. Low-cost, high-impact option in peri-urban areas.
Grid extension	Medium-voltage lines deployed from isolated JIRAMA networks to nearby towns and villages (around 15km). Effective where demand density is moderate.
Mini-grids (LV/MV)	Autonomous systems for small to medium-sized rural settlements. Typically solar-powered with storage. Suitable when grid expansion is too costly.
Standalone solar home systems (SHS)	Individual Tier 1 or Tier 2 systems for highly dispersed rural households. Low capacity but easy to deploy.

Table 2.3: Author-generated summary of the four main electrification modalities recommended in the PEI Madagascar report [7].

According to the PEI report [7], each electrification modality serves a distinct role within the broader national strategy. In areas already served by low-voltage infrastructure, the report highlights grid densification as the most efficient intervention. This ap-

proach connects nearby unserved households, generally within 600 meters of distribution transformers, at relatively low cost and with high return on investment. However, technical limitations such as voltage drops constrain the effective range for this option.

Where settlements are situated in proximity to one of the 96 isolated JIRAMA grids, medium-voltage grid extension is proposed as a viable solution. This strategy targets towns and villages located within approximately 15 kilometers of existing lines, where demand density is sufficient to justify investment but full integration into a national grid is either impractical or too costly. As explained in the PEI, this modality balances technical feasibility with financial sustainability under moderate load conditions.

For rural communities located beyond the reach of grid infrastructure, the PEI recommends the deployment of mini-grids. These autonomous systems are designed to serve both small villages (via low-voltage configurations) and more populous rural hubs (via medium-voltage setups). Typically powered by solar energy and coupled with battery storage, mini-grids offer flexibility and resilience, and are capable of delivering higher tiers of service independently of the national grid.

In the most isolated and sparsely populated areas, standalone solar home systems (SHS) are presented as the primary electrification solution. These systems, classified under Tier 1 and Tier 2 of the Multi-Tier Framework, can support basic needs such as lighting, mobile charging, and low-power appliances. The PEI forecasts that more than 5.7 million new SHS units will be necessary to meet future access targets. Nonetheless, several constraints are noted, particularly regarding affordability and maintenance. According to cost estimates from the PEI [7], a Tier 1-compliant SHS is priced at approximately USD 180, while a Tier 2 system is estimated at USD 350. These figures are compounded by relatively short operational lifespans, typically three to five years, primarily due to the limited durability of battery components [7].

Looking ahead, the Nouvelle Politique de l'Énergie (NPE) outlines a strategic goal of achieving 70% national electrification by 2030 [7]. The implementation plan is based on a two-pronged approach: first, by intensifying network densification in peri-urban zones where infrastructure is already present, and second, by accelerating the rollout of decentralized technologies such as SHS and mini-grids in rural and remote regions. Achieving this vision will require the creation of an estimated 4.3 million new electricity connections within the coming decade, nearly three times the current number, under the universal access scenario presented in national energy planning documents [7].

Chapter 3

Existing microgrids

Understanding and analyzing a wide range of microgrid implementations is essential to draw robust and transferable insights. Studying other projects not only helps to validate technical and socio-economic assumptions, but also uncovers operational patterns, design strategies, and institutional models that may not be visible in a single case.

By comparing different microgrids, it becomes possible to identify recurring challenges, such as battery degradation, payment recovery, or maintenance gaps, and explore the effectiveness of different mitigation strategies. These comparisons also inform the selection of realistic parameter values for simulation or techno-economic modeling, including load profiles, tariff levels, or demand elasticity.

Moreover, learning from existing deployments allows future projects to avoid past mistakes, adopt proven innovations, and contextualize design choices within local constraints. This process strengthens the credibility of research conclusions and enhances the replicability of proposed solutions.

In practice, however, identifying comparable microgrids with sufficiently detailed data proved challenging. While information on installed capacity is often available, particularly for projects supported by international organizations or NGOs, operational, data such as the number of connected customers, their consumption patterns, or payment behavior are rarely disclosed by private operators. Since installed capacity alone has little meaning without knowledge of the demand it serves, the number of case studies that could be rigorously analyzed for this work was limited.

3.1   DC Nanogrid by Nanoé in Madagascar

3.1.1   General Context

Ambohimena is a rural village in the Diana region of northern Madagascar where electrification is extremely limited. The social enterprise Nanoé has deployed an innovative

energy access model based on decentralized direct current (DC) nanogrids. These small-scale systems interconnect clusters of 3–5 households with solar photovoltaic generation and battery storage, thereby providing essential electricity access in areas where extending the national grid would be economically unviable [9, 10].

Nanoé initially installed 27 nanogrids in Ambohimena. In November 2021, five of these were interconnected into a larger DC microgrid. By the end of 2022, 24 nanogrids were interconnected, significantly extending electricity access and resilience throughout the village [9].

Each nanogrid typically includes 100–200 Wp of installed PV capacity and 90–130 Ah of battery storage. The model prioritizes local ownership and affordability, offering a flexible pay-per-use structure via mobile payments. Customers enter a code into a keypad to access electricity on the days they need it, and must purchase certified energy-efficient appliances directly from Nanoé [9].

The choice of Ambohimena as a case study is strategic. It provides access to detailed socio-economic data and historic electricity consumption patterns, allowing robust techno-economic and behavioral analysis [10].

3.1.2 Household Characteristics

Survey data collected by Nanoé indicate the following household characteristics [10]:

- 74.7% of households are owner-occupied.

- Median household composition: 2 adults and 2 children.

- Median income: MGA 150,000/month (approx. EUR 30).

- Housing types vary: walls made of Ravinala wood (40%), concrete-stone (22%), or wood-concrete hybrid (18%); roofs mostly tin (73%) or leaves (9%); floors mainly concrete (77%).

- Appliance ownership includes LED bulbs and spots, USB phone chargers, 12 V sockets, and occasionally TVs.

- Reported professions and usages: farmers (31.6%), traders (22.2%), employees (6.8%) and public lighting users (32.5%).

3.1.3 Residential Load Profile

Historical consumption data from 2018 to 2021 revealed very low household demand, focused primarily on evening lighting and phone charging. Cluster analysis identified three typical user groups [10]:

- **Group 0 (17%)**: High-consumption users (approx. 40 Wh/day) with 15 W evening peaks.

- **Group 1 (66%)**: Low-consumption users (approx. 10 Wh/day), peaking around 4 W.

- **Group 2 (17%)**: Used for public lighting. 30 Wh/day, a 10 W evening peak, and a stable 8 W nighttime base load.
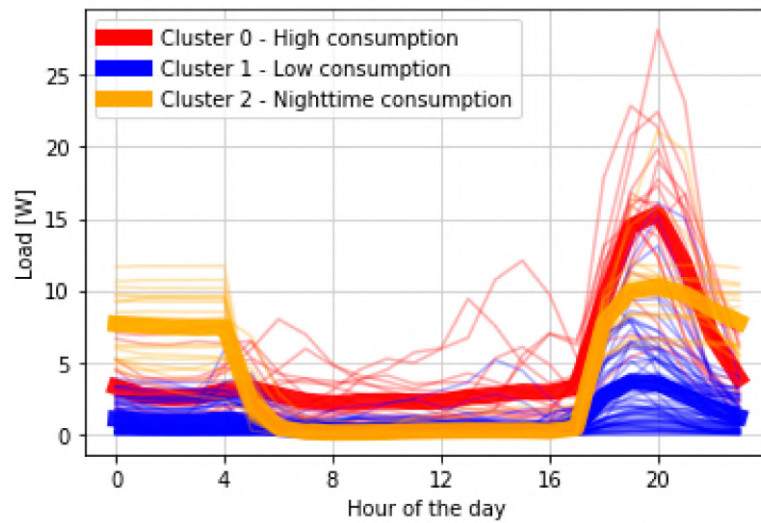
Figure 3.1: Average load profiles by household cluster. Source: [10].

3.1.4   Tariff System and Affordability

Nanoé applies a prepaid tariff model where users pay per day of consumption. Payments are made via mobile phone, unlocking electricity via a digital keypad. This model supports both flexibility and affordability, while the sale of efficient appliances ensures system compatibility and creates an additional revenue stream [9].

19

Fee for Device		Fee for Service	
Device	Initial Fee (in $)	Service	Daily Fee (in $/Day)
3 W	10	10 Wp 50 Wh/Day	0.15
4 W	~10	18 Wp 90 Wh/Day	0.23
USB 5 W	~10	30 Wp 150 Wh/Day	0.3
8 W	~15	42 Wp 210 Wh/Day	0.45
PL 12 W	~30	66 Wp 330 Wh/Day	0.6
15 W	~100	100 Wp 500 Wh/Day	0.91
60 W	~850	125 Wp 1,250 Wh/Day	1.5

Figure 3.2: Electricity and appliance pricing scheme. Source: [9].

3.1.5 Productive Use and Limitations

The integration of productive use of electricity (PUE) remains limited. In comparable villages, diesel-powered rice hullers are still necessary to meet high energy demands, especially during harvest season. Without hybridization or increased system flexibility, DC nanogrids cannot currently support such loads effectively [10].

3.1.6 Battery Utilization and Resilience

Between July and September 2020, the average depth of discharge (DoD) of batteries was 13.9%, suggesting underutilization and generous reserve capacity. This conservative strategy is consistent with the goal of uninterrupted service, even in poor solar conditions [9].
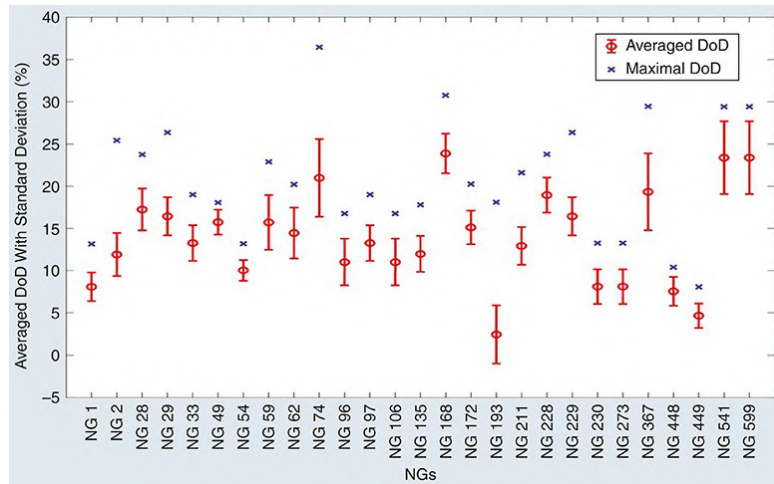
Figure 3.3: Average battery depth of discharge in Ambohimena. Source: [9].

3.1.7 Initial Adoption

In the initial years, the average Daily Household Electricity Consumption increased significantly, as reported by [10]. Table 3.1 presents the observed evolution of the measured data:

Year	Average Daily Household Electricity Consumption	Annual Change in Average Daily Electricity Consumption	Average Daily Maximum Household Power Demand	Annual Change in Maximum Average Power Consumption
2018	8.16 Wh	-	2.26 W	-
2019	21.88 Wh	168.27 %	2.25 W	-0.75 %
2020	35.47 Wh	62.11 %	2.27 W	0.92 %
2021	50.62 Wh	42.72 %	2.99 W	32.11 %

Table 3.1: Annual trends in average household electricity consumption and power demand. Source: [10]

However, this annual change in electricity consumption may only be temporary, as consumers acquired the required appliances from Nanoé.

3.1.8 Seasonality

Seasonal variations are reported in [10], as shown in Figure 3.4. Being Madagascar in the south hemisphere, and having precipitation data (see Figure 4.4b), we know that the rainy season starts around November and ends around April. During the rainy season,

we see energy consumption at around 6-7Wh daily, instead of the 9Wh seen during the dry season.
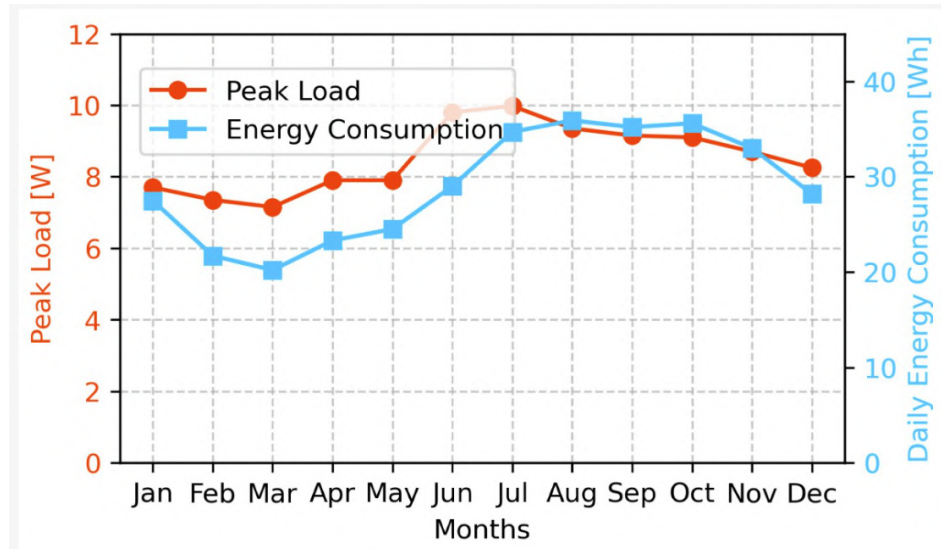
Figure 3.4: Variations in energy consumption by season. Source: [10].

If the demand during the rainy season decreases, this could reduce the need for solar panels and batteries, since the rainy season is the least beneficial to solar microgrids (more cloud cover). However, in [10] they list "fewer hours of sunshine" as one of the possibilities for the decline in demand, which would actually be a forced decline of demand due to lower supply. Therefore, we can't suppose for our microgrid, based only on this data, that demand naturally decreases during the rainy season.

3.1.9 Seasonal Productive Loads: the Rice Huller

Field interviews and modeling studies indicate that productive equipment such as rice hullers have highly seasonal usage. In Ambohimena, diesel rice hullers typically operate between 1–2 hours per day during the rainy season, but up to 9 hours daily in June, coinciding with the rice harvest. Load modeling based on local surveys suggests early-morning and afternoon peaks during this time [10].

3.1.10 Lessons Learned from Nanoé

The Nanoé experience in Ambohimena provides several lessons that are directly relevant for the design and operation of rural microgrids:

- **Business models:** The project shows that innovative business models can improve both affordability and system reliability. Flexible prepaid payment options enable

households with irregular income to access electricity, while requiring users to purchase certified appliances ensures technical compatibility and reduces operational risks. Nevertheless, this model also creates dependency on a single vendor, which can raise concerns about affordability and market competition.

- **Risk of overdimensioning:** The low observed depth of discharge (around 14%) indicates that the systems were significantly oversized relative to actual demand. While this conservative approach improves resilience and reduces the probability of outages, it also results in underutilized assets and higher investment costs. Future projects should carefully balance resilience with cost efficiency by aligning system sizing more closely to realistic demand growth.

- **Local capacity building:** Long-term sustainability depends on developing local technical expertise. Training community-based technicians is essential to ensure regular maintenance, reduce dependence on external operators, and strengthen user trust in the system [10].

3.2 Microgrids in the DIANA Region, Madagascar

3.2.1 Introduction

In Madagascar's DIANA region, four microgrids were installed around 2008 by Mad'Eole, with support from Experts-Solidaires, in the rural villages of Ambolobozobe, Ambolobozokely, Ivovona, and Sahasifotra [11]. A fifth microgrid was later deployed in Ampasindava (2016–2017), incorporating the operational feedback and limitations observed in these earlier systems [12].

3.2.2 Technical Summary

The legacy microgrids combined photovoltaic generation, wind turbines, OPzS lead-acid batteries, and diesel generators. However, detailed technical data could only be found for Ambolobozobe and Ambolobozokely. Both sites were equipped with PV installations of 11 kWp and battery banks rated at 240 V and 852 Ah [11]. This corresponds to approximately 102 kWh of nominal energy storage per site, assuming 50% depth of discharge due to the OPzs battery technology.

    Table 3.2 presents verified data for January-April 2015, as reported in the same source [11].

Village	PV (kWc)	Wind (kW)	Energy sold (kWh)	Recovery rate (%)
Ambolobozobe	11	0	701	26
Ambolobozokely	11	10	766	31

Table 3.2: Operational data for four legacy micro grids (energy sold and recovery rate are the average between January and April 2015). Source: [11]

3.2.3 Performance and Challenges

Reported issues in [11] include:

- Degraded technical performance: The average technical efficiency in Ambolobozokely was below 40%, indicating poor energy conversion or storage performance. Despite having photovoltaic and wind resources, the actual electricity sold remained significantly lower than the theoretical generation potential. This is evident in the low energy yields reported in Table 3.2.

- Battery degradation: After seven years of operation, battery banks in both Ambolobozobe and Ambolobozokely, each rated at 240 V, 852 Ah (approximately 102 kWh usable at 50% depth of discharge), showed clear signs of end-of-life. The increased reliance on diesel generators suggests insufficient charge retention and deteriorated storage capacity.

- Excessive diesel consumption: Fuel use was disproportionately high, especially in Ambolobozokely, where generator usage often exceeded renewable generation. This implies either battery malfunction or a possible misappropriation of diesel fuel.

- Low reliability and trust: Irregular service delivery, insufficient supply duration, and infrastructure failures (such as non-functional wind turbines), which contributed to user dissatisfaction and reluctance to pay.

- Weak governance and communication: The operational team struggled with internal coordination, accountability, and consistent field presence. These issues undermined system maintenance, user engagement, and payment enforcement.

- Socioeconomic mismatch: Seasonal migration in fishing communities such as Ambolobozokely resulted in fluctuating electricity demand, often misaligned with peak renewable generation (e.g., high wind availability during periods of low occupancy).

These challenges illustrate a vicious cycle of degraded service quality, declining user engagement, and insufficient revenue, ultimately threatening the sustainability of rural electrification efforts. Indeed, users were reluctant to pay for the unreliable electricity. Recovery rates, defined as the percentage of users paying their monthly fees, remained critically low in April 2015: 24% in Ambolobozobe, 31% in Ambolobozokely, 19% in Ivovona, and only 7% in Sahasifotra [11].

3.3 Minigrids in Tanzania

3.3.1 Data on Sites A and D

Two mini-grid sites in Tanzania, referred to as Site A and Site D, are analyzed in [13]. Sites B and C are not considered in the available dataset.

Site A, an island community, included 358 households, while Site D, a mainland village, comprised 135 households. Average daily electricity consumption per household was 0.104 kWh in Site A (standard deviation 0.262) and 0.089 kWh in Site D (standard deviation 0.134) [13]. Figure 3.5 shows the mean daily load profiles for both sites, with a gradual increase during the day and a pronounced peak in the evening.
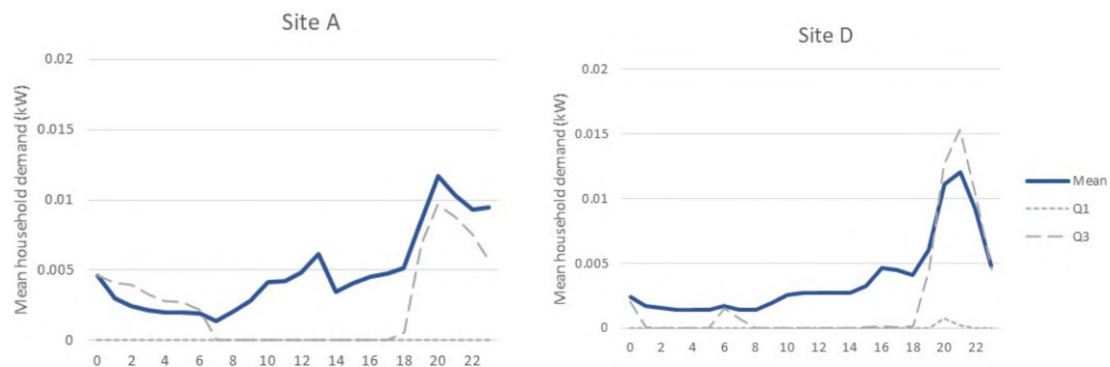
Figure 3.5: Average daily load profiles in two Tanzanian mini-grid sites. Source: [13].

Weekly and seasonal variations were also identified. Consumption in Site A remained stable throughout the week, whereas Site D showed slightly higher usage during weekends. On a yearly scale, both sites exhibited seasonality, with demand falling by approximately 20% between May and November before rising again towards the end of the year [13].

Customer numbers stabilized shortly after initial connection. Site D was commissioned in early 2018, while Site A started in 2019. By mid-2019, growth had stagnated and some disconnections were observed, resulting in fewer active households than reg-

istered accounts. However, data on the share of households that chose not to connect is not available [13].

An important finding relates to price elasticity: electricity consumption increased when tariffs were reduced, highlighting the sensitivity of demand to price levels (Figure 3.6) [13].
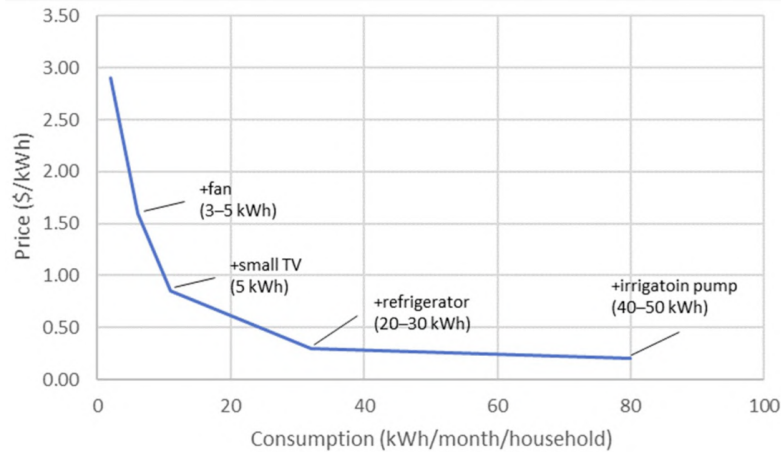
Figure 3.6: Influence of electricity tariffs on household consumption. Source: [13].

3.3.2   Lessons Learned from Tanzanian Mini-Grids

The case of Sites A and D highlights several important lessons for rural mini-grid planning:

- **Low household consumption:** Average daily demand remained below 0.11 kWh per household, showing that electricity use can be extremely limited even when supply is available.

- **Concentration of demand:** Load profiles showed clear evening peaks, with a small share of households responsible for most of the total consumption.

- **Seasonal and weekly variations:** A 20% seasonal decline in demand was observed, and slight weekend increases appeared in Site D, suggesting that both temporal and cultural factors influence load.

- **Customer growth stagnation:** Connections stabilized shortly after commissioning, and some disconnections occurred. This indicates that access alone does not guarantee expanding demand or sustained participation.

- **Tariff sensitivity:** Consumption rose when electricity prices decreased, confirming that affordability strongly shapes usage levels.

3.4 Southeast Asian Off-Grid Villages

3.4.1 Consumption Estimation

This section summarises selected results from [14] on three unelectrified villages in Myanmar, Indonesia, and Laos. The study combined demographic data, appliance ownership, and load profiles to project electricity demand. This is not real data from installed micro grids, but estimations.

Electricity use in all three cases concentrated in morning and evening periods, with distinct daily patterns shown in Figures 3.7–3.9. In Myanmar and Laos, evening peaks dominate due to post-sunset activity, while in Indonesia demand rises earlier, partly driven by religious routines.
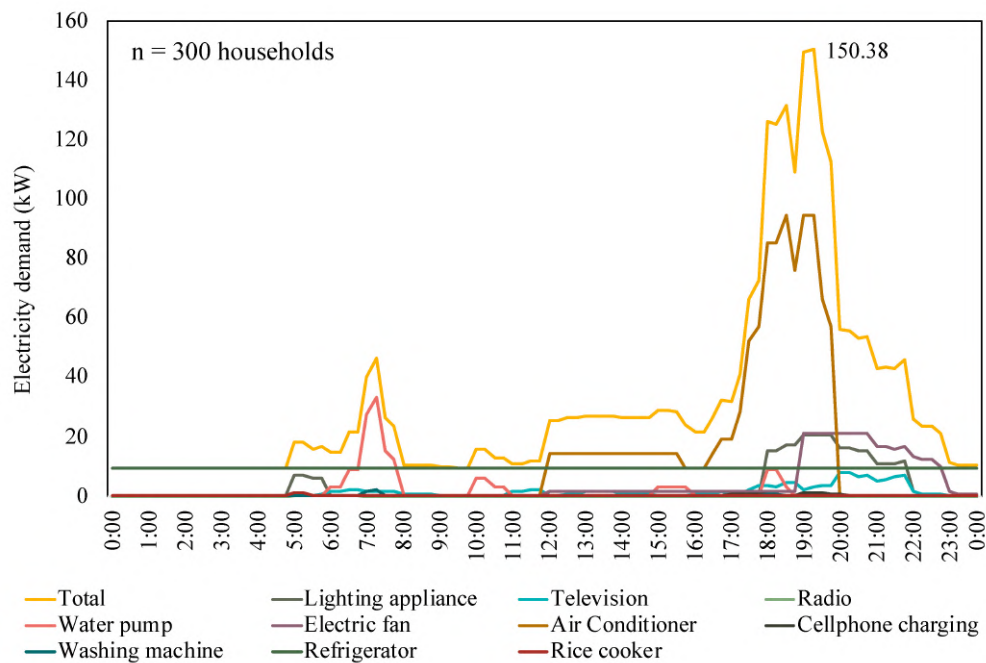
Figure 3.7: Daily load profile in Myanmar. Source: [14]
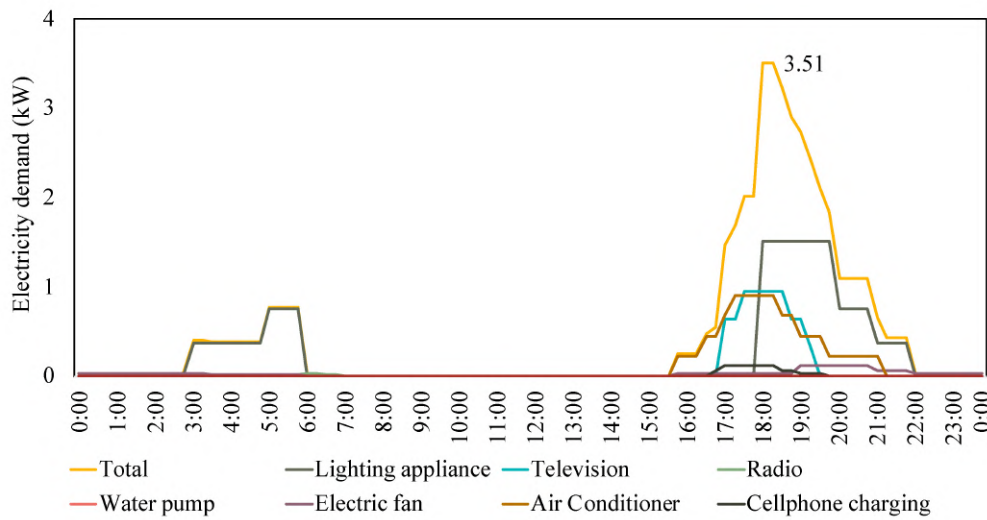
Figure 3.8: Daily load profile in Indonesia. Source: [14]
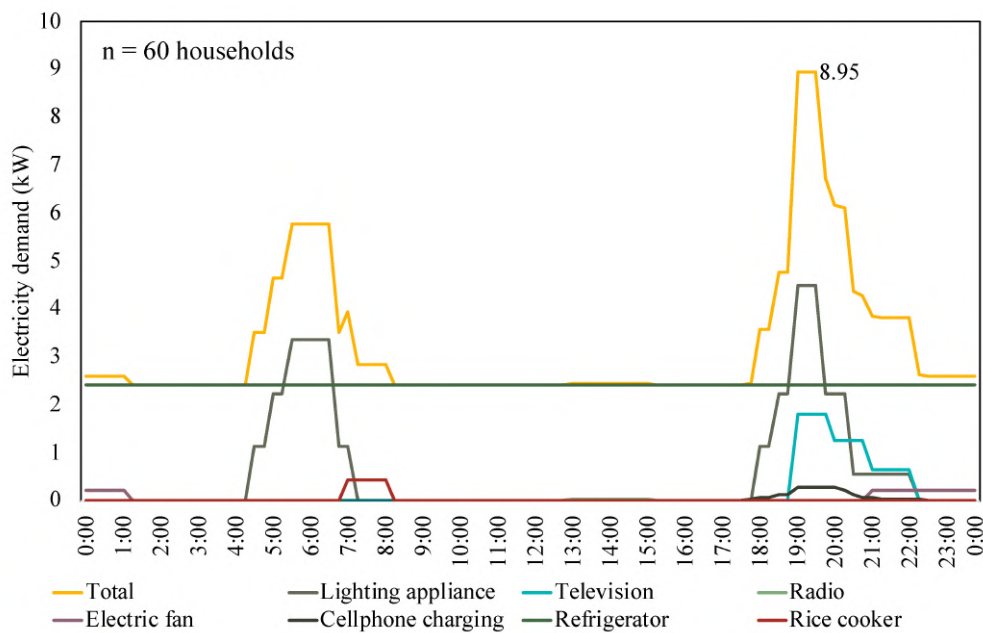
Figure 3.9: Daily load profile in Laos. Source: [14]

Appliance diversity was highest in Myanmar, limited in Indonesia by degraded PV kits, and focused on rice cookers and lighting in Laos (Table 3.3). This variation in appliance penetration, combined with climatic and cultural factors, explains the wide range in projected peak loads: from 3.5 kW in Indonesia to 150 kW in Myanmar, a

42 fold increase. Battery degradation in Indonesian PV kits within 2–3 years underlined the importance of maintenance, while lighting and mobile charging were the most valued benefits across all three locations.

Appliance	Myanmar	Indonesia	Laos
Lighting	95.1 %	54.7 %	100 %
TV	86.4 %	30.2 %	60 %
Fan	74.1 %	1.9 %	17 %
Air Conditioner	49.4 %	1.9 %	0 %
Refrigerator	16.0 %	0 %	20 %
Water Pump	79.0 %	3.8 %	0 %
Rice Cooker	22.2 %	0 %	40 %

Table 3.3: Appliance ownership by village. Source: [14]

3.4.2 Lessons Learned from Southeast Villages Load Estimation

The Southeast Asian case studies provide several insights for demand estimation in un-electrified rural villages:

- **Daily patterns:** Cultural factors such as religious routines can shift demand profiles, as seen in Indonesia.

- **Appliance diversity:** Appliance penetration varies strongly by context, these differences translate into widely varying projected peak loads.

- **Scale of demand:** Projected peaks range from only 3.5 kW in Indonesia to 150 kW in Myanmar, showing the potential 42-fold difference depending on socioeconomic, cultural, and technical conditions.

- **Maintenance needs:** The rapid degradation of Indonesian PV kits within 2–3 years highlights the importance of proper maintenance and system quality for sustained service.

- **Valued services:** Across all three locations, lighting and mobile charging were consistently identified as the most valued benefits, confirming their central role in early stages of rural electrification.

Chapter 4

Socio-Economic and Infrastructural Analysis of Antanamalaza

4.1 Study Area Profile

4.1.1 Why Antanamalaza

Antanamalaza has been selected as the primary case study for this work. Although the methodology is applicable to other rural villages in Madagascar, this site was chosen for both practical and methodological reasons.

A small solar microgrid has already been installed in Antanamalaza by Électriciens Sans Frontières [15]. However, no reliable data exist regarding the number of connected households, consumption patterns, or maintenance records. Preliminary evidence suggests that this installation is considerably smaller than the system analyzed in this study. For this reason, the present analysis proceeds as if no microgrid were currently in operation, thereby ensuring that assumptions and conclusions remain independent.

The choice of Antanamalaza is also linked to the availability of contextual information. Previous collaborations between this works director and non-governmental organizations in the area have facilitated access to data on productive activities, such as wood workshops and rice dehusking facilities. Such information is generally difficult to obtain without direct fieldwork, which lies beyond the scope of this project. Apart from these general insights, no privileged or non-public technical data have been used.

In addition, Antanamalaza represents a prime candidate for a microgrid. As discussed in Table 2.3, densification is not feasible since no distribution lines are present in the vicinity. Grid extension is also economically prohibitive, given that the nearest line is more than 15 km away, exceeding the recommended distance for extensions (see Section 2.2.2). At the same time, the village has sufficient population density and number of households to justify the deployment of a microgrid system, as will be quantified

later in this chapter.

Finally, Antanamalaza is broadly representative of rural Madagascar. Its geographical isolation, lack of centralized energy infrastructure, and socioeconomic profile, centered on small-scale agriculture and artisanal activities, make it an appropriate example for modeling decentralized energy solutions. This representativeness will also be further substantiated in the following sections, where demographic structure and productive activities are examined in more detail. These characteristics are not unique but rather illustrative of the broader rural context in the country, thereby reinforcing the relevance and replicability of the conclusions drawn from this case.

4.1.2 Location

Understanding the local context of the proposed energy system requires situating the village of Antanamalaza within the administrative and territorial structure of Madagascar.

The country is organized into four main administrative levels: regions, districts, communes, and fokontany. Each level contributes to the governance, provision of public services, and community representation.

Figure 4.1 illustrates the position of the Vakinankaratra region within Madagascar. This region is located in the central highlands, to the south of the capital Antananarivo.

At the regional scale, Figure 4.2 presents an administrative map of Vakinankaratra, indicating the boundaries of its districts and communes. Antanamalaza belongs to the district of Ambatolampy and constitutes a rural commune named after its main settlement, which is the focus of this study. In other words, Antanamalaza is both the name of the commune and the village under analysis. The commune of Antanamalaza is part of the Ambatolampy district, one of the seven districts forming the Vakinankaratra region.

Within each commune, the territory is further subdivided into fokontany, which correspond to village clusters or neighborhoods and represent the most local level of administration. Fokontany are used for community coordination, collection of statistics, and provision of basic public functions. Unlike higher administrative divisions, their boundaries are often poorly defined or inconsistently updated in official records.

Figure 4.1: Location of the Vakinankaratra region within Madagascar [16].

Figure 4.2: Administrative map of the Vakinankaratra region. Source: Region Vakinankaratra [17], with minor annotations by the author.

4.1.3 Geographic and Climatic Characteristics

Antanamalaza is situated at an altitude of approximately 1660 meters above sea level, consistent with the elevation of Madagascar's central highlands. As shown in Figure 4.3, the village lies on slightly higher ground than the surrounding terrain. This location likely provides protection against flooding, while lower-lying areas are more suitable for rice cultivation. The topography is characterized by gentle hills and shallow valleys, creating a landscape well adapted to agriculture and rural settlement.

The surrounding land is predominantly agricultural, with plots used for subsistence farming and small-scale crop processing. These physical characteristics are relevant both for understanding land-use patterns and for evaluating the feasibility of transporting materials and maintaining infrastructure.

Figure 4.3: Aerial view of Antanamalaza. Source: Facebook group of Antanamalaza [18].

Climatically, Antanamalaza falls within a humid subtropical zone, marked by a distinct rainy season from November to April. Heavy precipitation during this period reduces road accessibility and complicates infrastructure maintenance. According to satellite-based data from NASA POWER [19], average daily rainfall ranges from 17.1 mm in January to 1.9 mm in September. Monthly average temperatures vary between 18.3 °C in December and 11.4 °C in July, with recorded extremes of 27.5 °C in October and 2.6 °C in June.

Time Series of Climatology Temperature at 2 Meters 2001/01/01 to 2020/12/31 in LST (Lat: -19.43, Lon: 47.63)

Source: GMAO MERRA-2 data accessed from NASA POWER at 2025-05-10 10:34:56 UTC.
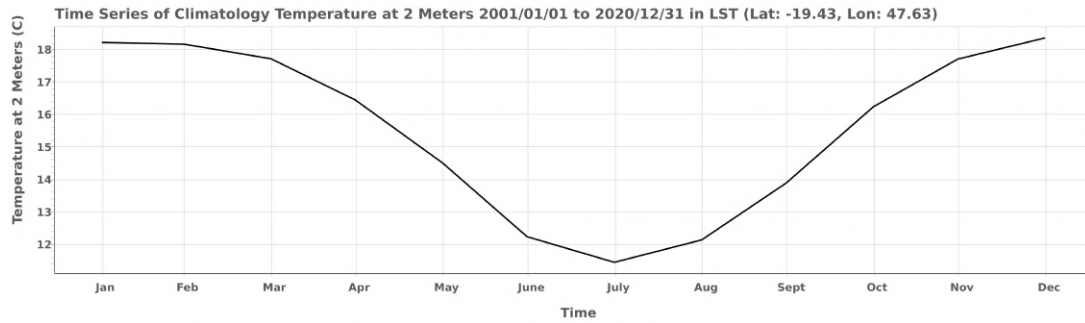
(a) Average monthly temperature in Antanamalaza.

Time Series of Climatology Precipitation Corrected 2001/01/01 to 2020/12/31 in LST (Lat:-19.43, Lon: 47.63)

Source: GMAO MERRA-2 data accessed from NASA POWER at 2025-05-10 10:34:56 UTC.
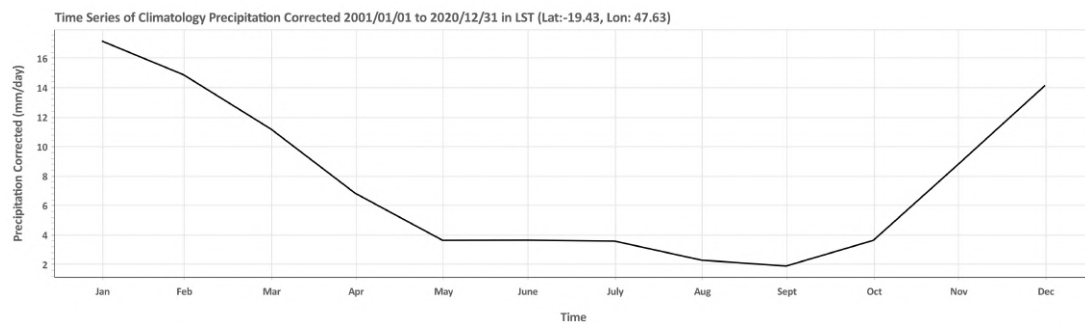
(b) Average monthly precipitation in Antanamalaza.

Figure 4.4: Climatic data for Antanamalaza. Source: NASA POWER [19].

Hydropower does not appear to be a viable option, as no rivers in the immediate vicinity provide sufficient or consistent flow to support even small-scale installations, particularly during the dry season. The renewable energy potential of the site is therefore primarily solar, with wind energy considered a possible secondary option, pending detailed local resource assessments.

4.2 Demographics and Population Estimates

4.2.1 Methodological Approach

The estimation of the population of Antanamalaza required combining multiple sources, given the absence of recent disaggregated census data at the fokontany level. The approach followed three main steps: (i) commune-level population figures from 2001 and 2013, and national yearly data were used to establish a growth trend; (ii) this growth was extrapolated to 2023 by comparison with national rural growth rates; and (iii) the

resulting commune-level estimate was downscaled to the village using satellite-derived building footprints and average household size from national surveys.

4.2.2 Population of the Commune Antanamalaza

Estimating electricity demand requires an understanding of the number of people who will potentially use energy services. Unfortunately, Madagascar lacks disaggregated official population figures at the fokontany (village) level, and even at the commune level data remain scarce and are published irregularly.

For the commune of Antanamalaza, two population estimates are available:

- In 2001, the population was estimated at 12,217 inhabitants, according to the Ilo program of Cornell University [20].

- In 2013, the population was estimated at 17,365 inhabitants by the Centre de Recherches, d'Études et d'Appui à l'Analyse Économique à Madagascar (CREAM) [21].

The compounded annual growth rate (CAGR) between 2001 and 2013 is calculated as:

$$P(t) = P_0 \cdot (1+r)^t \quad \Rightarrow \quad 1+r = \left(\frac{P(t)}{P_0} \right)^{1/t} = \left(\frac{17{,}365}{12{,}217} \right)^{1/12} \approx 1.0297 \Rightarrow r \approx 2.97\%.$$

This corresponds to an average annual growth rate of approximately 2.97%. However, this value cannot be applied directly for long-term projections. National demographic data reveal that rural population growth in Madagascar has been declining over time, as shown in Figure 4.5. It is therefore reasonable to assume that Antanamalaza did not experience a constant 2.97% annual growth rate, but rather a declining trend starting above this value and gradually decreasing.
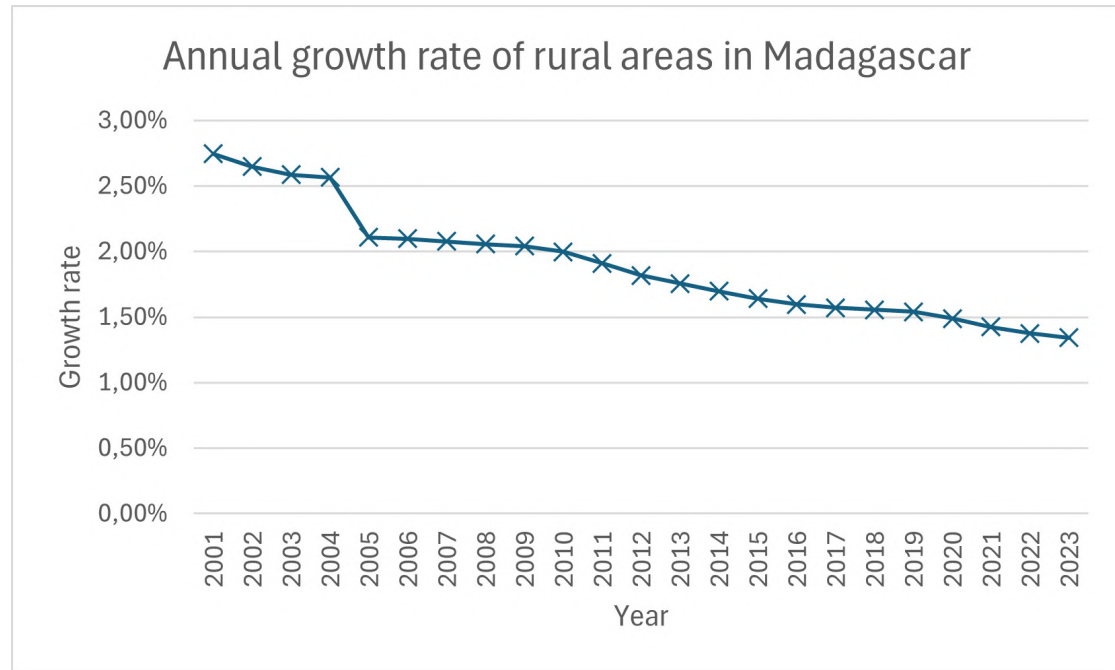
Figure 4.5: Rural population growth in Madagascar (2001–2023). Chart elaborated by the author using World Bank data [22].

To refine the projection, the historical growth of Antanamalaza was compared to national rural growth data from 2001 to 2013. Let r_i denote the national rural growth rate in year i. The cumulative growth factor is given by:

$$F = \prod_{i=2001}^{2013} (1 + r_i).$$

From this, the national CAGR is derived as:

$$\text{CAGR}_{\text{national}} = F^{1/12} - 1 \approx 2.23\%.$$

Antanamalaza's growth was therefore approximately 33% higher than the national rural average. A proportionality factor can be defined as:

$$\alpha = \frac{2.97\%}{2.23\%} \approx 1.33.$$

Year	Rural Growth Rate (%)
2001	2.746
2002	2.649
2003	2.585
2004	2.566
2005	2.108
2006	2.097
2007	2.077
2008	2.056
2009	2.042
2010	1.997
2011	1.910
2012	1.818
2013	1.755
2014	1.698
2015	1.641
2016	1.598
2017	1.572
2018	1.556
2019	1.541
2020	1.490
2021	1.424
2022	1.375
2023	1.343

Table 4.1: Rural population growth in Madagascar (2001–2023). Data elaborated by the author using World Bank figures [22].

To project Antanamalaza's population to 2023, it is assumed that the commune continued to grow faster than the national rural average, maintaining the same proportional relationship as in the past. For any year t, the adjusted growth rate is defined as:

$$r_{\text{Anta},t} = \alpha \cdot r_{\text{Nat},t}.$$

Using the national rural growth rates from 2014 to 2023 (Table 4.1), the adjusted local rates yield a cumulative growth factor:

$$P_{2023} = 17{,}365 \times \prod_{i=2014}^{2023} (1 + r_{\text{Anta},i}) \approx 17{,}365 \times 1.223 \approx 21{,}229.$$

The population of the commune of Antanamalaza in 2023 is therefore estimated at approximately **21,230 inhabitants**.

4.2.3 Population of the Village Antanamalaza

The previous subsection estimated that the commune of Antanamalaza had approximately 21,230 inhabitants in 2023. According to the SDG 7 Dashboard [8], there are 5,343 structures in the commune with an area greater than 9 m^2 (see Table 4.2). Based on household data from INSTAT [23], rural households in Madagascar consist on average of 4.4 individuals, compared to 4.0 in urban areas. Assuming that each structure accommodates at most one household, it is estimated that 4,825 of these structures are residential. This implies that approximately 90.3% of all structures larger than 9 m^2 in the commune are households, with the remainder being non-residential buildings.

To estimate the number of households and individuals who could be connected to the proposed microgrid, a specific area of the village was delineated (Figure 4.6). The selected area is compact, with a longest dimension of 1.3 km, a perimeter of 4,300 m, and a total area of 330,000 m^2. It displays a high density of similarly sized structures arranged along wide roads and appears to encompass nearly the entire village of Antanamalaza, although official boundaries were not available to the author.

Manual counting of structures within this area would not be reliable. Instead, the Open Buildings dataset [24] was analyzed using QGIS software. The analysis included only structures larger than 9 m^2 and tagged with a confidence level above 70% in Google's classification system. In Figure 4.7, qualifying structures are marked in green. A total of 998 structures were identified within the selected area.

Assuming that the ratio of structures to households in the village mirrors the commune-wide estimate, approximately 901 households can be inferred within the defined area. With an average household size of 4.4 individuals, this corresponds to an estimated population of 3,965 residents.

Indicator	Commune Level	Village (selected area)
Estimated population	21,230	3,965
Number of structures > 9 m^2	5,343	998
Estimated residential structures	4,825	901

Table 4.2: Demographic and structural estimates for Antanamalaza.

Demographic estimates and number of households (see Table 4.2) provide the foundation for the electricity demand projections developed in the following chapter.

Figure 4.6: Satelite view of the village of Antanamalaza, with the area considered for potential microgrid connections. Source: Google Earth, with area boundary drawn by the author.

Figure 4.7: Screenshot from QGIS showing the structures identified within the selected area.

4.3 Socio-Economic and Infrastructural Characteristics

Understanding the socio-economic and infrastructural context of Antanamalaza is critical for evaluating its electricity demand and assessing the feasibility of decentralized energy systems. The data used in this section are drawn from three key sources: the

commune-level census conducted in 2001 [20], a 2013 regional monograph with commune-level data by CREAM [21], and a national survey conducted by INSTAT in 2018 [25], of which 298 households were in the commune of Antanamalaza. Although most of this data corresponds to the commune as a whole rather than the village specifically, it provides an essential approximation of local conditions.

4.3.1 Institutional Presence and Basic Services

Table 4.3 provides a snapshot of the commune's demographic and institutional landscape in 2001. With a population of 12,217, Antanamalaza was slightly below the national commune average of 15,026 inhabitants but slightly above the median. Yet public infrastructure remained limited: there was only one ministry representation and no hospital, bank, post office, or senior secondary school. Nevertheless, the commune had a health center and access to both primary and junior secondary education, placing it in line with the national norm in these areas.

The commune also lacked access to a national road, though it was served by a provincial road and had a functioning minibus stop, ensuring a minimum level of internal mobility and regional connectivity. No piped water was supplied by JIRAMA or by other providers, reflecting the general scarcity of such infrastructure in rural communes.

Information	Antanamalaza commune (2001)	Comparison to Other Communes
Population	12 217	Average is 15 026 and median is 10 850
Number of different ministry representations	1	Average is 1.58
Availability of a hospital	No	8.4% of communes have it
Availability of a health center	Yes	94% of communes have it
Availability of a bank or savings institution	No	7.5% of communes have it
Availability of a post office	No	28% of communes have it
Availability of a primary school	Yes	99.6% of communes have it
Availability of a junior secondary school	Yes	52.6% of communes have it
Availability of a senior secondary school / high school	No	8.9% of communes have it
Presence of a national road	No	33.4% of communes have it
Presence of a provincial road	Yes	40.4% of communes have it

Continued on next page

Information	Antanamalaza commune (2001)	Comparison to Other Communes
Presence of a minibus stop	Yes	38.8% of communes have it
Presence of a permanent court	No	2.7% of communes have it
Presence of a daily market	Yes	36.7% of communes have it
Presence of a agricultural input sales point	Yes	17% of communes have it
Presence of a public phone	No	9.8% of communes have it
Drinking water supplied by JIRAMA	No	7.0% of communes have it
Drinking water supplied by a provider other than JIRAMA	No	33.8% of communes have it

Table 4.3: Demographic and institutional characteristics of the commune of Antanamalaza in 2001, compared with national commune averages and medians. Source: [20], comparison calculations by the author.

Twelve years later, CREAM [21] reported an expansion of services. Antanamalaza hosted a market (see Figure 4.8), a police post, a private radio station, and access to landline phone services. In 2013, the commune had nine public and eighteen private primary schools, collectively serving 2,296 students with 60 teachers, for a student–teacher ratio of approximately 38:1. It also had one public and one private secondary school. While specific locations were not provided, it is likely that these institutions are situated in the main village of Antanamalaza, given its centrality within the commune. No high school (senior secondary institution) was reported in the commune.

Health infrastructure included one CSB II (Centre de Santé de Base Niveau II), a basic health facility with at least one doctor. External sources confirm that this center is located in the village of Antanamalaza. The commune does not host any industrial mining operations, nor does it contain known deposits of precious metals, in contrast with other communes in the same district where gold mining is present.
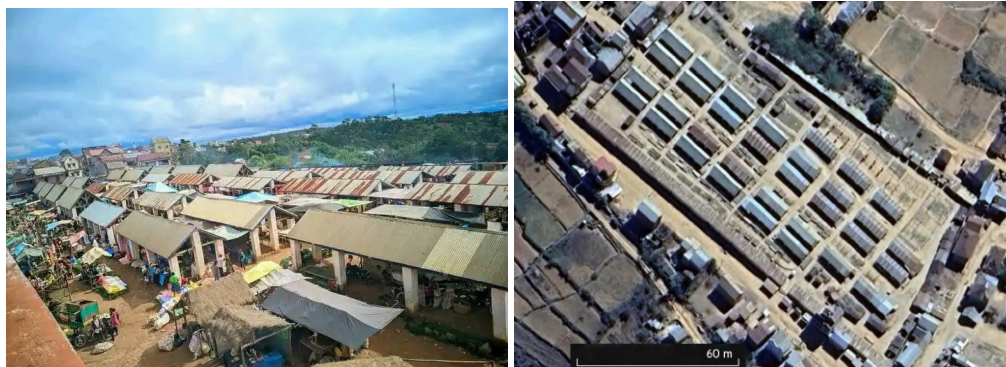
(a) Photo of the market of Antanamalaza. Source: [18].

(b) Google Earth view of the market of Antanamalaza

Figure 4.8: Market of Antanamalaza.

In summary, Antanamalaza offers only a limited set of public services. Education and health facilities are present but at a basic level, while higher-order infrastructure such as hospitals, high schools, banking, and piped water are absent. For the purposes of this study, the key institutional loads are therefore expected to come from the CSB II health center, the schools, and the daily market.

4.3.2 Economic Activity and Employment Structure

As illustrated in Table 4.4, Antanamalaza is a predominantly agriculture-dependent commune. In 2001, 85% of the population worked in agriculture, slightly higher than the national rural average of 80%. The service sector accounted for the remaining 15% of employment, while the industrial, fishing, and livestock sectors were entirely absent. These figures highlight the commune's narrow economic base and its vulnerability to climatic or market shocks affecting agricultural production.

Rice is the most common crop by surface area, followed by corn. In terms of market value, however, potatoes, dry beans, and cassava take precedence, reflecting the diversity of agricultural priorities beyond subsistence farming. Agricultural practices also appear more intensive than in many other rural areas: over 75% of farmers in Antanamalaza reported using chemical fertilizers, compared with a national average of just 13%. This high adoption rate suggests a relatively advanced approach to farming within the commune.

Information	Antanamalaza commune (2001)	Comparison to Other Communes
Presence of Industrial mining	No	26.8% of communes have it
Presence of a business with over 50 employees	No	7.4% of communes have it
Presence of a business with 10 to 50 employees	No	8.2% of communes have it
Presence of a business with under 10 employees	Yes	13.7% of communes have it
Share of the population in the agricultural sector (%)	85%	Average is 80% across all communes
Share of the population in the fishing sector (%)	0%	Average is 3.5% across all communes
Share of the population in the livestock sector (%)	0%	Average is 10.6% across all communes
Share of the population in the industrial sector (%)	0%	Average is 1.5% across all communes
Share of the population in the service sector (%)	15%	Average is 10% across all communes
Most important agricultural product by area	Rice	71.6% of communes report rice as the most important crop, 53.8% as the second most important, and 10.4% report maize as third
Second agricultural product by area	Rice	
Third agricultural product by area	Corn	
Most important agricultural product by value	Potato	7.8% of communes report potato, 24.0% dry beans, and 60.1% cassava as one of the three most valuable crops by value
Second agricultural product by value	Dry beans	
Third agricultural product by value	Cassava	
Percentage of rice fields irrigated by pump/dam	15%	Average of 16.3%. Most communes are at 0%, so Antanamalaza is in the fourth quintile
Proportion of farmers using chemical fertilizers	>75%	Only 13.07% of communes report this

Table 4.4: Economic activity and employment structure of the commune of Antanamalaza in 2001, compared with national commune averages. Source: [20], comparison calculations by the author.

4.3.3   Income, Poverty, and Vulnerability

Table 4.5 summarizes the income distribution and development priorities of Antanamalaza. The commune's profile closely mirrors national patterns: 40% of the population is considered middle-income (facing food issues only in bad years), 43% is categorized as poor (experiencing seasonal food insecurity), and 10% as extremely poor (facing year-round food insecurity). The proportion of wealthy households (7%) is also close to the national average. The lean season lasts approximately five months, slightly longer than the national median of four.

Information	**Antanamalaza commune (2001)**	**Comparison to Other Communes**
Percentage of wealthy population (no food issues even with crop failure)	7%	Average is 8.7%, median is 5%. Antanamalaza is in the fourth quintile
Percentage of middle-income population (food issues only in bad years)	40%	Average is 39%, median is 35%. Antanamalaza is in the third quintile
Percentage of poor population (seasonal food difficulties)	43%	Average is 44%, median is 40%. Antanamalaza is in the third quintile
Percentage of extremely poor population (food insecure year-round)	10%	Average is 8%, median is 5%. Antanamalaza is in the fourth quintile
Duration of the lean season	5 months	Average is 4.4 months, median is 4 months. Antanamalaza is in the third quintile
Top development priority in the commune	Health	60.4% of communes list health as one of the top 3 priorities
Second development priority in the commune	Agriculture	62.0% of communes list agriculture as one of the top 3 priorities
Third development priority in the commune	Education	56.8% of communes list education as one of the top 3 priorities. Health, agriculture, and education are the most frequently cited top 3 priorities

Table 4.5: Income distribution, poverty levels, and development priorities in Antanamalaza (2001), compared with national commune averages. Source: [20], comparison calculations by the author.

Household size, measured in number of rooms, provides an additional proxy for socio-economic conditions. As shown in Table 4.6, nearly two-thirds of households in Antanamalaza occupy single-room dwellings, while more than 94% have no more than two rooms. This distribution reflects the commune's income profile: a majority of households are low-income or extremely poor (53% combined), with limited capacity to invest in larger dwellings. Conversely, only 6% of households report having three or more rooms, a proportion that aligns with the 7% of wealthier households in the income data. These housing conditions reinforce the economic vulnerability highlighted in Table 4.5.

Number of rooms	Percentage of households (%)
1	65.8
2	28.2
3	3.7
4	2.0
5	0.3

Table 4.6: Distribution of households by number of rooms in Antanamalaza (2018). Calculated by the author based on data from [25].

The most frequently cited development priorities in the commune were health, agriculture, and education, matching national trends in rural Madagascar. This alignment indicates that Antanamalaza's socio-economic structure and aspirations are broadly representative of the national rural context, highlighting both the commune's persistent vulnerabilities and its shared development priorities with other rural areas of Madagascar.

4.3.4 Accessibility and Transport Conditions

Table 4.7 summarizes the commune's transport and accessibility profile. Antanamalaza does not have paved roads, but it is connected by unpaved routes that, in principle, remain usable year-round by minibus. Travel time to the nearest urban center is approximately three hours in both the dry and rainy seasons, a consistency largely due to the availability of minibus services. These indicators place the commune in the second national quintile for accessibility, both for passenger transport and for the movement of agricultural goods (see cost metrics for 50 kg sacks).

In practice, however, these roads deteriorate significantly during the rainy season. As illustrated in Figure 4.9, unpaved segments often become muddy and may be impassable for larger vehicles. CREAM [21] notes that, during this period, access to the commune is restricted to small vehicles.

Information	Antanamalaza commune (2001)	Comparison to Other Communes
Presence of an Airport	No	5.8% of communes have it
Transport cost for one person to the main urban center (dry season)	12 500 Ar	Second quintile. Median is 35 000 Ar
Transport cost for one person to the main urban center (rainy season)	12 500 Ar	Second quintile. Median is 35 000 Ar
Travel time to the main urban center (dry season)	3h	Second quintile
Travel time to the main urban center (rainy season)	3h	Same as in the dry season. This occurs in 49% of communes. Average increase is 33% during the rainy season
First mode of transport to urban centers	Mini bus	Relatively fast 3h time and consistency is possible because of the minibus
Second mode of transport to urban centers	Mini bus	
Transport cost for a 50kg sack to the main urban center (dry season)	5 000 Ar	Second quintile. Median is 10 000 Ar
Transport cost for a 50kg sack to the main urban center (rainy season)	5 000 Ar	Second quintile. Median is 10 000 Ar
Availability of paved roads in the commune	No	77% are in the same situation
Availability of unpaved roads passable year-round by mini bus	Yes	47% are in the same situation

Table 4.7: Transport and accessibility indicators for Antanamalaza (2001), compared with national commune averages. Source: [20], comparison calculations by the author.

(a) Flooded road segment.   (b) Vehicles partially stuck.
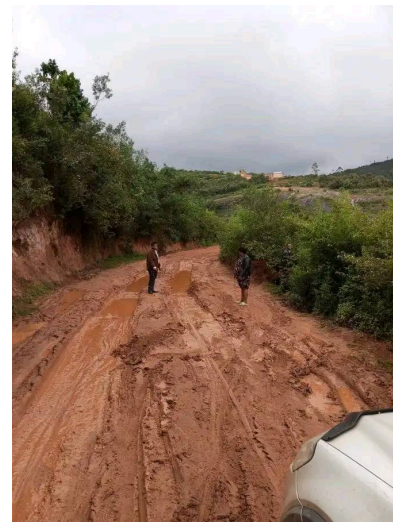
Figure 4.9: Road to Antanamalaza partially flooded. Source: [18].

4.3.5 Transport Modes and Employment at Household Level

A more detailed picture of household conditions emerges from the INSTAT survey [25], which sampled 298 households in Antanamalaza. Only 2.0% of households owned a car and 7.4% a scooter, while 55.0% reported owning at least one bicycle. Strikingly, 42.6% of households had none of these three transport modes, underscoring the commune's reliance on walking, informal means of transport, and shared or public services.

Transport Mode	Number of Households	Percentage
Bicycle	164	55.0%
Scooter	22	7.4%
Car	6	2.0%
None of the above	127	42.6%

Table 4.8: Household ownership of transport modes in Antanamalaza (2018). Source: [25], comparison calculations by the author.

With respect to employment, 92.6% of households reported having at least one member engaged in agricultural activities. Only three households (1.0%) declared no involvement in either agriculture or livestock. These results highlight the commune's overwhelming dependence on primary sector activities and suggest that any diversification of livelihoods would require significant and targeted policy support.

4.4 Energy Access and Appliance Ownership

Appliance ownership data from the 2018 INSTAT survey [25] reveals a clear picture of low electrification levels. As shown in Table 4.9, mobile phones are the most commonly owned device (49.3%), followed by radios (30.2%). Landline phones, televisions, video players, and computers are rare, and no households reported owning refrigerators, washing machines, or electric cookstoves. This lack of high-demand appliances confirms that most households have not yet reached higher tiers of electricity access.

Appliance	Percentage of Households
Mobile phone	49.3%
Radio	30.2%
Television	5.0%
Landline phone	4.0%
Video player	3.0%
Internet equipment	2.0%
Sewing machine	2.0%
Air conditioner	0.3%
Computer	0.3%
Cookstove	0.0%
Refrigerator	0.0%
Washing machine	0.0%

Table 4.9: Household appliance ownership (excluding lighting) in Antanamalaza in 2018. Table made by the author using data from [25]

Lighting sources provide further insight. As seen in Table 4.10, kerosene lamps remain the most common source (56.7%), while 28.9% of households report having electricity for lighting. This is particularly relevant given that in 2017–2018, the commune had no access to the national grid or a local microgrid. This strongly suggests that solar home systems (SHS) and other off-grid solutions were the primary sources of electricity.

Lighting Source	Percentage of Households
Kerosene lamp	56.7%
Electricity	28.9%
Candle	9.1%
Other	5.4%

Table 4.10: Main sources of lighting in households in Antanamalaza in 2018. Table made by the author using data from [25]

At the time of the survey (2017–2018), the commune lacked both grid and microgrid access, indicating that electricity was primarily supplied through off-grid sources such as solar home systems.

4.5 Representativeness Within the National Context

Overall, Antanamalaza can be regarded as broadly representative of rural communes in Madagascar. Its demographic size, income distribution, institutional access, and economic base align closely with national medians. Development priorities such as health, agriculture, and education mirror those most frequently cited at the national level, while the commune's heavy reliance on agriculture reflects the typical rural economic structure.

Certain features, such as relatively high fertilizer use and year-round road access by minibus, set Antanamalaza somewhat apart from the average commune. Nevertheless, these variations remain within the spectrum of rural conditions in Madagascar and do not undermine its validity as a case study. On the contrary, they provide useful nuance, reinforcing both the relevance of the findings and the broader applicability of the study's conclusions.

Chapter 5

Estimating Demand of Electricity

5.1   Importance

To evaluate the potential impact, cost, and scale of the proposed project, it is essential to estimate the future electricity demand within the microgrid. Forecasting electricity demand in this context is particularly challenging due to the conditions of the village. The project will introduce reliable electricity for the first time, and while some residents may have previously managed to intermittently charge small devices such as lamps or mobile phones, access has been neither stable nor dependable. For the majority of households, the use of substantial electrical appliances was previously inconceivable.

The implementation of a microgrid in a previously unconnected rural village represents a transformative development. Devices that had relied on small, individual solar kits, often abandoned after their short and costly operational life, are expected to be integrated into the new grid. In addition, households are likely to progressively acquire new appliances as electricity access becomes normalized and more affordable.

Demand estimation, while essential, remains inherently uncertain. It depends on a range of assumptions, many of which are difficult to verify or have a strong influence on the results. For this reason, it is crucial that the microgrid infrastructure is designed with flexibility, allowing it to adapt efficiently to evolving consumption patterns after deployment.

This chapter develops demand estimates using two complementary approaches: a top-down method, based on income distribution and adoption scenarios, and a bottom-up method, based on appliance ownership and usage. The two approaches are then compared and reconciled to provide a robust basis for subsequent system dimensioning.

5.2 Estimating Household Demand

5.2.1 Top-down Method

5.2.1.1 Method overview and household income distribution

The top-down estimation method relies on the tool developed by [26], which simulates hourly household consumption profiles. The model requires only four input parameters:

- Total number of households

- Share of connected households classified as high-income

- Share of connected households classified as medium-income

- Share of connected households classified as low-income

While the tool does not generate pricing information, it provides a useful preliminary approximation of household demand patterns over time.

Obtaining reliable values for these parameters is not straightforward. The total number of households has been estimated at 901, as discussed in Section 4.2.3. To determine the income composition of potential users, a two-step approach is applied. First, the distribution of households by income level is established. Second, the likely adoption rate for each group is inferred.

According to Table 4.5, the 2001 dataset indicates that 7% of households were classified as high-income, 40% as medium-income, 43% as low-income, and 10% as very low-income. Although somewhat outdated, this is the most recent source that reports all four categories, and is therefore adopted as the basis for this analysis under the assumption that household-level income shares remain broadly applicable.

The relevance of this assumption is supported by long-term poverty trends. The World Bank [27] reports that national monetary poverty rates remained largely stable between 2012 and 2022. Similarly, [28] show only a modest 2.4% increase in the population living below the $5.50/day threshold between 2001 and 2012. Taken together, these findings suggest that the 2001 income distribution remains a reasonable approximation for the present study.

5.2.1.2 Adoption scenarios

The income distribution of actual microgrid users is expected to differ from that of the general population. Higher-income households are more likely to connect to the grid due to greater financial capacity, whereas affordability constraints may prevent lower-income groups from gaining access. Assumptions regarding connection rates by income level must therefore be incorporated into the model.

Empirical evidence supports the view that affordability is the primary determinant of microgrid adoption. Aklin et al. [29] demonstrated that in rural India, high perceived costs were the main barrier to adoption, even when systems were designed to be affordable. Harrington et al. [30] further highlighted that improvements in reliability and lighting quality, particularly during evening hours, were among the most valued outcomes. These findings suggest that while affordability influences initial adoption, continued use is reinforced by the quality and reliability of the service.

Based on this evidence, a set of assumptions has been formulated regarding household connection behavior. High-income households are assumed to connect unconditionally, while very low-income households are assumed not to connect due to financial barriers. For medium- and low-income households, adoption is considered conditional. In the short term, these groups are expected to connect primarily if existing electricity solutions become unviable and the grid offers a more cost-effective alternative. In the medium term, wider adoption is anticipated if the service is affordable and accessible. Appliance ownership is also expected to influence these decisions.

At present, only 49% of households report owning at least one mobile phone, the most common appliance (see Table 4.9). This figure is close to the combined share of high- and medium-income households (47%). However, this does not imply that only 49% of households will connect to the grid. Appliance ownership and usage are likely to rise once the microgrid is installed, since the cost of owning a device will fall with the removal of the need to purchase personal photovoltaic systems, currently one of the most prevalent electricity sources (see Table 2.2), and with the expected improvement in supply reliability.

Two scenarios are therefore considered in this analysis. In the primary scenario, electricity is assumed to be both affordable and highly valued, resulting in all households except those in the very low-income category connecting to the grid. In the alternative scenario, electricity is assumed to be less affordable, though still beneficial; under this condition, only medium- and high-income households are expected to connect. In this latter case, low- and very low-income households, together representing 50% of the population, remain unconnected.

Income group	Share of households	Assumed connection rate, scenario 1	Assumed connection rate, scenario 2
High income	7%	100%	100%
Medium income	40%	100%	100%
Low income	43%	100%	0%
Very low income	10%	0%	0%

Table 5.1: Estimated income distribution and assumed connection rates

Income group	Share of households	Number of connected households scenario 1	Number of connected households scenario 2
High income	7%	63	63
Medium income	40%	360	360
Low income	43%	387	0
Very low income	10%	0	0
Total	100%	810	423

Table 5.2: Number of households connected in each category

Input data	Share of connected households scenario 1	Share of connected households scenario 2
Connected households	810	423
High income	7.8%	14.9%
Medium income	44.4%	85.1%
Low income	47.8%	0%

Table 5.3: Input data for both scenarios

5.2.1.3   Load profile results

As shown in Table 5.1, the majority of household connections in scenario 1 are expected to come from medium- and low-income groups.

Using these figures as inputs to the tool developed by [26], the daily load profile shown in Figure 5.1 was obtained.
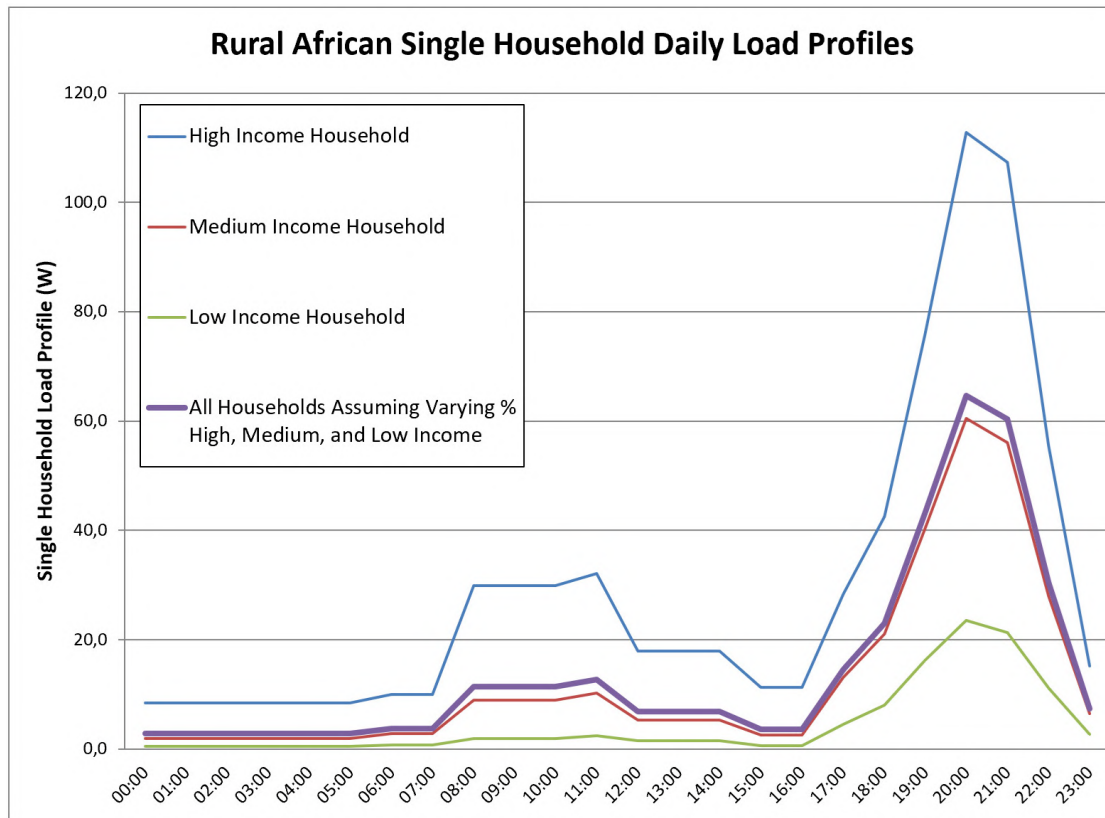
Figure 5.1: Daily load profile for households in Antanamalaza under scenario 1 (obtained with the tool developed by [26]).

The simulated household load profile displays the following characteristics: total daily electricity consumption is estimated at 194 kWh, corresponding to an annual demand of approximately 70,954 kWh. Peak demand occurs at 20:00, reaching 30.09 kW, while the minimum demand of 1.62 kW is observed at 03:00. This pattern is consistent with typical weekday household usage, showing relatively stable consumption during daylight hours followed by a marked increase in the early evening.

For comparison, the alternative scenario (scenario 2) yields a lower overall demand profile, as fewer households are assumed to connect. Total household consumption is estimated at 153 kWh/day (55,898 kWh/year), with a maximum daily peak of 22.9 kW and a minimum of 1.39 kW. These values are consistently lower than those of scenario 1, reflecting the reduced number of connected households. Nonetheless, scenario 1 is retained as the primary reference for this study, as it better captures the expected outcome under conditions of affordable and reliable electricity supply.

Seasonal and weekend variations are not considered in this estimation. Although such effects may exist, available data are insufficient to assess them with accuracy. Moreover, no distinctive factors indicating strong seasonality in household demand have

been identified. In contrast to certain microgrid systems, such as Ambolobozokely (Section 3.2), where demand fluctuates with fishing-related migration, the Antanamalaza context does not exhibit comparable characteristics.

Seasonal influences are further expected to be negligible due to the nature of appliance ownership (see Table 4.9). The very limited presence of climate-sensitive devices—such as fans, refrigerators, air conditioners, or heating systems—suggests that temperature-related demand shifts will play only a minor role in overall consumption.

5.2.1.4   Long-term projections

In the simulations, demand is projected over a 25-year horizon. Growth is expected to result from two main drivers: (i) population increase and (ii) higher per-capita consumption, provided the grid proves reliable and the village continues to expand.

Between 2010 and 2023, electricity access in Madagascar rose markedly, from 12.3% to 39.4% of the population [3]. Over the same period, national per-capita electricity consumption increased from 62.2 kWh to 80.4 kWh [31]. At first glance, this suggests substantial progress in infrastructure and availability. However, when adjusted for the share of the population actually connected to the grid, a different pattern emerges.

The average electricity consumption per connected person can be estimated as:

$$C_{\text{connected}} = \frac{C_{\text{national}}}{P_{\text{connected}}}$$

Applying this formula yields:

$$C_{2010} = \frac{62.2}{0.123} \approx 506 \text{ kWh/person}, \quad C_{2023} = \frac{80.4}{0.394} \approx 204 \text{ kWh/person}$$

This indicates that average consumption per connected person declined by nearly 60% over the 13-year period. Several factors may help explain this counterintuitive trend. First, electrification has expanded primarily into rural areas, where households typically consume far less electricity than urban users. Second, Madagascar's generation capacity remains limited and unstable, reducing supply reliability. Third, in 2010 a relatively small number of already-connected industrial and urban users with disproportionately high demand likely inflated per-user averages.

Given these dynamics, projecting future consumption per connected person is highly uncertain. For the purposes of this study, an annual compound growth rate of 2% is assumed, reflecting both population growth of approximately 1.5% (see Section 4.2.2) and increased household demand driven by the acquisition of higher-power appliances. While this assumption may not fully capture future developments, the overall results are unlikely to be significantly affected. The proposed system is designed to be modular, allowing periodic resizing to align capacity with evolving demand (see later chapters).

The results presented here reflect the demand estimated under the top-down approach, based on income distribution and household connection scenarios. These findings will later be compared (see Section 5.4) with those obtained through the bottom-up method (see Section 5.2.2), in order to cross-validate the two approaches and refine the overall demand estimate for Antanamalaza.

5.2.2 Bottom-up Method

5.2.2.1 Methodology

The second approach to estimating electricity demand relies on a bottom-up framework, as outlined in [32] and [14]. In this method, energy requirements are calculated by aggregating the consumption of individual appliances, rather than inferring demand from household categories. The procedure typically yields two key outputs: the total daily energy demand, which informs the sizing of solar generation capacity, and, in the case of [32], the nighttime energy demand, which determines the required level of battery storage.

In its conventional form, the bottom-up method classifies households into categories according to appliance ownership, usage duration, and device power ratings. For the commune of Antanamalaza, however, such categorization is not optimal. More reliable information is available on aggregate appliance ownership at the community level than on their distribution across household types. For this reason, the present analysis focuses directly on overall appliance counts and usage patterns, thereby adapting the standard approach to the data available.

The results derived from this bottom-up method will later be compared (see Section 5.4) against those obtained through the top-down approach presented in Section 5.2.1. This comparison will help assess the consistency of both methods and provide a more robust estimate of future electricity demand.

5.2.2.2 Appliance Ownership and Assumptions

Based on the assessment of appliance ownership in Antanamalaza (see Section 4.4), the following appliances were identified: radios, televisions, VCRs, sewing machines, computers, internet modems, air conditioners, landline phones, mobile phones, and electric lighting.

Table 4.9 provides the percentage of households that own each appliance. However, the dataset does not specify how many units of each appliance are owned per household. Among all appliances, mobile phones are considered the most likely to be present in multiple units, given their high ownership rate. Radios, although the second most common, are more easily shared within a household, making multiple ownership less likely. All

other appliances are found in less than 5% of households, suggesting that the marginal impact of multiple ownership is negligible.

To account for possible multiple ownership of mobile phones, it is assumed that high-income households (7% of the total, see Table 4.5) own two phones, while all other connected households own one. Given that 43% of households are expected to connect to the grid and own at least one phone (see Section 4.2.3), the resulting average number of phones per connected household is:

$$\frac{(0.07 \times 2) + (0.43 \times 1)}{0.50} = \frac{0.14 + 0.43}{0.50} = 1.14 \text{ phones per connected household}$$

Lighting is another component that may be present in multiple units per household. While not all lighting sources in the commune are electric (see Table 4.10), it is reasonable to expect that grid-powered lighting would progressively replace kerosene or candles if it proves cheaper . The main barrier is the upfront cost of purchasing lamps, which is unlikely to be met by the poorest households. Therefore, it is assumed that all but the 10% classified as very low-income will adopt electric lighting.

The distribution of households by number of rooms is presented in Table 4.6. Since these data are given as percentages from a survey, the calculation can be made directly in relative terms without resorting to absolute household counts. Assuming that all very low-income households are concentrated in one-room dwellings, the share of one-room connected households is reduced by 10 percentage points, while the distribution of multi-room households remains unchanged.

The average number of rooms per connected household is then obtained as a weighted average:

$$\bar{R} = \frac{(55.8 \times 1) + (28.2 \times 2) + (3.7 \times 3) + (2.0 \times 4) + (0.3 \times 5)}{90} \approx 1.48$$

where the denominator reflects the 90% of households assumed to adopt electric lighting.

Assuming one lighting point per room, the average number of electric lamps per connected household is therefore approximately 1.48. This value will serve as the basis for estimating total lighting energy demand.

These ownership and usage assumptions form the input for the demand calculation in the following subsection.

5.2.2.3 Appliance Specific Consumption

To estimate appliance-specific demand using a bottom-up approach, information on the typical power ratings and usage durations of devices is required. For this purpose, the

author relies on the "Energy Cheat Sheet" provided by the South African government [33]. Although the data originates from South Africa rather than Madagascar, appliance usage patterns and power ratings appear sufficiently consistent to justify its use in this context.

Device	Radio	TV	VCR	Sewing Machine	Computer
Ownership (%) (See Table 4.9)	30.20%	5.03%	3.02%	2.01%	0.34%
Typical Power (W) (Source: [33])	12–70	30–340	17–22	100	30–150
Utilisation (hours/day) (Source: [33])	3	6	4.7	0.4	4
Percentage at night (%)	20	80	100	10	50
Number per connected household	1	1	1	1	1

Table 5.4: Estimated consumption of rural electrical devices – Part 1

Device	Internet Modem	Air Conditioner	Landline Phone	Mobile Phone	Lighting
Ownership (%) (See Table 4.9)	2.01%	0.34%	4.03%	49.33%	90.00%
Typical Power (W) (Source: [33])	8–12	500–1440	2	5	5–10
Utilisation (hours/day) (Source: [33])	24	2.4	15	2	4–6
Percentage at night (%)	60	90	50	90	100
Number per connected household	1	1	1	1.14	1.48

Table 5.5: Estimated consumption of rural electrical devices – Part 2

Where a range of typical power values exists, both lower and upper bounds are used to compute energy demand, as detailed in the following section.

Regarding the proportion of appliance usage occurring at night, there is a lack of country-specific data to support a data-driven assumption. Consequently, a broad estimation is introduced. These figures are carried forward into the next step for completeness, but as explained later, only total daily demand will be retained in the final demand estimate.

5.2.2.4 Demand Calculation and Results

Although both total and night-only demand are calculated for completeness, only total daily consumption will be retained in the final demand estimate. Night-only figures are reported here as an intermediate step, to illustrate potential implications for battery sizing.

To estimate electricity demand across 901 households, two metrics were calculated for each appliance:

- **Total daily consumption**, using the formula:

$$E_{\text{total}} = N \times f \times q \times P \times t$$

- **Night-only consumption**, using the formula:

$$E_{\text{night}} = N \times f \times q \times P \times t \times r$$

Where:

- N is the total number of connected households (901),

- f is the ownership frequency of the appliance (in decimal),

- q is the number of units per connected household,

- P is the rated power (evaluated at both its lower and upper bound, in watts),

- t is the average daily use (in hours),

- r is the proportion of use that occurs at night.

Table 5.6 summarizes the lower and upper bounds for both total and nighttime energy use.

Device	Total (Wh) Low	Total (Wh) High	Night (Wh) Low	Night (Wh) High
Radio	9795.7	57141.4	1959.1	11428.3
TV	8157.7	92453.4	6526.1	73962.7
VCR	2174.1	2813.5	2174.1	2813.5
Sewing Machine	724.4	724.4	72.4	72.4
Computer	367.6	1838.0	183.8	919.0
Internet Modem	3477.1	5215.7	2086.3	3129.4
Air Conditioner	3676.1	10587.1	3308.5	9528.4
Landline Phone	1089.3	1089.3	544.7	544.7
Mobile Phone	5066.9	5066.9	4560.2	4560.2
Lighting	30003.3	60006.6	30003.3	60006.6
Total	**64532.2**	**236936.3**	**57418.5**	**166965.9**

Table 5.6: Estimated daily and night-only energy use per appliance across 901 households (in Wh)

As shown in Table 5.6, the difference between the lower and upper bound estimates is significant for many appliances. This variability arises primarily from the wide range of rated power values found in rural settings, where devices may vary greatly in efficiency, age, and design (e.g., older CRT televisions vs. newer LED models).

To obtain a single estimate for both daily and night-only electricity consumption, the arithmetic mean of the lower and upper bounds was taken for each appliance i:

$$E_{\text{avg},i} = \frac{E_{\text{low},i} + E_{\text{high},i}}{2}$$

The community-wide average demand is then obtained by summing across all appliances:

$$E_{\text{total, avg}} = \sum_{i=1}^{n} E_{\text{avg},i} \quad \text{and} \quad E_{\text{night, avg}} = \sum_{i=1}^{n} \frac{E_{\text{night, low},i} + E_{\text{night, high},i}}{2}$$

Numerically, this yields:

$$E_{\text{total, avg}} = \frac{64{,}532.2 \text{ Wh} + 236{,}936.3 \text{ Wh}}{2} = 150{,}734.2 \text{ Wh/day}$$

$$E_{\text{night, avg}} = \frac{57{,}418.5 \text{ Wh} + 166{,}965.9 \text{ Wh}}{2} = 112{,}191.9 \text{ Wh/night}$$

These values correspond to a scenario where 90% of all households in Antanamalaza are connected to the grid, representing a total of 811 households. Among these, 366 are expected to connect solely for lighting purposes. This corresponds to a community-wide demand of roughly 151 kWh per day, or 0.19 kWh per household per day, which lies within the expected range for rural electrification projects, as detailed next.

5.2.2.5 Benchmarking Against Other Microgrids

Although the estimated demand for Antanamalaza may appear low, it is consistent with consumption levels observed in other rural microgrids, as discussed in Chapter 3. Not all of the projects reviewed in that chapter provide directly comparable measured data: some report only projections, while others present real consumption figures (see Section 3.4). In addition, certain measurements were taken from systems experiencing operational difficulties, which likely depressed electricity usage (see Section 3.2).

Nevertheless, three microgrids with measured data are available for comparison, drawing from two independent sources.

In Section 3.1.3, we reported on a functioning DC microgrid in Madagascar. As shown in Table 3.1, the average daily household demand rose sharply from 0.08 kWh/(day·hh) in 2018 to 0.50 kWh/(day·hh) in 2021. The authors of [10] attributed this increase to the progressive adoption of DC-compatible appliances. Since Antanamalaza's system will be AC-based, and users already own AC appliances, the 2021 value of 0.50 kWh/(day·hh) is the most relevant comparison.

In Section 3.3, we reviewed data from two rural sites in Tanzania. Average household consumption was reported at 0.104 kWh/(day·hh) for a site with 358 households, and 0.089 kWh/(day·hh) for a site with 135 households.

The estimated values for Antanamalaza (0.19 kWh/(day·hh)) are of the same order of magnitude as those observed in Tanzania, although roughly twice as high. In contrast, they are about half the level measured in the Madagascan village of Ambohimena in 2021. These comparisons suggest that the Antanamalaza estimates are plausible, while also highlighting the strong influence of local factors on household demand. As such, benchmarking supports the credibility of the estimates, even though it cannot validate them with certainty.

5.3 Estimating Services and Industry Demand

Based on information obtained through the director's contact with individuals familiar with the area, the main businesses and services present in Antanamalaza are known. These include: three wood workshops, three rice workshops for processing paddy into white or brown rice, one CSB II health center, one repair shop, three schools, two churches, one small SIM card shop, and one small commercial bank shop.

Among these, only the rice and wood workshops are expected to contribute significantly to overall electricity demand, since they rely on motor-driven equipment with sustained power draw. The remaining establishments, such as schools, churches, and small commercial services, are assumed to rely primarily on lighting and therefore exhibit relatively low electricity consumption. Each category is assessed in the following subsections.

5.3.1 Rice Workshops Electricity Consumption

The operational assumptions for rice processing workshops applied in this work are not defined by the author but follow those presented in [10], which are representative of small-scale rural rice milling facilities in Madagascar. According to this reference, rice milling equipment operates at a constant power of $1100\,\text{W}$, with a fixed daily schedule that varies by month: two hours per day in December, January, April, and August; one hour per day in February, March, September, October, and November; and eight hours per day in May, June, and July. When the daily operation exceeds three hours, a fixed midday break from 11:00 a.m. to 2:00 p.m. is assumed.

These patterns align with observations reported in other microgrids (see Section 3.1.9), where productive equipment such as rice hullers exhibit pronounced seasonal variability. For example, in Ambohimena, operation peaks during the harvest months (June to August) and reaches its lowest levels during the rainy season (December to March), following similar temporal trends to those assumed here.

The resulting yearly electricity consumption for a rice workshop is shown in Figure 5.2, amounting to approximately $2.0\,\text{MWh}$ per workshop annually. With three such facilities in Antanamalaza, the aggregate consumption reaches roughly $6.0\,\text{MWh/year}$, making rice processing one of the largest non-household loads in the village.
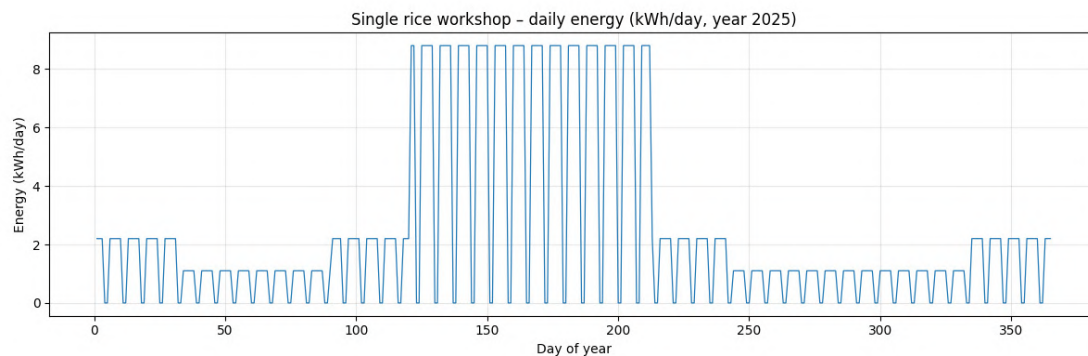
Figure 5.2: Yearly consumption of a rice workshop, based on the operational hypotheses from [10].

5.3.2 Wood Workshops Electricity Consumption

According to [34], a typical carpentry business in Africa consumes approximately $18\,\text{kWh}$ per month. Unlike rice workshops, carpentry tools are not operated continuously. Instead of assuming a constant low-power load, it is assumed that each workshop operates a single tool in a binary mode (fully on or fully off), active only during half of business hours. Activation periods are distributed randomly and independently across workshops, and the model is calibrated to reproduce the reported mean monthly consumption of $18\,\text{kWh}$ per business.

Business hours are assumed to span from 6:00 a.m. to 6:00 p.m., consistent with the rice workshop schedule. The simulated electricity consumption for one week is presented in Figure 5.3, where days 3 and 4 correspond to the weekend (as labeled by the `datetime` module). The resulting pattern displays the expected randomness, with sporadic peaks and idle periods. A maximum daily load of approximately $340\,\text{Wh}$ is observed, corresponding to the rare event in which all three carpentry workshops operate simultaneously.

Overall, the annual electricity consumption of a carpentry workshop ($216\,\text{kWh}$) is modest compared to that of a rice workshop ($2000\,\text{kWh}$). Nevertheless, the stochastic behavior of these loads adds variability to the aggregate demand profile.
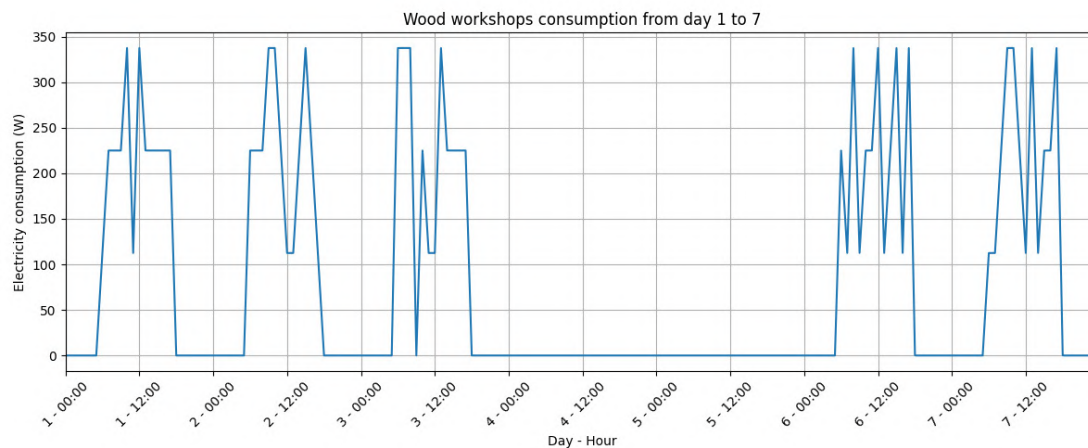
Figure 5.3: Estimated weekly consumption of the three wood workshops.

5.3.3 Miscellaneous Business Electricity Consumption

The electricity consumption of non-intensive businesses is presented in Figure 5.4, where days 3 and 4 correspond to the weekend. With the exception of the CSB II, which also includes a vaccine refrigerator, these establishments are assumed to rely exclusively on lighting. The following assumptions are adopted: the CSB II is equipped with three

lights and one refrigerator; each school has eight lights, a figure consistent with the reported 2.44 classrooms per school in 2013 according to CREAM [21]; each church contains four lights; and each of the two small shops is equipped with a single light.

All lights are assumed to consume 10 W and to operate from 6:00 a.m. to 6:00 p.m.. This corresponds to the upper end of the range reported in [33], since these institutions are expected to use more powerful fixtures than households. Although this assumption likely overestimates lighting demand, it accounts for the possibility that some buildings may be poorly lit and therefore require daytime lighting.

The vaccine refrigerator in the CSB II is assumed to consume power comparable to that of a household refrigerator. Although medical refrigerators could be more efficient, detailed specifications were unavailable. Following [35], the compressor is considered to consume 50 W when active, operating in cycles of 20 minutes on followed by 8 minutes off. This assumption provides a conservative estimate that may slightly overstate real consumption.
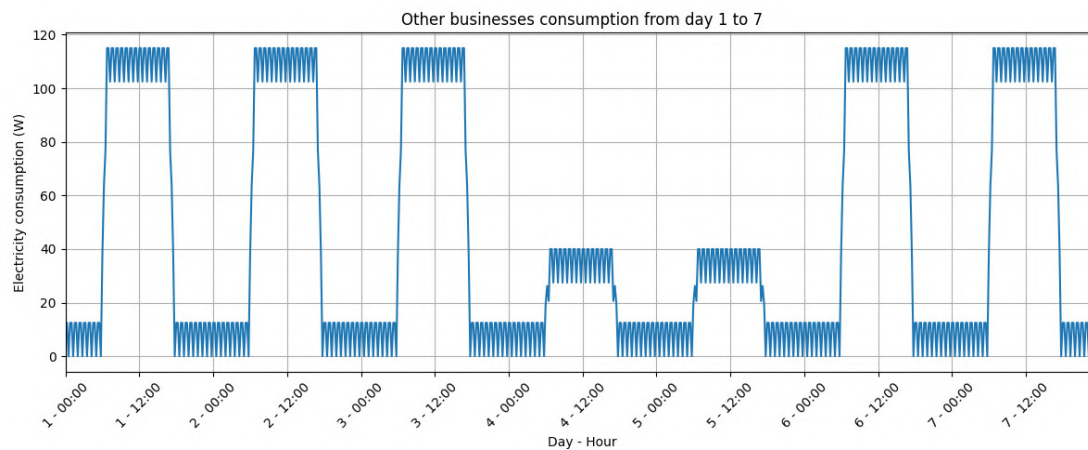
Figure 5.4: Estimated weekly consumption of the non-electric intensive businesses.

5.3.4 Synthesis of Productive and Service Loads

Taken together, these productive and service loads represent a relatively small fraction of total village demand compared to household consumption. However, their seasonal concentration (rice milling) and stochastic variability (wood workshops) mean that they play a role in determining system adequacy and in shaping the design requirements for storage and generation capacity.

Moreover, it is essential to account for productive industries, since they have the potential to drive local economic development. By enabling higher-value activities such as rice processing and carpentry, reliable electricity access can directly enhance income

generation, employment opportunities, and ultimately contribute to making the entire village more prosperous.

5.4   Total Estimated Electricity Demand

The estimated residential consumption of 151 kWh/day derived from the bottom-up method (see Section 5.2.2) is broadly consistent with the value obtained through the top-down approach (see Section 5.2.1), which yields 194 kWh/day. The top-down estimate exceeds the bottom-up result by approximately 28.5%. This discrepancy may stem from the inherent uncertainties in both methods, but it could also reflect the fact that the bottom-up approach does not capture the surge in electricity use that often accompanies initial electrification, as households gradually acquire new appliances. As discussed in Section 5.2.2.5, the resulting per-household consumption (0.19–0.24 kWh/day) falls within the same order of magnitude as other rural microgrids in Madagascar and Tanzania, supporting the plausibility of the estimates. For this reason, and to avoid underestimation, the top-down estimate is retained as the basis for household demand calculations in this study.

For businesses and services, demand growth is modeled using the same 2% annual increase as for households (see Section 5.2.1).
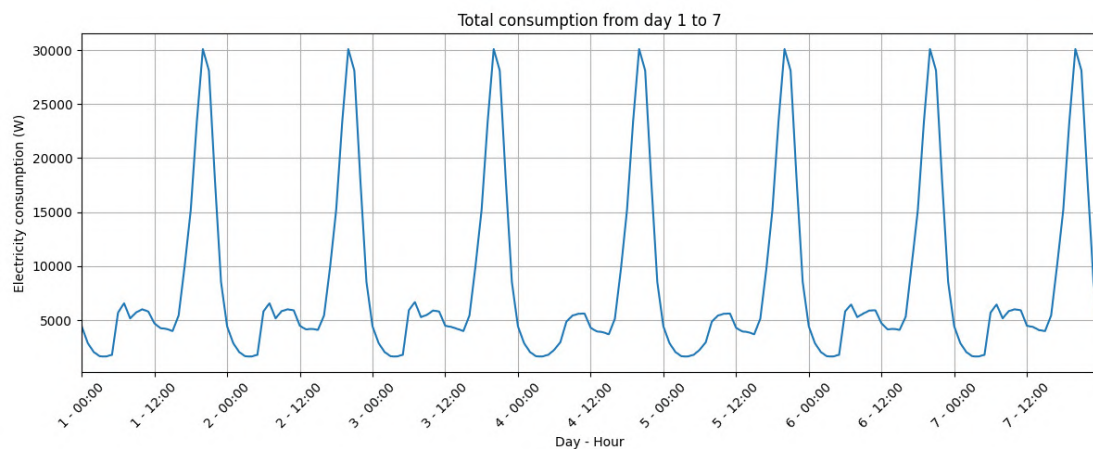
Figure 5.5: Estimated electricity consumption during one week in January.
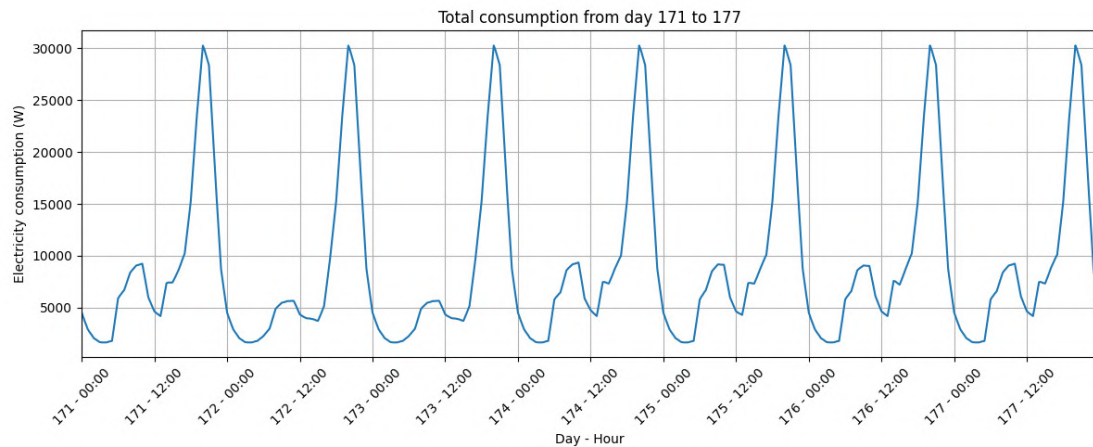
Figure 5.6: Estimated electricity consumption during one week in June.

Figure 5.5 illustrates the electricity consumption over a single week in January 2025. A clear daily pattern emerges, reflecting the dominance of household demand. The regular peaks and troughs correspond to residential activity cycles, with little variation between weekdays and weekends. This suggests that, in this period, business operations contribute minimally to the aggregate profile. By contrast, in June (Figure 5.6), the effect of productive activities is more visible, though still modest compared to the prominent evening household peak.
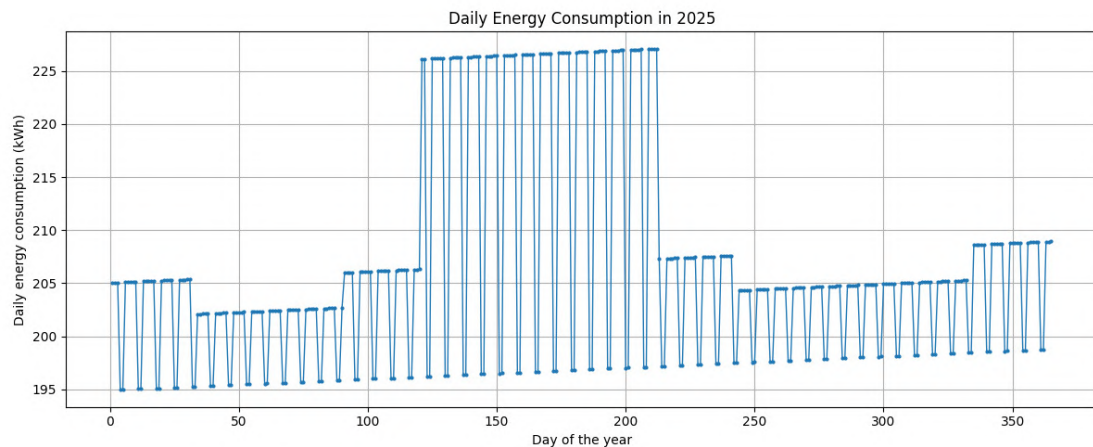
Figure 5.7: Electricity consumption for the year 2025.

At the annual scale (Figure 5.7), longer-term variations become evident. Seasonal increases in industrial activity, particularly rice processing, drive notable rises in demand during specific months. Weekday–weekend contrasts also appear, with reduced loads on

weekends when workshops and services are largely inactive. The 2% annual growth assumption was implemented continuously, resulting in a smooth exponential trajectory rather than discrete year-on-year steps.
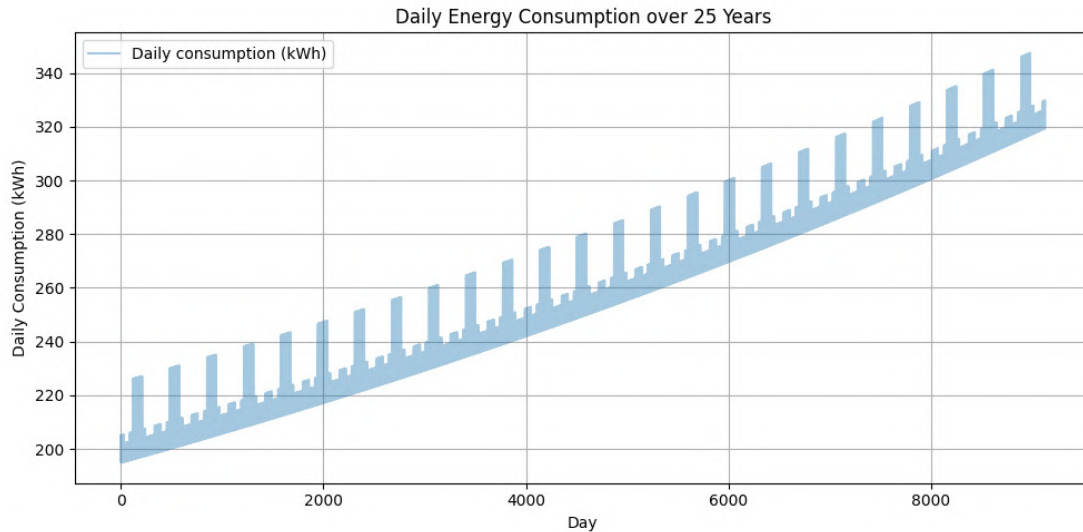
Figure 5.8: Daily electricity consumption over 25 years.

Finally, Figure 5.8 shows the evolution of daily electricity consumption over a 25-year horizon. With a sustained 2% annual growth rate, total demand increases by a factor of approximately 1.64. This upward trajectory highlights the compounding effect of incremental growth, underscoring the need to size the system with sufficient headroom for long-term expansion.

Designing a suitable energy system must therefore account not only for present requirements but also for the dynamics of future demand. The next chapter lays the groundwork by defining the technical components to be deployed in Antanamalaza, while the subsequent chapter addresses the dimensioning of these components to ensure that the evolving load can be met reliably under local climatic and operational conditions.

Chapter 6

System Architecture and Components

This chapter presents the selection and justification of the elements that define the proposed microgrid in Antanamalaza. The objective is to establish realistic technical, economic, and environmental parameters that will serve as inputs for the dimensioning and optimisation study in the following chapter. The analysis begins with the rationale for the distribution architecture and continues with the main system components: inverters, photovoltaic modules, batteries, and a backup diesel generator. Each element is examined in terms of local availability, cost, technical performance, and life-cycle considerations.

6.1 System Configuration and Rationale

Before analysing the individual components of the microgrid, it is necessary to define the overall distribution architecture that will structure the system.

The proposed microgrid will use a three-phase alternating current (AC) distribution system. This choice reflects both the geographical characteristics of the site and the expected types of electrical loads. As noted in [34], direct current (DC) distribution becomes unsuitable for distances exceeding 200 meters due to transmission losses and voltage drops. In Antanamalaza, the settlement extends over approximately 1.3 kilometers along its longest axis (see Section 4.2.3), surpassing the recommended threshold for DC by more than a factor of six.

While single-phase supply may suffice for purely residential loads, a three-phase configuration is preferred in anticipation of productive electricity uses. Medium- and high-power industrial motors, which dominate such applications, are generally three-phase. According to [34], these motors are readily available in Madagascar, facilitating procurement and maintenance. Although three-phase infrastructure increases upfront investment by an estimated 5-20%, it provides important advantages in robustness, scalability, and industrial compatibility.

Finally, adopting 230 V and 50 Hz operation ensures full alignment with Madagascar's national electrical standards [36], guaranteeing compatibility with locally available equipment and simplifying future integration.

With the distribution architecture defined, the following sections examine the selection of individual components.

6.2 Main Components of the System

With the distribution architecture defined, the focus now shifts to the main components that will supply and regulate electricity within the microgrid. The system is designed to rely primarily on photovoltaic (PV) generation, supported by battery storage and managed through inverters. A diesel generator is also considered as a backup option to provide resilience during peak demand periods or extended episodes of low solar irradiation.

The overall configuration is illustrated in Figure 6.1. Multiple inverters can be connected in parallel, each linked to a dedicated PV array and interfaced with the battery storage system. In this arrangement, the inverter typically integrates maximum power point tracking (MPPT) and charge-controller functions. The generator, while not central to the system, is shown as a complementary source of supply for contingency scenarios.

It should be noted that the layout in Figure 6.1 is intended to illustrate functional relationships rather than final dimensions. The equipment sizes shown do not correspond to the capacities that will ultimately be installed in Antanamalaza. Precise sizing of photovoltaic capacity, storage, and backup generation will be determined in the optimisation study presented in the following chapter.

Although not represented in the diagram, adequate protection systems (circuit breakers, fuses, surge protection devices) are indispensable to guarantee safety, reliability, and compliance with electrical standards.

The following subsections examine each major component in detail: inverter, photovoltaic modules, batteries, and the backup generator. For each, technical characteristics, local availability, costs, and life-cycle impacts are reviewed, providing the baseline parameters for the optimisation analysis.
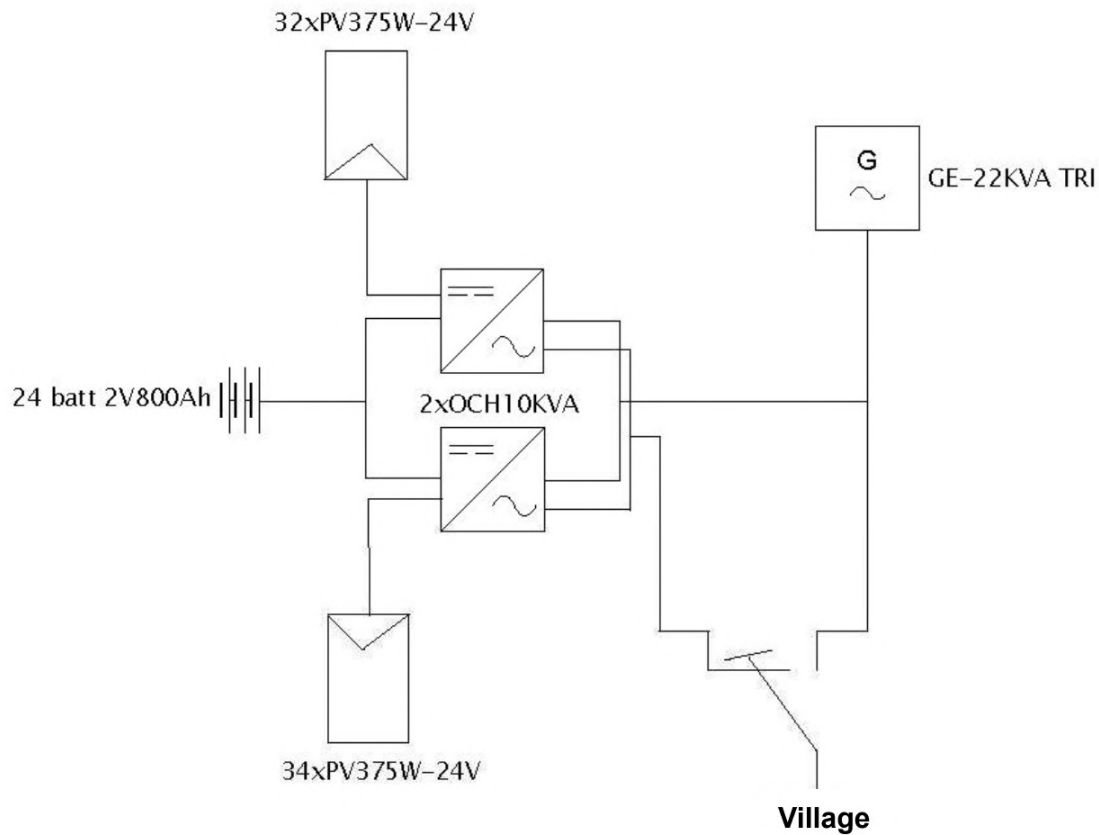
Figure 6.1: Electrical diagram of an isolated PV–battery–generator microgrid. Source: [37]

6.2.1 Inverter

The inverter is a central element of the microgrid, as it sets key technical constraints on the sizing and compatibility of other components such as photovoltaic modules, batteries, and backup generators. Most commercial inverters designed for microgrids integrate maximum power point tracking (MPPT) and charge-controller functions, thereby eliminating the need for separate control devices.

Whenever possible, procuring inverters locally is recommended in order to ensure compliance with grid standards and to facilitate future maintenance. According to the ENF Solar directory [38], several companies active in Madagascar offer microgrid solutions. The brands most frequently represented were Victron Energy (listed by three companies), SMA (two companies), and Fronius (one company). In addition, four companies offered inverters under proprietary branding, which likely correspond to rebranded products or local assembly.

Among the available listings, only one supplier published a retail price: a 5 kW Victron Energy inverter (model 48/5000), shown in Figure 6.2, offered at 9,260,665 Ar [39]. Using the mid-market exchange rate of 27 July 2025 (1 MGA = 0.00019295 €), this corresponds to approximately 1,787 €.

Figure 6.2: Victron Energy 48/5000 inverter. Source: [39]

While this quotation provides a useful reference, more competitive prices could likely be obtained either through negotiation or by comparing multiple suppliers. However, for the demand levels projected in this study, an inverter with higher capacity is required.

An alternative procurement option would be to purchase equipment abroad and import it into Madagascar. For example, a 20 kW inverter was identified at a price of 1800 € including European VAT [40]. Nevertheless, such equipment would be subject to an additional 20% VAT on import, as indicated in [41], unless a specific exemption were obtained. This reduces the cost advantage of international sourcing.

In parallel, a quotation was obtained from Solar Technologies, one of the companies listed in the ENF Solar directory [38]. The company proposed a 10 kW all-in-one inverter with integrated charge controller and dual MPPT, priced at 4600 €. The unit is presented in Figure 6.3.

Figure 6.3: Solar Technologies 48/10000 inverter. Source: [42]

The main technical and environmental specifications of this model are summarised in Table 6.1.

Specification	Value
Phases	3-phase
Nominal power	10,000 VA
Max input current	40 A
Frequency range	50 Hz / 60 Hz
Transfer time	10 ms
Waveform	Pure sine wave
Max DC-to-AC efficiency	91%
Nominal / Max DC voltage	720 V / 900 V
MPPT voltage range	400 V – 800 V
Max solar charging current	2×18.6 A
Max charging current	10 A – 200 A
Estimated lifetime	>10 years [43]

Table 6.1: Technical specifications of the Solar Technologies 48/10000 inverter. Source: [42], unless otherwise indicated

For the remainder of this work, the 10 kW Solar Technologies inverter is considered as the reference configuration, due to its higher nominal power, integrated control fea-

tures, and confirmed local availability. With the inverter defined, attention now turns to the generation technology, namely the photovoltaic modules.

6.2.2 Solar Panels

PV modules define the generation potential of the microgrid and directly affect both energy yield and project economics. For this study, the Amerisolar AS-7M 144-HC was chosen. This module was selected primarily because it was the only PV product with a listed retail price identified in Madagascar (two separate units), therefore providing a transparent and verifiable basis for cost estimation. In addition, it exhibits all the usual technical characteristics of modern modules, meaning there was no reason to discard it in favour of alternatives. The Amerisolar AS-7M 144-HC is a monocrystalline PERC half-cell module with a rated output of 550 W and a conversion efficiency of 21.28% [44]. Under standard test conditions (STC), it operates at 41.8 V and 13.16 A. The module dimensions are 2279 mm × 1134 mm, and its weight is 29 kg. The main specifications are summarised in Table 6.2. A figure of the model available in Madagascar is shown in Figure 6.4.

Parameter	Value
Technology	Monocrystalline PERC, half-cell
Rated power (P_{max})	550 W
Module efficiency	21.28%
Voltage at P_{max}	41.8 V
Current at P_{max}	13.16 A
Dimensions	2279 × 1134 mm
Weight	29 kg
Standards	IEC 61215, IEC 61730
Unit price (local)	Ar 952,000
Approx. price per W	0.353 €/W

Table 6.2: Main specifications of the selected solar panel (Amerisolar AS-7M 144-HC). Data from [44].
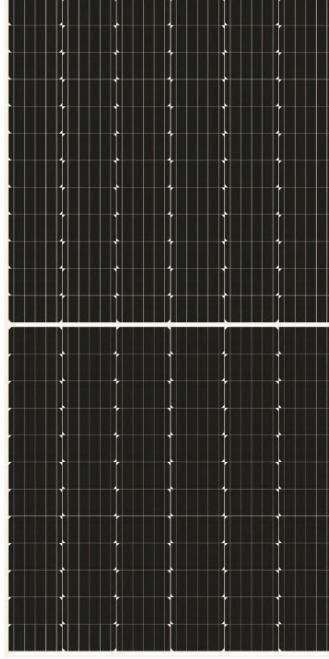
Figure 6.4: Photograph of the 550 W panel. Source: Gaia Madagascar [44]

The local unit cost corresponds to approximately 0.353 €/W. This value is significantly higher than international benchmarks. According to [45], Tier 1 solar module prices in 2025 are expected to range between 0.14 and 0.15 USD/W, equivalent to 0.13–0.14 €/W. Tier 1 refers to manufacturers recognised by BloombergNEF for strong financial performance and reliable delivery to large-scale, bank-financed projects. The elevated local price in Madagascar can be explained by the limited market size, transport costs, import duties, and distribution margins.

A second quotation was obtained from the supplier that also provided the Victron inverter (Figure 6.2), listed in the ENF Solar directory [38]. This offer included a 550 W panel priced at 236 € including taxes, corresponding to 0.429 €/W. Technical specifications are comparable to those of the Amerisolar panel. For consistency, the Amerisolar module is adopted for the system design and economic modelling.

The performance parameters of the selected panel are essential for the energy production estimates presented later in this work. The nominal cell temperature is $T_n = 25\,°\mathrm{C}$, under standard irradiance $G_n = 1000\,\mathrm{W/m^2}$. The temperature coefficient of power is $\gamma = -0.36\,\%/°\mathrm{C}$, and the nominal operating cell temperature is NOCT $= 43\,°\mathrm{C}$. In addition, the manufacturer specifies a linear annual degradation rate of $0.67\,\%$, guaranteeing at least $80\,\%$ of the initial output after 30 years. The values used in this study are shown in Table 6.3. The initial value of $97.5\,\%$ reflects the standard one-year warranty drop before linear degradation begins.

Year	Performance (%)	Year	Performance (%)
0	97.50	16	88.48
1	97.50	17	87.88
2	96.90	18	87.27
3	96.30	19	86.67
4	95.69	20	86.07
5	95.09	21	85.47
6	94.49	22	84.87
7	93.89	23	84.27
8	93.29	24	83.67
9	92.69	25	83.06
10	92.09	26	82.46
11	91.48	27	81.86
12	90.88	28	81.26
13	90.28	29	80.66
14	89.68	30	80.00
15	89.08		

Table 6.3: Warranted PV performance by year, based on the linear degradation warranty from Amerisolar [44]. Values represent the minimum guaranteed output relative to the initial rated power.

The environmental footprint of photovoltaic modules has been assessed in [46], showing that emissions depend strongly on the electricity mix used during manufacturing. Panels produced in coal-intensive grids, such as in China, reach approximately 810 kg CO_2-eq/kWp, while those manufactured in Germany or other EU countries average between 480 and 580 kg CO_2-eq/kWp. Module design also has an effect: glass–glass configurations typically exhibit higher embodied emissions but benefit from reduced degradation and longer lifetimes, lowering their normalised impact per kWh. Transport contributes only marginally to the overall footprint.

Amerisolar operates manufacturing facilities in several countries. For the purposes of this study, production in China is assumed, as it represents the largest global hub for solar panel manufacturing and is therefore considered most representative. Accordingly, embodied emissions of 810 kg CO_2-eq/kWp are adopted for the environmental assessment of the selected panels.

Having defined the generation technology, the next subsection turns to battery storage, the key element that determines the reliability of supply.

6.2.3 Batteries

The choice of battery technology plays a decisive role in determining both the cost and reliability of an off-grid solar microgrid. Unlike inverters or PV modules, batteries differ significantly in usable capacity, cycle life, maintenance requirements, and cost per kWh delivered. In rural contexts such as Madagascar, where technical support is scarce, minimising operational complexity is a central priority.

6.2.3.1 Technology selection and specifications

A comparative study by Ruiz et al. [47] assessed lead-acid and lithium-ion batteries in PV-based microgrids under realistic operating conditions. The authors found that lithium-ion batteries reduced the levelised cost of electricity (LCOE) by about 5% compared to lead-acid systems (0.32 vs. 0.34 €/kWh), while requiring 40% fewer replacements over the project lifetime. These findings underscore the economic and logistical advantages of lithium-ion storage, particularly in remote installations. Based on this evidence, lithium iron phosphate ($LiFePO_4$) batteries are adopted as the reference technology for Antanamalaza, offering a favourable balance between upfront cost, durability, and ease of operation.

As highlighted by Singh et al. [48], $LiFePO_4$ batteries are particularly well-suited for rural and remote grid-scale applications. Their advantages include a strong safety profile, long cycle life, and minimal maintenance requirements. Although $LiFePO_4$ batteries have a lower energy density than LCO or LMO chemistries, they offer superior thermal stability, a much lower risk of thermal runaway, and gradual capacity fading. These characteristics make them a robust choice for isolated rural microgrids, where reliability and safety are more important than volumetric density.

During the market review in Madagascar, no $LiFePO_4$ batteries of sufficient capacity were found with publicly listed local retail prices. To ensure transparent and reproducible costing, a specific manufacturer is therefore selected for reference and pricing purposes. Among commercially available $LiFePO_4$ options, the 48 V 200 Ah (10.24 kWh) Powerwall model from GSL Energy is adopted as a reference (see Figure 6.5). This manufacturer provides direct sales through international platforms with clear, publicly available pricing, which facilitates cost estimation and procurement planning. Because the unit would be imported, the delivered price in Madagascar is expected to exceed the factory price due to shipping and import duties; a detailed estimate of these surcharges is therefore developed in the next subsection. The final installed storage capacity will be determined in the system sizing chapter (Chapter 7).

Figure 6.5: Photograph of the selected battery. Source: GSL Energy [49]

Once the technology has been selected, the next step is to estimate the delivered cost and assess its environmental footprint.

6.2.3.2 Cost and environmental performance

To estimate the delivered cost of the GSL 48 V 200 Ah LiFePO$_4$ battery in Madagascar, we begin with the listed price of 1,197.07 USD. Using the EUR/USD exchange rate on August 5, 2025 (1 EUR = 1.097 USD), this corresponds to 1091.00 e. The product dimensions are $800 \times 550 \times 200$ mm, giving a volume of about 0.088 m^3.

Transport costs are estimated from a less-than-container load (LCL) shipping rate of 110 USD/m^3 in [50], equivalent to 100.21 e/m^3. This results in a shipping cost per unit of:

$$C_{\text{shipping}} = 100.21 \times 0.088 \approx 8.82\,\text{e} \tag{6.1}$$

It should be noted that the actual shipping cost of a single unit may be higher, since freight forwarders often apply minimum charges based on size or weight. However, as batteries will be purchased in batches, the unit shipping cost remains reasonable when shipping without filling a full container.

Madagascar applies an average MFN import duty of 11.4% on electrical machinery, including lithium-ion batteries [51]. In addition, a 20% VAT is applied to the cumulative value of product and duty [52]. The final delivered cost is therefore:

$$
\begin{aligned}
C_{\text{FOB}} &= 1091.00\,\text{e} \\
C_{\text{duty}} &= 0.114 \times (1091.00 + 8.82) \approx 125.23\,\text{e} \\
C_{\text{VAT}} &= 0.20 \times (1091.00 + 8.82 + 125.23) \approx 245.41\,\text{e} \\
C_{\text{final}} &= 1091.00 + 8.82 + 125.23 + 245.41 \approx \boxed{1470.46\,\text{e}}
\end{aligned}
\tag{6.2}
$$

Thus, the estimated delivered cost of a single unit is approximately $1470\,\text{e}$, including shipping, import duties, and VAT. This value is used as the reference cost basis for subsequent economic calculations.

In addition to cost, environmental performance is an important consideration. The ecological impact of batteries is generally quantified through their life-cycle greenhouse gas (GHG) emissions, expressed in $\text{kg.CO}_2-\text{eq/kWh}$ of storage capacity. This indicator accounts for raw material extraction, manufacturing processes, transport, and—in some cases—end-of-life treatment. For lithium iron phosphate (LiFePO_4) batteries, recent analyses highlight comparatively low values relative to other chemistries. Peiseler et al. [53] report a range of $54\,\text{kg.CO}_2-\text{eq/kWh}$ to $69\,\text{kg.CO}_2-\text{eq/kWh}$, while Lin et al. [54] estimate $90.8\,\text{kg.CO}_2-\text{eq/kWh}$ without accounting for recycling. For a 10.24 kWh battery, these values correspond to a total impact between $540\,\text{kg.CO}_2-\text{eq}$ to $908\,\text{kg.CO}_2-\text{eq}$.

Parameter	Value
Battery model	GSL Energy Powerwall
Battery chemistry	LiFePO_4
Nominal capacity	$200\,\text{A h}$
Nominal voltage	$48\,\text{V}$
Nominal energy	$10.24\,\text{kW h}$
Cycle life	>6500 cycles at 80% DoD
Maintenance requirement	Minimal
Unit price (excl. delivery)	$1091.00\,\text{e}$
Shipping volume	$0.088\,\text{m}^3$
Shipping cost (LCL)	$8.82\,\text{e}$
Import duty (11.4%)	$125.23\,\text{e}$
VAT (20%)	$245.41\,\text{e}$
Delivered cost	$1470.46\,\text{e}$
Cost per Wh (delivered)	$0.147\,\text{e/Wh}$
GHG emissions	$540\,\text{kg.CO}_2-\text{eq}$ to $908\,\text{kg.CO}_2-\text{eq}$

Table 6.4: Technical, economic, and environmental specifications of the selected LiFePO_4 battery. Based on [49, 50, 51, 52, 53, 54].

Beyond upfront costs and environmental impact, the useful service life of the battery determines replacement schedules and long-term economics.

6.2.3.3 Lifetime and degradation

According to manufacturer specifications (Table 6.4), the battery is rated for about 6500 cycles under controlled test conditions: 80% depth of discharge (DoD), charge/discharge rates of $0.5C/1C$, nominal temperature of $25\,°C$, and operation within voltage limits. Here, a rate of $1C$ corresponds to charging or discharging the full nominal capacity in one hour, while $0.5C$ indicates a two-hour process. The integrated battery management system (BMS) ensures compliance with these parameters during testing. In practice, however, real-world performance is influenced by fluctuations in DoD, C-rates, and ambient temperature.

Published Cycles–DoD curves reveal substantial variation across studies. Cheng et al. [55] report only $\sim$1000 cycles at 80% DoD (Figure 6.6), whereas PowerTech [56] suggests about 4500 cycles (Figure 6.7). Alattar et al. [57] indicate an intermediate value of around 2200 cycles (Figure 6.8). Taken together, these results show that lifetime estimates vary by more than a factor of four depending on the specific cell chemistry, quality, and test protocol, underscoring the uncertainty of predicting service life without model-specific data.
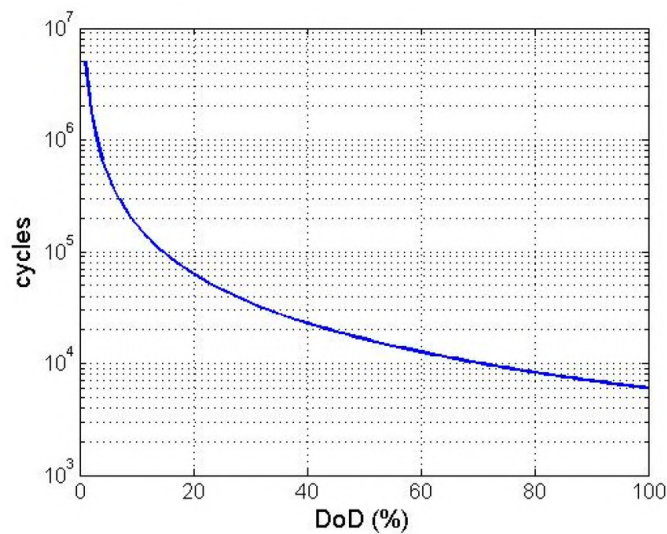
Figure 6.6: Cycles vs. DoD for LiFePO$_4$ batteries. Source: [55]
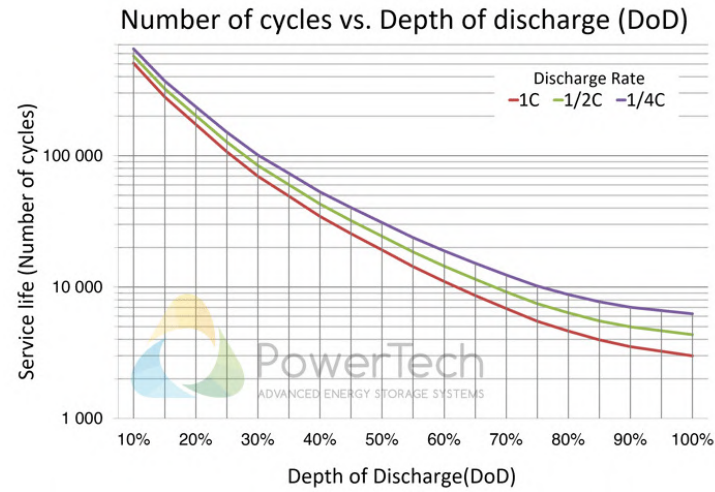
Figure 6.7: Cycles vs. DoD for LiFePO$_4$ batteries. Source: [56]
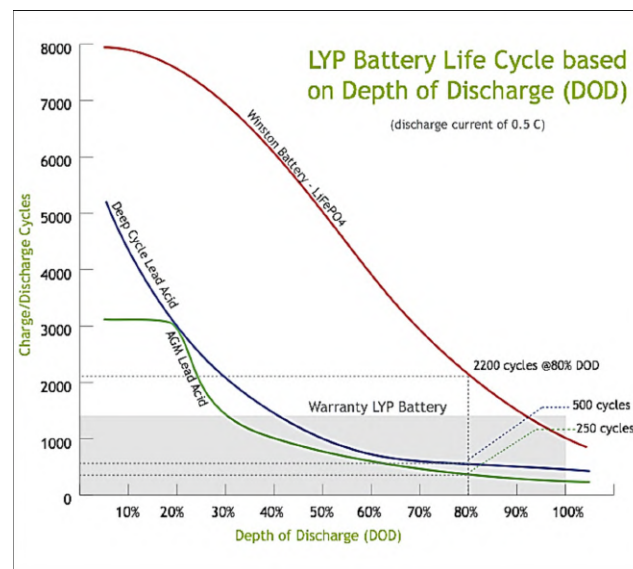
Figure 6.8: Cycles vs. DoD for LiFePO$_4$ batteries. Source: [57]

Vinci et al. [58] estimate a first-life duration of about 15 years at 80% DoD, corresponding to roughly 5475 cycles. For the Antanamalaza project, where the microgrid is expected to cycle daily at slightly lower DoD, a 15-year planning horizon is adopted. It should nevertheless be emphasised that actual performance will depend on temperature, DoD patterns, calendar ageing, and the quality of the BMS.

In addition, lithium-ion batteries of different ages should not be directly paralleled. Differences in internal resistance and capacity between aged and new cells lead to un-

even current sharing during operation. Weng et al. [59] show that aged cells, typically exhibiting higher resistance, provide less current during discharge, forcing newer cells to handle a disproportionate load. This imbalance reduces overall efficiency and accelerates the degradation of the new cells, thereby shortening the effective capacity of the entire bank. For this reason, unless cells are carefully matched or reconditioned, full replacement of the battery bank at year 15 is assumed. In practice, however, periodic state-of-health (SOH) assessments should guide replacement timing more precisely.

6.2.4 Generator

In parallel with the PV–battery system, some simulations will explicitly incorporate a diesel generator as part of the microgrid architecture. Although not renewable, diesel generation remains a common solution for rural electrification in Madagascar due to its reliability and immediate availability. Integrating a generator can significantly reduce the required capacities of PV modules and batteries, thereby lowering upfront investment costs. At the same time, however, reliance on diesel introduces recurrent fuel expenditures and greenhouse gas emissions. For this reason, generator-based configurations are analysed alongside fully renewable alternatives, allowing a systematic comparison of their technical, economic, and environmental performance.

6.2.4.1 Sizing considerations

The first step is to define the required generator size. Figures 6.9 and 6.10 present the average daily load profile for the first year of dimensioning (2025) and the final year (2049). The general shape of the profile remains similar over time, but the magnitude increases. In 2025, peak demand reaches 30 kW, while by 2049 it rises to approximately 50 kW. Relative to the base load, the additional capacity needed corresponds to about 25 kW in 2025 and 40 kW in 2049.
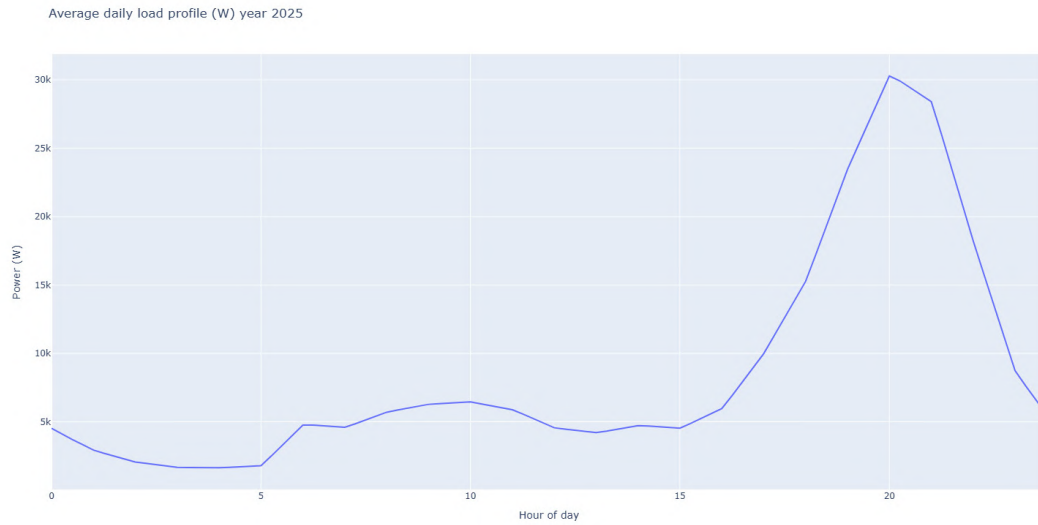
Figure 6.9: Average daily load profile in 2025
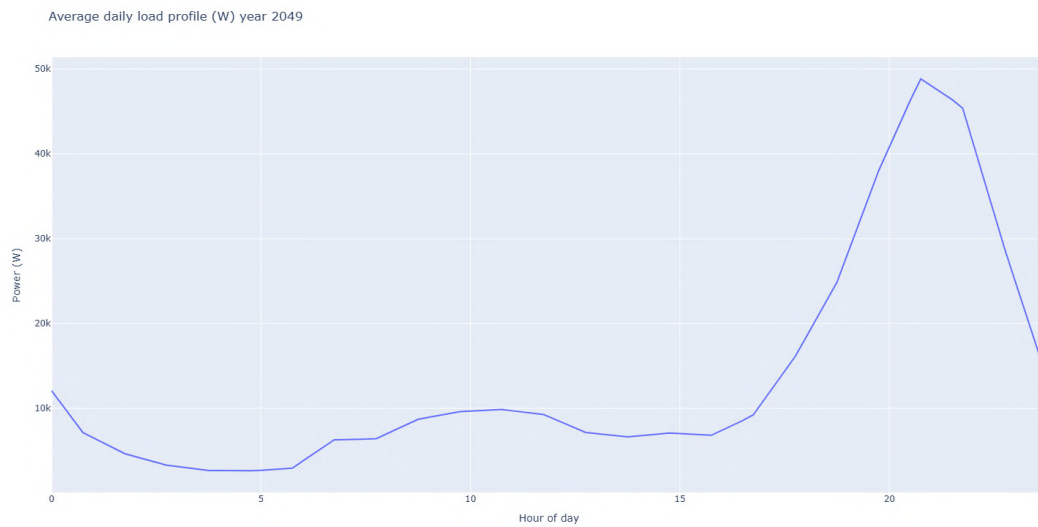
Figure 6.10: Average daily load profile in 2049

A generator in the 25-40 kW range is therefore considered adequate. With such a rating, PV and batteries still cover a significant share of the demand. By contrast, a 50 kW generator would be sufficient to meet the entire load, eliminating the need for renewable generation or storage.

For on-site generation needs, a Greaves 50 kVA diesel generator has been selected as

reference equipment. The main rationale is its availability in Madagascar, which reduces logistical and supply chain risks. The generator's rated capacity of 50 kVA corresponds to a real power of approximately 40 kW, assuming a typical power factor of 0.8. In practice, diesel generators should not be operated continuously at full rated power. A maximum recommended load of 80% is generally applied to ensure efficiency and longevity, which corresponds here to about 32 kW. This range fits well with the project's expected demand. The selected generator is shown in Figure 6.11.

Figure 6.11: Greaves 50 kVA diesel generator. Source: [60]

6.2.4.2   Economic and operational aspects

Manufacturer specifications for the Greaves 50 kVA generator indicate the following diesel consumption levels:

Load	Consumption (L/h)
100%	12.35
75%	9.97
50%	7.20
25%	4.70

Table 6.5: Diesel consumption of the Greaves 50 kVA generator. Source: [61]

At full load, this implies roughly 12.35 L/h of diesel consumption. Over 1000 hours of annual operation (about 3 h/day), this corresponds to 12,350 L of diesel. At 2000 hours (about 6 h/day), fuel use rises to nearly 25,000 L per year. Such volumes translate into important and recurring costs for the community, as well as substantial greenhouse gas emissions (Section 6.2.4.4). Thus, fuel expenditures become a decisive factor when evaluating generator-based microgrids.

According to a local supplier [60], the cost of this generator is 79,353,500 Ar. Using the exchange rate on 16 August 2025, this corresponds to approximately 15,265 €. This investment must be amortised over the generator's expected lifetime if it is ultimately included in the system design.

6.2.4.3   Lifetime and maintenance requirements

Regular maintenance is critical to ensure long-term performance. The manufacturer specifies oil changes every 500 hours of operation [61], highlighting the need for consistent technical support and spare part availability. Access to these services in Madagascar should be carefully evaluated. At 1000 hours of annual operation, this implies two full maintenance cycles per year; at 2000 hours, four cycles would be required, further increasing operational complexity and cost.

Reported lifespans for diesel generators vary widely. Some sources estimate 15,000–50,000 hours before major servicing [62], while others suggest 10,000–30,000 hours under typical conditions [63]. More optimistic estimates indicate 20,000–40,000 hours with proper maintenance, potentially corresponding to 25 years of operation [64]. For this study, a conservative lifetime of 20,000 hours is adopted in simulations, equivalent to around 10 years of service at 2000 hours per year.

6.2.4.4   Environmental footprint

The ecological footprint of diesel generators has been assessed in [65], which shows that the majority of life-cycle emissions are generated during the operational phase, primarily from diesel combustion. Manufacturing and transport account for only a minor share of the total. ADEME's official method sheet [66] reports a well-to-wheel emission factor

of approximately 3.16 kg CO_2 per litre of diesel, which includes extraction, refining, and transport. This factor is used in later comparisons of system alternatives.

6.2.4.5   Role in comparative analysis

In summary, the diesel generator is not considered merely as a backup device but as a genuine design alternative to a fully renewable system. Subsequent chapter compare both options on the basis of cost, reliability, and environmental impact, providing a clear picture of the trade-offs involved in generator-based versus renewable-only microgrids.

Chapter 7

Microgrid Dimensioning

7.1 Introduction

This chapter aims to define the technical characteristics of the microgrid required to supply electricity to Antanamalaza throughout the project horizon. The dimensioning process must balance three fundamental criteria: coverage of the projected demand, compliance with component constraints, and overall cost efficiency. To this end, the system is represented in discrete increments of photovoltaic (PV) modules and battery units, ensuring technical consistency with the selected inverter. The expected PV output is modelled under real operating conditions, using site-specific environmental datasets. These elements provide the basis for the optimization process developed in the following sections.

The chapter first introduces input data, then presents the optimization framework, and finally evaluates sizing results across scenarios

7.1.1 Electrical Increments and Modularity

The number of PV modules and batteries cannot be chosen arbitrarily; both must be installed in integer quantities that comply with the electrical constraints of the selected inverter.

The Amerisolar panels (Table 6.2) are connected to a hybrid inverter with integrated MPPT functionality. According to the inverter specifications (Table 6.1), the maximum input voltage is $900\,\mathrm{V}$, with a nominal operating voltage of $720\,\mathrm{V}$. Given that each panel has a maximum voltage of $41.8\,\mathrm{V}$ under standard test conditions, the maximum permissible number of panels in series is:

$$\left\lfloor \frac{900}{41.8} \right\rfloor = 21 \text{ panels.} \tag{7.1}$$

To maintain a safety margin, each string is limited to 20 panels, resulting in a string voltage of:

$$20 \times 41.8 = 836\,\text{V}. \tag{7.2}$$

With a nominal output of $550\,\text{Wp}$ per panel, one string provides:

$$20 \times 550 = 11\,000\,\text{Wp}. \tag{7.3}$$

Since the inverter is equipped with two MPPT inputs, a single unit can accommodate two strings, corresponding to $22\,\text{kWp}$. To prevent overloading, PV expansion is defined in increments of $11\,\text{kWp}$ (one string). Every $22\,\text{kWp}$ of PV capacity requires one inverter. For instance, systems of $11\,\text{kWp}$ or $22\,\text{kWp}$ require one inverter, whereas $33\,\text{kWp}$ or $44\,\text{kWp}$ require two.

The selected batteries operate at $48\,\text{V}$ (Table 6.4), fully compatible with the inverter input. No series connection is necessary, and units can be connected in parallel. Each battery provides $10\,\text{kW h}$ of storage, so capacity is increased in increments of $10\,\text{kW h}$.

Combining these constraints, the design space is defined as a grid of feasible configurations based on discrete increments of PV capacity ($11\,\text{kWp}$) and battery storage ($10\,\text{kW h}$). Each point in this grid is assessed during the optimization process, ensuring that all candidate systems remain technically consistent while preserving flexibility to balance demand and budget requirements.

7.1.2 PV Output Modelling

To simulate the expected electricity production of the PV system, manufacturer-rated values are corrected to account for real operating conditions. Two adjustments are applied sequentially.

First, the cell temperature is estimated as a function of ambient temperature and incident irradiance:

$$T_c = T_a + \frac{\text{NOCT} - 20}{800} \cdot G_a \tag{7.4}$$

Second, the nominal output is corrected for both irradiance and temperature effects:

$$P_{\text{PV}} = P_{\text{STC}} \cdot \frac{G_a}{G_n} \cdot [1 + \gamma \cdot (T_c - T_n)] \tag{7.5}$$

These formulations, validated by Sun et al. [67], are widely adopted in PV performance modelling.

In addition to these corrections, an annual degradation factor is introduced to capture the gradual efficiency loss of PV modules over time. Yearly efficiency values, taken from manufacturer data, are reported in Table 6.3.

Since these equations require irradiance and temperature inputs, the next step is to obtain and preprocess environmental datasets representative of the local conditions in Antanamalaza.

7.1.3   Environmental Data and Preprocessing

To simulate PV performance under site-specific conditions, hourly irradiance and temperature data were obtained from the Renewables.ninja platform [68]. Several historical years were analysed for each candidate configuration to ensure that the system design remains robust under interannual variability.

The optimal tilt angle was determined using the PVGIS tool (Joint Research Centre, European Commission) [69]. For Antanamalaza, with azimuth fixed at $180°$ (north-facing) and local horizon included, the optimal tilt was found to be $20°$. Figure 7.1 illustrates the PVGIS interface and the simulation setup.
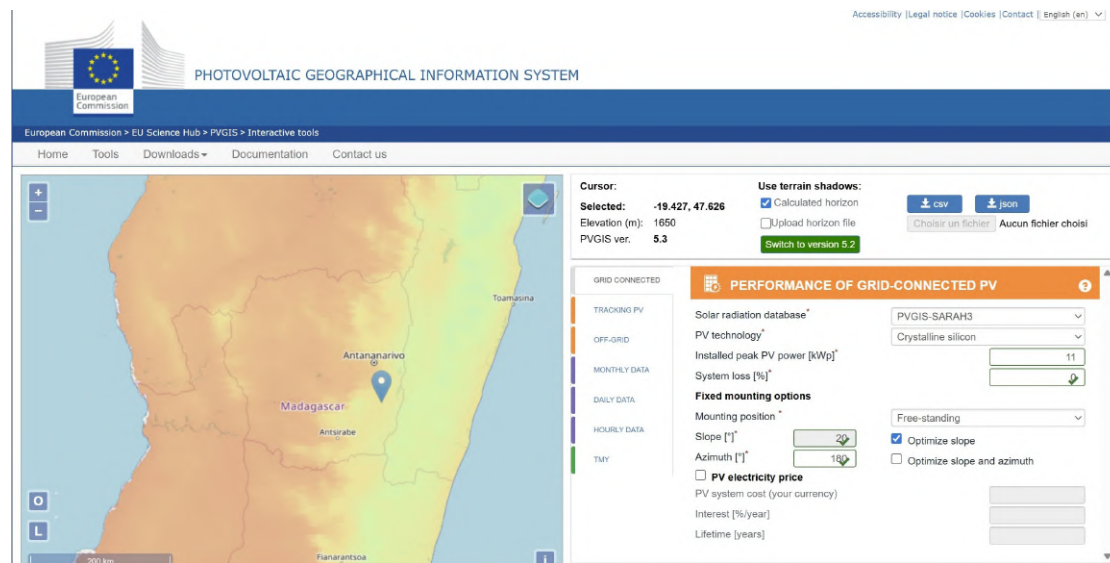
Figure 7.1: Simulation of optimal tilt angle using PVGIS [69] for Antanamalaza, Madagascar.

Because the model operates at 15-minute resolution, the hourly input values were linearly interpolated into four sub-hourly points. This procedure increases temporal resolution and improves the accuracy of simulated PV generation and battery dynamics.

Figure 7.2 presents the yearly irradiance for 2019 with the selected orientation. Over the full year, the maximum irradiance oscillates between approximately $1000\,\mathrm{W/m^2}$ and $800\,\mathrm{W/m^2}$ in July. The most significant variations, however, are caused by cloud cover. Extended periods of low irradiance are visible around March and December, when several consecutive days fall below $100\,\mathrm{W/m^2}$.
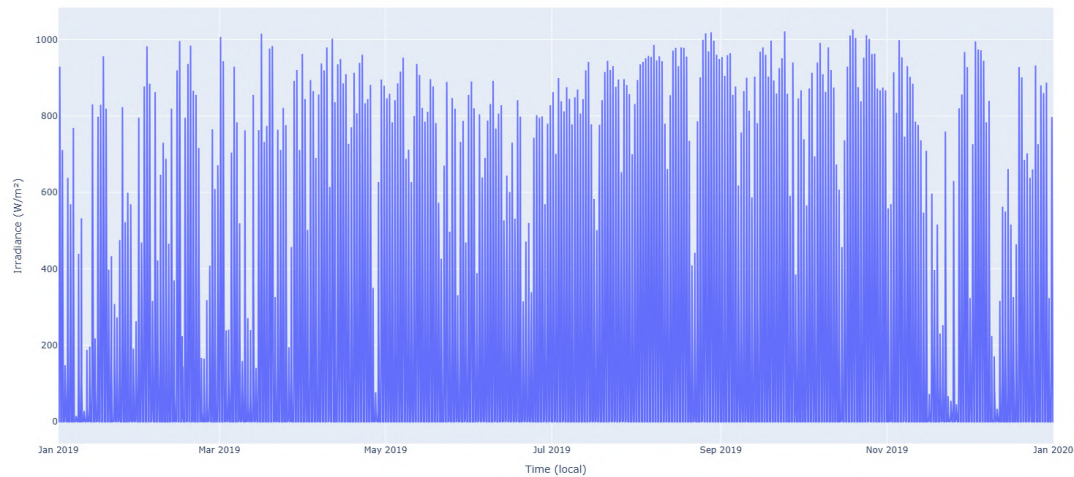
Figure 7.2: Irradiance profile for 2019 in Antanamalaza. Source: [68], representation by author.

A representative daily irradiance curve is shown in Figure 7.3. The profile is nearly symmetrical, with irradiance beginning around 06:00 and ending near 17:00 local time.
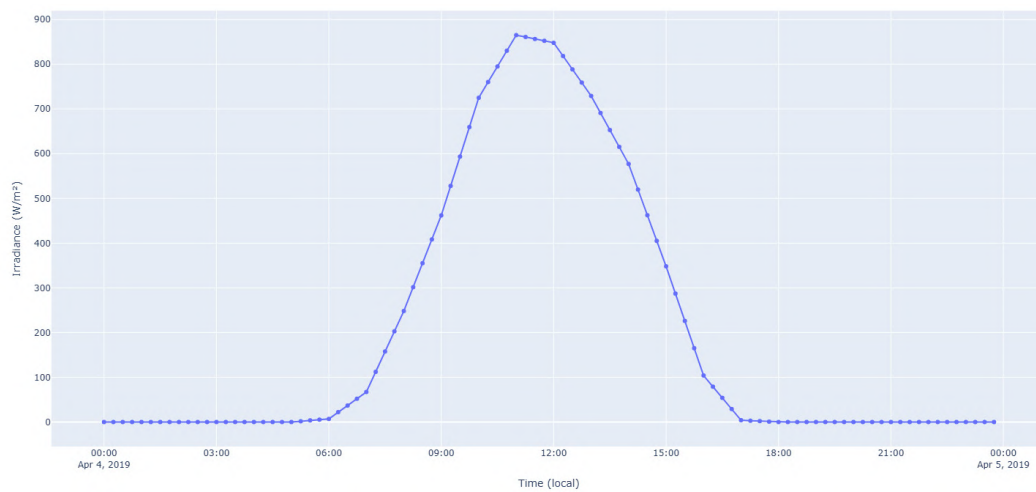
Figure 7.3: Irradiance on a representative day in 2019. Source: [68], interpolation and representation by author.

Temperature also exhibits seasonal variation. Figure 7.4 shows the annual profile, where the lowest values occur in June and July, corresponding to winter in Madagascar, which lies in the Southern Hemisphere.

91
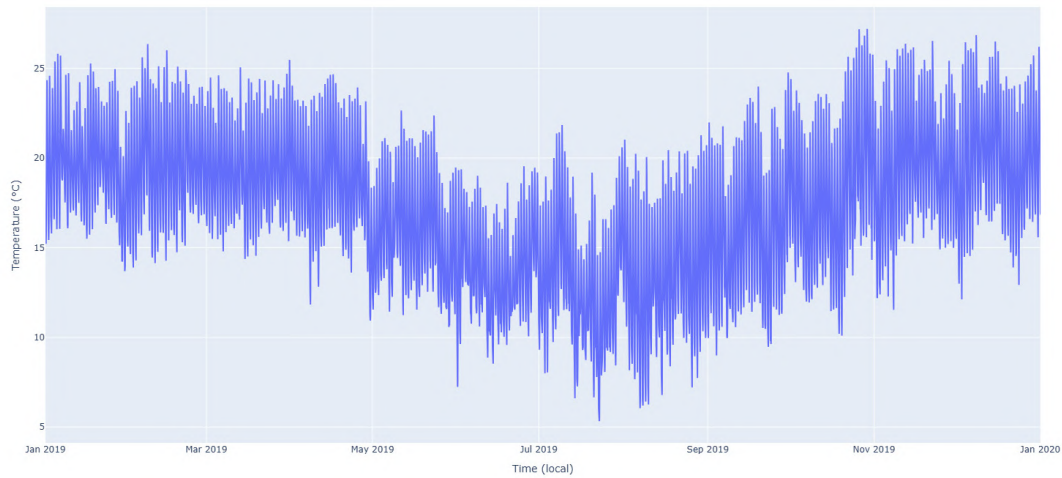
Figure 7.4: Temperature profile for 2019 in Antanamalaza. Source: [68], representation by author.

A representative daily temperature cycle is shown in Figure 7.5. Daytime temperatures closely follow solar irradiance, while during the night they decrease almost linearly until sunrise.
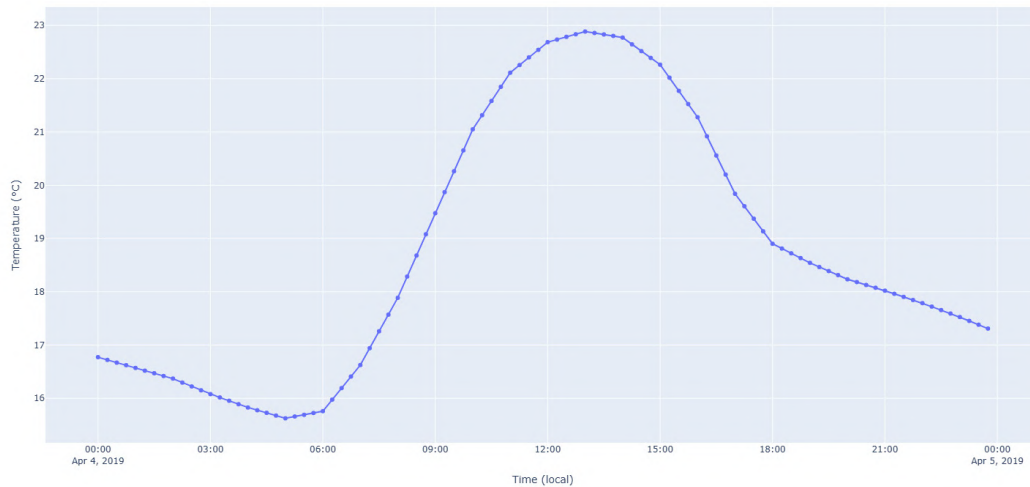
Figure 7.5: Temperature on a representative day in 2019. Source: [68], interpolation and representation by author.

With the technical parameters and environmental inputs defined, the next step is to describe the optimization framework used to evaluate feasible microgrid configurations.

7.2 Optimization framework

The optimization process evaluates a grid of feasible microgrid configurations, defined by discrete increments of photovoltaic (PV) capacity and battery storage (Section 7.1.1). Each candidate configuration is simulated over the full study horizon, from 1 January 2025 to 31 December 2049, using the demand and environmental data described earlier. Component ageing is explicitly modelled: PV output is reduced according to the degradation trajectory in Table 6.3, while the usable battery capacity decreases with the assumed SOH curve. In accordance with the discussion in Section 6.2.3.3, a full replacement of the battery bank is scheduled at year 15. Financial discounting or cost inflation is not applied; instead, the roll-out strategy prioritises deferring investments as long as technical feasibility is preserved.

Scenario-specific operational constraints determine the viability of each configuration. In the no-generator cases, electricity demand must be supplied entirely by PV and batteries, with a tolerance for unmet demand depending on the scenario definition (either 0% or 5%). In the generator cases, additional dispatch rules are enforced (e.g., SOC thresholds or night-only operation), with the generator allowed to supply the load and/or charge the battery when active.

For each valid configuration, a simplified annualised cost metric is computed. This indicator is not a full LCOE, but rather a consistent proxy used to rank system options. It is defined as the sum of the annualised investment costs of all components plus the yearly fuel cost when a generator is present:

$$C_{\text{annual}} = \frac{C_{\text{bat}}}{L_{\text{bat}}} + \frac{C_{\text{PV}}}{L_{\text{PV}}} + \frac{C_{\text{inv}}}{L_{\text{inv}}} + C_{\text{fuel}} + C_{\text{gen}}, \qquad (7.6)$$

where $L_{\text{bat}} = 15$ years, $L_{\text{PV}} = 30$ years, and $L_{\text{inv}} = 10$ years (see Section 6.2 for justifications).

The yearly fuel cost is expressed as

$$C_{\text{fuel}} = V_{\text{diesel}} \cdot p_{\text{diesel}}, \qquad (7.7)$$

with V_{diesel} denoting simulated annual diesel consumption and p_{diesel} the assumed unit price. The generator investment cost is annualised according to its effective service life in years:

$$C_{\text{gen}} = \frac{C_{\text{GEN}}}{\frac{\text{Life span (h)}}{\text{Operating hours per year}}}, \qquad (7.8)$$

so that higher utilisation leads to a shorter effective lifetime and, consequently, a higher annualised cost. In scenarios without a generator, both C_{fuel} and C_{gen} are set to zero.

The optimisation proceeds by simulating the entire configuration grid, discarding solutions that violate technical or scenario-specific constraints, and selecting the option

with the lowest C_{annual} for the target years (2039 and 2049). To approximate implementation practice, a just-in-time roll-out strategy is also constructed: beginning in 2025, PV capacity is expanded in increments of 11 kWp and inverters in 22 kWp steps only when required to maintain feasibility, while batteries are installed or replaced in bulk in 2025 and 2040. This staged roll-out does not affect the ranking metric itself but provides a realistic timeline of investment outlays used in subsequent analyses.

7.3 Optimization of PV and Battery Capacity Without Generator

In this configuration, the system is composed exclusively of photovoltaic (PV) panels, parallel-connected hybrid inverters (integrating both MPPT and inverter functions), and batteries. A diesel generator is not included. Two scenarios are analyzed without a generator:

1. Full demand satisfaction with a state-of-charge (SOC) constraint of 10–90

2. Allowing up to 5% unmet demand, with the same SOC constraint of 10–90%.

7.3.1 All-Demand-Met Scenario

In this baseline scenario, the battery state of charge (SOC) is constrained between 10% and 90%, corresponding to a maximum depth of discharge (DoD) of 80%.

Because all batteries are assumed to be replaced at the 15-year mark, and electricity demand increases annually, the system must be dimensioned to operate reliably in two distinct periods: 2025–2039 (first battery set) and 2040–2049 (second set). Demand beyond 2050 is not projected.

The resulting minimum PV and battery capacities, accounting for both battery degradation and PV efficiency losses, are reported in Table 7.1. These values represent useful capacities and must therefore be oversized at installation to compensate for expected degradation. At this stage, the focus is on identifying the minimum requirements that guarantee reliability under the strict SOC constraint, before turning to staged investment strategies.

Year	Required useful PV capacity (Wp)	Required useful battery capacity (Wh)
2039	264,000	880,640
2049	330,000	1,013,760

Table 7.1: Minimum required capacities without generator, enforcing SOC $\in$ [10%, 90%].

The aggregate results in Table 7.1 provide a static benchmark. However, to better understand the underlying dynamics, it is useful to visualise the full configuration space and the performance frontier between feasible and infeasible solutions.

Figures 7.6 and 7.7 show the simulation results for 2039, with each bubble representing a PV–battery configuration. Colours indicate viability, while viable (green) points are annotated with the annualized cost metric, defined as the ratio of investment cost to useful life. The optimal solution is located at the boundary between feasible and infeasible regions: increasing capacity beyond this point adds cost without improving performance, while reducing one component typically requires oversizing the other to maintain full coverage.

For 2039, the optimal configuration yields an annualized cost of 19,772 €, increasing to 22,649 €in 2049.
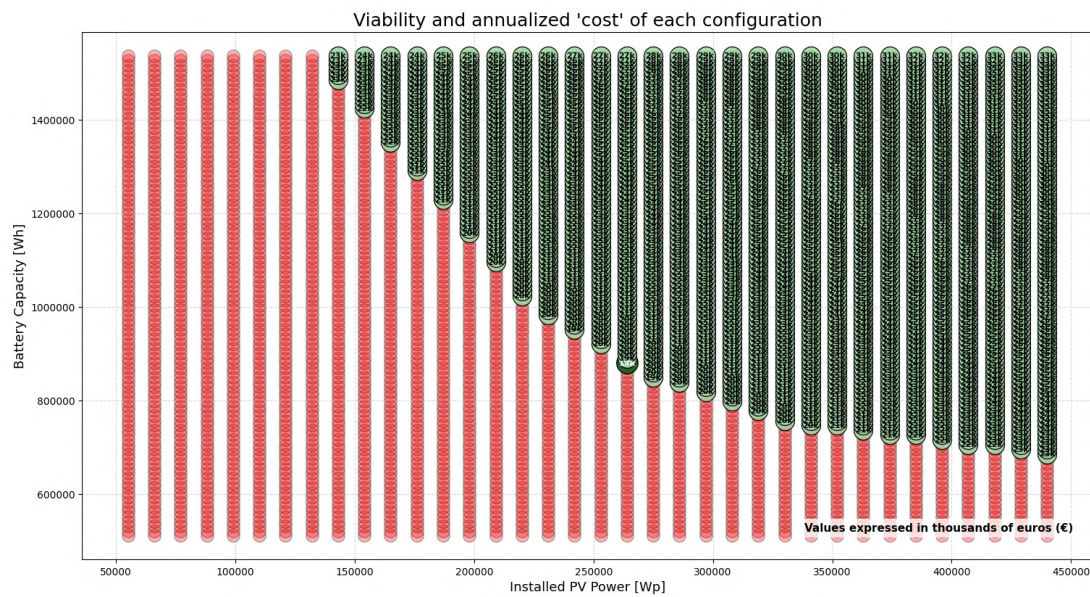
Figure 7.6: All tested PV–battery configurations for 2039, with viability (colour).
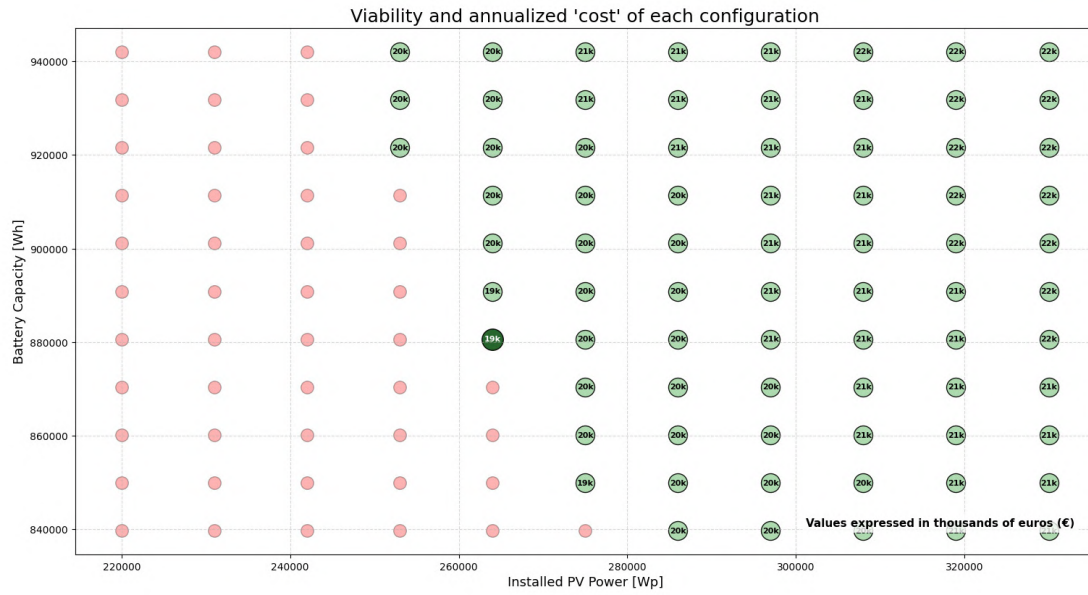
Figure 7.7: Zoom on viable PV–battery configurations around the selected 2039 optimal point.

Once the optimal configuration is identified, the next step is to examine its operational behaviour across the year.

Figures 7.8 and 7.9 present the simulated SOC profiles for 2039 and 2049, respectively. The resemblance between the two curves is expected, as both are generated under the same climatic conditions and with similar, though not identical, load profiles. SOC values are expressed relative to the maximum usable capacity in each year, after accounting for degradation. In both cases, SOC remains within the imposed 90%–10% operating limits.

The system is, however, substantially oversized to ensure uninterrupted demand coverage during prolonged periods of low irradiance. Consequently, SOC typically fluctuates between 90% and 65%, corresponding to an average depth of discharge (DoD) of approximately 25%. Such shallow cycling is favourable for extending battery lifespan but significantly increases system cost. The analysis therefore indicates that allowing limited levels of unmet demand could reduce the required oversizing of both PV and battery capacity and lower total investment.
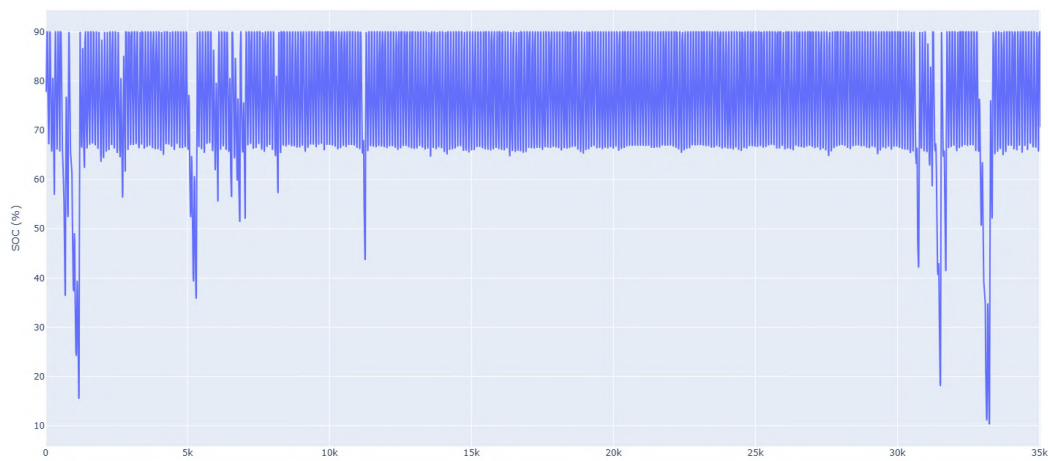
Figure 7.8: Estimated SOC in 2039, expressed relative to maximum achievable capacity (SOH-adjusted).
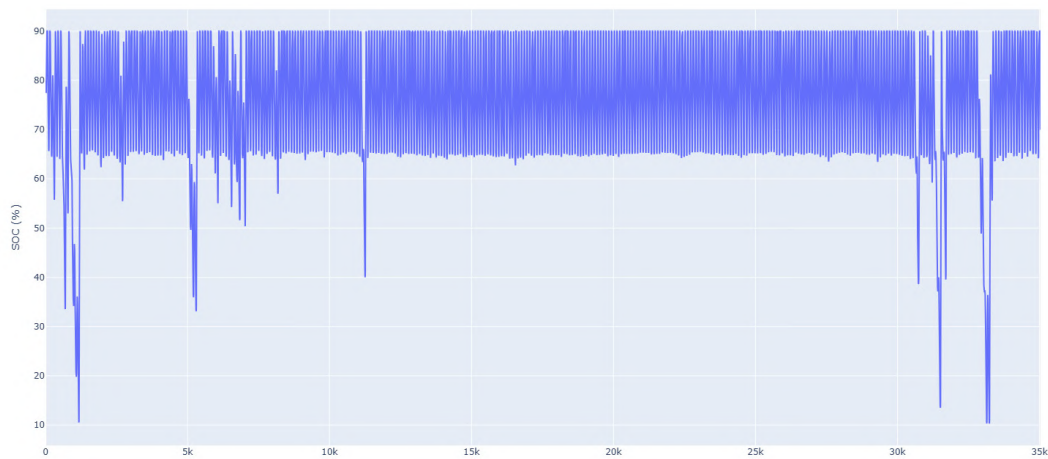
Figure 7.9: Estimated SOC in 2049, expressed relative to maximum achievable capacity (SOH-adjusted).

Beyond aggregated SOC curves, short time slices provide a clearer picture of how the system responds to fluctuations in demand and irradiance. Figure 7.10 illustrates the energy flows and battery state of charge (SOC) during the first three days of 2049. The green curve corresponds to electricity demand, while the blue curve represents PV generation, which is primarily determined by solar irradiance and ambient temperature. As expected, demand and generation peaks do not coincide, with the bulk of electricity consumption occurring during the night. During these hours, the required energy is supplied by the battery (red curve).

97

In the early daylight hours, the battery is recharged. The purple curve does not indicate internal component losses, but rather surplus energy that could theoretically have been used to meet demand or further charge the battery, after accounting for conversion losses, but instead remains unused due to system oversizing. Over the three-day window, even the second day—with noticeably lower solar irradiance and correspondingly reduced PV output—still allows the battery to reach near-full capacity (90% limit) before the onset of evening demand. As a result, the SOC never falls below 60%. This behaviour reflects the system's design philosophy, which prioritises resilience under worst-case conditions involving extended periods of low irradiance, at the expense of frequent surplus generation under typical conditions.
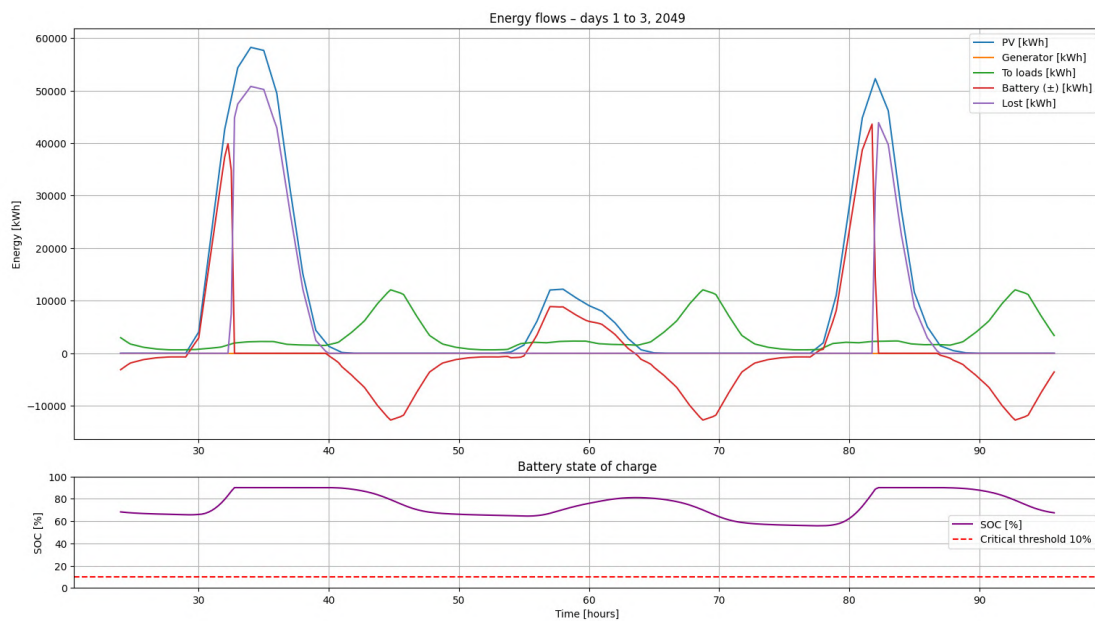
Figure 7.10: Estimated energy flows and SOC during the first three days of 2049

7.3.1.1 Roll-out plan 100% met

The static sizing results are translated into a dynamic investment pathway by applying a staged roll-out plan. The initial battery bank is replaced entirely at the fifteen-year mark to avoid parallel operation of cells with heterogeneous internal resistance and usable capacity [59]. In practice, replacement should be guided by continuous monitoring of the battery state of health (SOH), but for design purposes a deterministic midpoint replacement is assumed. Battery degradation is modelled linearly, reaching 80% of nominal capacity after fifteen years. Photovoltaic (PV) degradation is treated by cohorts: each yearly addition constitutes a cohort whose effective output is adjusted according to the warranted performance shown in Table 6.3, as a function of the cohort age. Hybrid

inverters are dimensioned in parallel according to the same convention as in the optimization stage.

The yearly roll-out plan is determined by applying the same feasibility criterion used in the optimization step: the simulated battery state of charge (SOC), evaluated at 15 min resolution, must remain above 10% throughout the year. A just-in-time strategy is adopted. Starting in 2025, PV is added in discrete increments of 11 kWp (20 panels of 550 Wp), and the smallest number of increments that satisfies the SOC constraint is selected. Inverters follow the same rule as the optimization code, with one unit installed per 22 kWp of PV capacity. Battery banks are sized to meet the end-of-period requirements in 2039 and 2049, accounting for degradation; the first bank is installed in 2025, the second in 2040.

The minimum capacities obtained in Table 7.1 are treated as target nameplate values to be reached by 2039 and 2049. Because PV degradation is applied per cohort while demand grows progressively, the just-in-time plan may slightly exceed these targets, though it still minimises early additions.

Table 7.2 presents the annual additions of PV capacity, inverters, and batteries, together with the associated investment costs. The cumulative installed nameplate and effective capacities are summarised in Table 7.3, while Figure 7.11 illustrates the yearly investment profile.

Year	Added kWp	Added Inverters	Added battery (kWh)	PV Cost [€]	Inverter Cost [€]	Battery Cost [€]	Total Cost [€]
2025	121.0	6	1085.44	42713.0	27600.0	159559.68	229872.68
2026	11.0	0	0.00	3883.0	0.0	0.0	3883.0
2027	11.0	1	0.00	3883.0	4600.0	0.0	8483.0
2028	11.0	0	0.00	3883.0	0.0	0.0	3883.0
2029	11.0	1	0.00	3883.0	4600.0	0.0	8483.0
2030	11.0	0	0.00	3883.0	0.0	0.0	3883.0
2031	11.0	1	0.00	3883.0	4600.0	0.0	8483.0
2032	11.0	0	0.00	3883.0	0.0	0.0	3883.0
2033	0.0	0	0.00	0.0	0.0	0.0	0.0
2034	11.0	1	0.00	3883.0	4600.0	0.0	8483.0
2035	11.0	6	0.00	3883.0	27600.0	0.0	31483.0
2036	11.0	1	0.00	3883.0	4600.0	0.0	8483.0
2037	22.0	2	0.00	7766.0	9200.0	0.0	16966.0
2038	22.0	1	0.00	7766.0	4600.0	0.0	12366.0

Year	Added kWp	Added Inverters	Added battery (kWh)	PV Cost [€]	Inverter Cost [€]	Battery Cost [€]	Total Cost [€]
2039	11.0	1	0.00	3883.0	4600.0	0.0	8483.0
2040	0.0	0	1157.12	0.0	0.0	170096.64	170096.64
2041	0.0	1	0.00	0.0	4600.0	0.0	4600.0
2042	0.0	0	0.00	0.0	0.0	0.0	0.0
2043	0.0	0	0.00	0.0	0.0	0.0	0.0
2044	0.0	1	0.00	0.0	4600.0	0.0	4600.0
2045	22.0	7	0.00	7766.0	32200.0	0.0	39966.0
2046	11.0	2	0.00	3883.0	9200.0	0.0	13083.0
2047	22.0	3	0.00	7766.0	13800.0	0.0	21566.0
2048	11.0	1	0.00	3883.0	4600.0	0.0	8483.0
2049	22.0	2	0.00	7766.0	9200.0	0.0	16966.0

Table 7.2: Annual additions of PV capacity, inverters, and battery nominal capacity with associated costs, when meeting all demand and enforcing SOC $\in [10\%, 90\%]$.

Year	PV nameplate (kWp)	PV effective (kWp)	Inverters	Battery effective (kWh)	SOC min (%)
2025	121.0	118.0	6	1085.4	10.31
2026	132.0	128.7	6	1071.0	11.48
2027	143.0	138.7	7	1056.5	12.21
2028	154.0	148.6	7	1042.0	12.92
2029	165.0	158.5	8	1027.5	13.62
2030	176.0	168.3	8	1013.1	13.50
2031	187.0	178.1	9	998.6	13.97
2032	198.0	187.8	9	984.1	15.17
2033	198.0	186.2	9	969.7	10.27
2034	209.0	195.6	10	955.2	10.40
2035	220.0	204.9	10	940.7	10.41
2036	231.0	214.1	11	926.2	10.48
2037	253.0	232.3	12	911.8	12.01
2038	275.0	250.1	13	897.3	12.26
2039	286.0	258.6	13	882.8	10.55
2040	286.0	255.9	13	1157.1	27.66

Year	PV nameplate (kWp)	PV effective (kWp)	Inverters	Battery effective (kWh)	SOC min (%)
2041	286.0	253.2	13	1141.7	25.04
2042	286.0	250.5	13	1126.3	21.35
2043	286.0	247.8	13	1110.8	17.46
2044	286.0	245.2	13	1095.4	12.63
2045	308.0	262.5	14	1080.0	12.35
2046	319.0	270.7	15	1064.6	10.44
2047	341.0	287.2	16	1049.1	11.91
2048	352.0	294.9	16	1033.7	10.91
2049	374.0	311.0	17	1018.3	11.02

Table 7.3: Installed PV capacity, number of inverters, and battery capacities (nominal and effective after degradation) when meeting all demand and enforcing SOC $\in$ [10%, 90%].

Two main insights emerge from the roll-out results. First, the optimisation favours a gradual ramp-up of PV capacity during the early years, adding only the increments strictly required to keep the state of charge (SOC) above the 10% threshold without front-loading investments (Table 7.2). This approach limits unnecessary upfront capital expenditure while preserving operational reliability. Second, by 2039 and 2049 the installed PV capacity falls slightly short of the minimum targets reported in Table 7.1. This undershoot is offset by a marginally larger battery capacity than the minimum requirement, which compensates for the reduced PV deployment.

A further observation concerns the optimisation horizon. Because the problem is solved separately for 2025–2039 and 2040–2049, the resulting strategy is not globally optimal over the entire period. This is illustrated in 2040, when the minimum SOC lies well above the 10% limit due to surplus PV capacity inherited from the first period. Consequently, PV additions are deferred until 2045, as shown in Table 7.1. A single joint optimisation covering 2025–2049 could, in principle, distribute capacity expansions more smoothly across time and achieve a marginal reduction in total lifecycle costs.
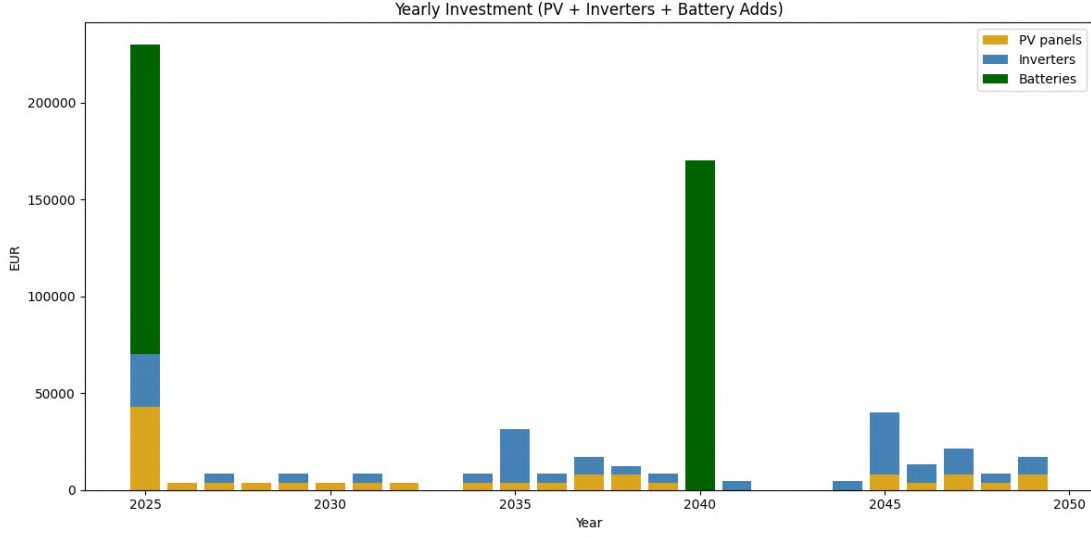
Figure 7.11: Annual investment for the progressive PV roll-out, with full demand satisfaction and SOC constrained to the range $[10\%, 90\%]$.

Figure 7.11 illustrates the annual investment profile for the progressive PV roll-out, including PV modules, inverters, and full battery replacements in 2025 and 2040. Most years involve only minor expenditures, reflecting the just-in-time approach of adding PV in small increments. Investment peaks correspond to battery purchases, which dominate capital outlays, while inverter costs appear intermittently when PV expansion exceeds the existing inverter capacity. The absence of investment in certain years highlights the optimisation's reliance on residual capacity from earlier additions until the SOC threshold approaches violation. This lumpy investment pattern illustrates the trade-off between cost minimisation and operational security, as well as the influence of splitting the horizon into two sub-problems—producing, for example, the noticeable gap in PV additions immediately after the 2040 battery replacement.

In summary, while the all-demand-met scenario ensures full reliability under stringent SOC constraints, it does so at the expense of significant oversizing and a lumpy investment trajectory, setting the stage for exploring scenarios with limited unmet demand.

7.3.2 5% unmet-demand scenario

Figure 7.12 shows the cost–reliability trade-off in 2039. Allowing even a small share of unmet demand leads to a sharp drop in annualized investment cost, with 29% savings achieved when moving from 0% to 1%. To balance affordability with reliability, a 5% unmet-demand threshold is adopted for the subsequent analysis. Within this framework, the battery remains constrained to operate within SOC $\in [10\%, 90\%]$. In practice,

once the SOC reaches 10%, the battery ceases discharging and any residual shortfall is recorded as unmet demand.
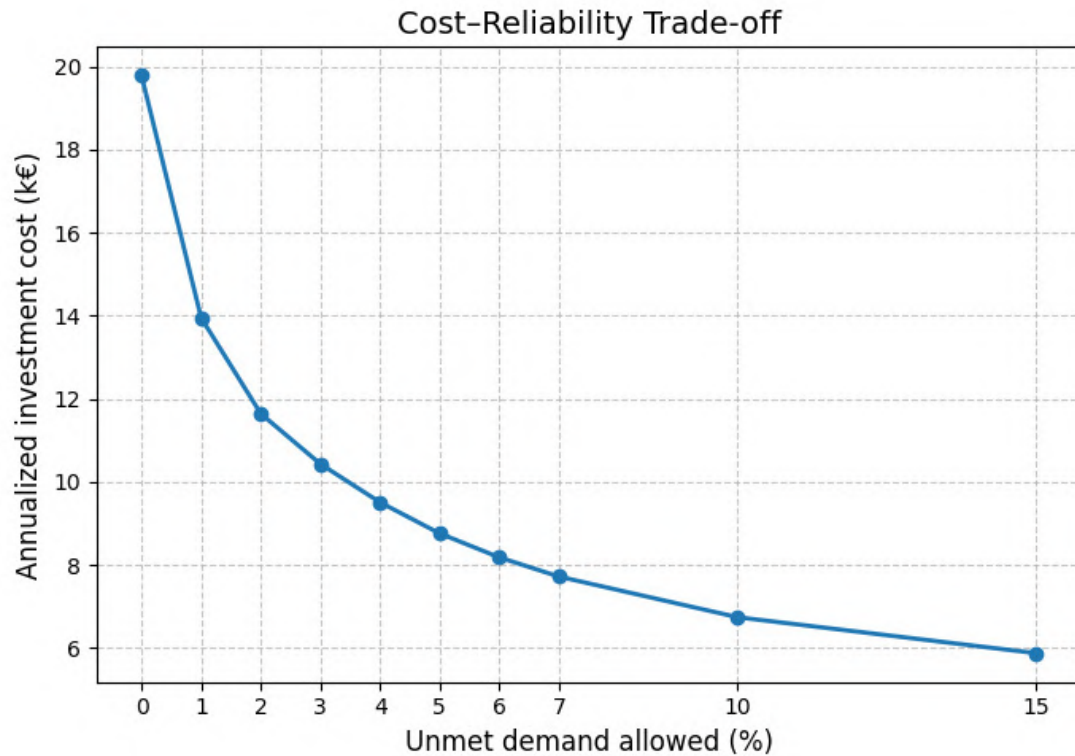
Figure 7.12: Annualized investment cost per accepted maximum unmet demand

Table 7.4 shows the required nameplate capacities. Relative to the all-demand-met case in Table 7.1, the reductions are substantial. In 2039, required PV capacity falls from 264 kWp to 154 kWp (–42%), and storage from 880.6 kWh to 327.7 kWh (–63%). In 2049, PV decreases from 330 kWp to 176 kWp (–47%) and storage from 1,013.8 kWh to 419.8 kWh (–59%). Thus, most of the additional capacity in the strict scenario is dedicated to covering the final 5% of demand.

Year	Required useful PV capacity (Wp)	Required useful battery capacity (Wh)
2039	154,000	327,680
2049	176,000	419,840

Table 7.4: Sizing without generator, with SOC limited to 90% (max) and 10% (min), accepting 5% unmet demand.

103

These sizing reductions directly translate into different operational dynamics, as illustrated in the SOC trajectories of Figures 7.13 and 7.14 with respect to Figures 7.8 and 7.9. Three changes stand out. First, cycling is deeper and more frequent, with recurrent visits to the 10% floor; in the all-demand-met case, SOC oscillated within a shallower 90%–65% band. The typical DoD rises from 25% to about 65%. Second, on cloudy days, the SOC peak often fails to reach the 90% ceiling, reflecting the reduced PV margin. Third, inter-day variability increases after cloudy sequences, since the smaller storage buffer must simultaneously cover immediate demand and recharge from previous deficits.
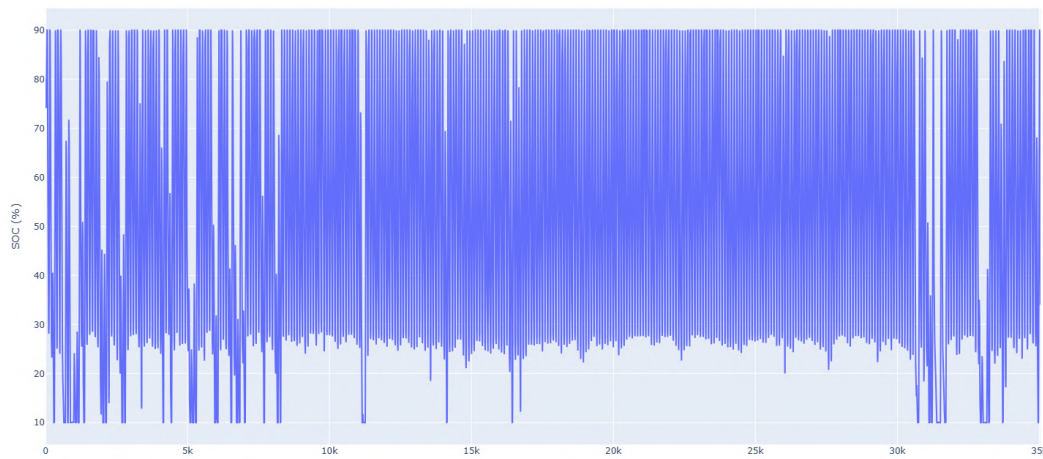
Figure 7.13: Estimated SOC in 2039, expressed relative to maximum achievable capacity (SOH-adjusted), when optimized for 5% unmet demand.
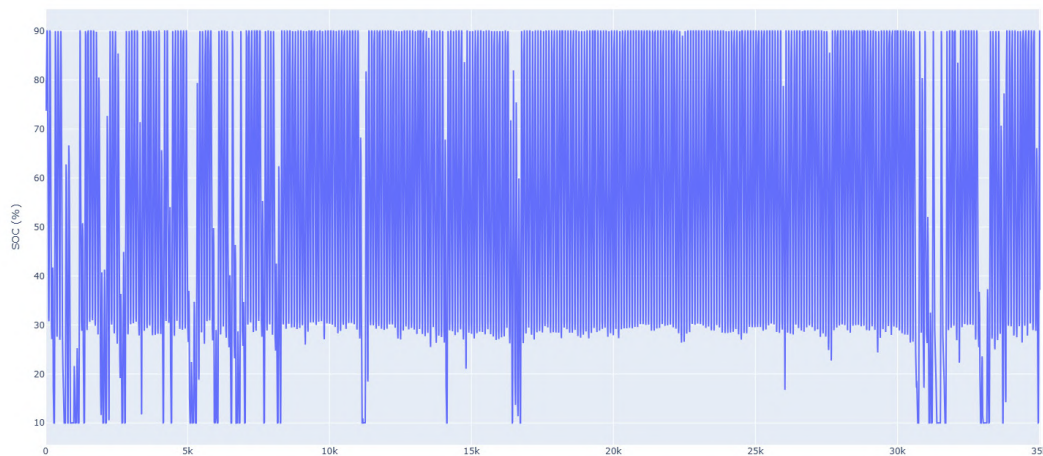
Figure 7.14: Estimated SOC in 2049, expressed relative to maximum achievable capacity (SOH-adjusted), when optimized for 5% unmet demand.

Operation over three representative days in 2049 is illustrated in Figure 7.15. In contrast with Figure 7.10, some demand is left unsupplied. On the second, cloudier day, PV output is reduced, so the SOC recovers only to about 40% by the evening peak, having previously dropped to 30%. At hour 68 (20:00), demand is no longer served: solar generation is absent, and the battery reaches the 10% limit, halting further discharge.
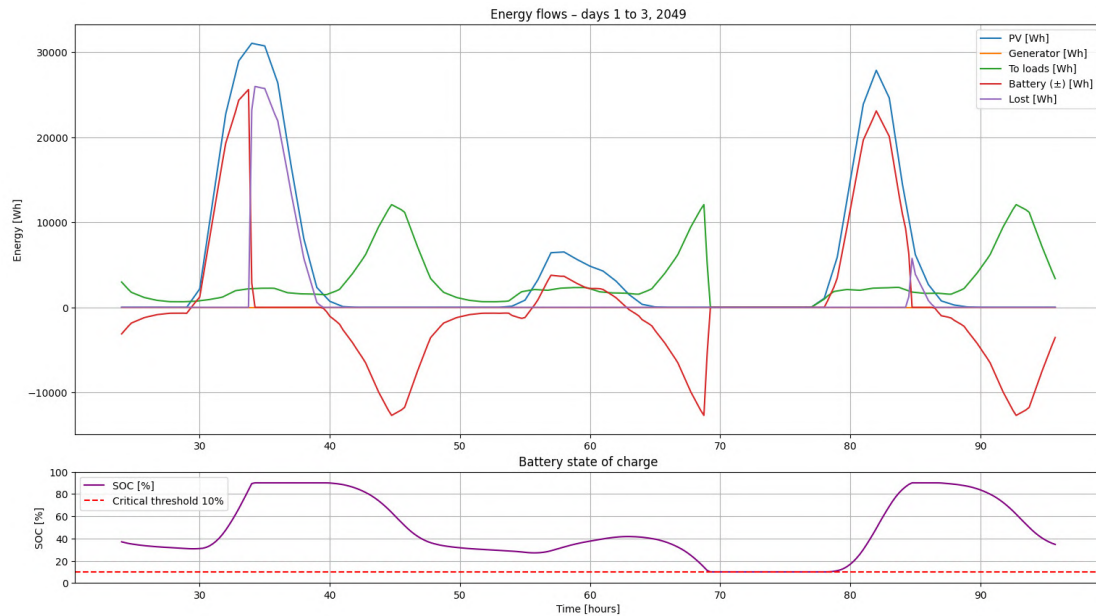
Figure 7.15: Estimated energy flows and SOC during the first three days of 2049, optimized for 5% unmet demand.

The long-term deployment strategy under this scenario, including annual additions and associated costs, is presented next.

7.3.2.1   Roll-out plan for the 5% unmet-demand scenario

The long-term deployment strategy under this scenario, including annual additions and associated costs, is presented in Table 7.5. Table 7.6 complements this by reporting the cumulative installed capacities and the effective SOH-adjusted values.

The results indicate that in 2039 and 2049, installed battery capacity slightly exceeds the minimum targets in Table 7.4. This oversizing allows for small reductions in PV capacity while still meeting the imposed constraints. In addition, following the 2040 battery replacement, the proportion of unmet demand temporarily decreases to around 3%, an artefact of the two-stage optimisation approach (2025–2039 and 2040–2049).

Year	Added PV (kWp)	Added Inverters	Added battery (kWh)	PV Cost (€)	Inverter Cost (€)	Battery Cost (€)	Total Cost (€)
2025	88.0	4	409.60	31040	18400	58800	108240
2026	0.0	0	0.00	0	0	0	0
2027	11.0	1	0.00	3880	4600	0	8480
2028	0.0	0	0.00	0	0	0	0
2029	0.0	0	0.00	0	0	0	0
2030	11.0	0	0.00	3880	0	0	3880
2031	0.0	0	0.00	0	0	0	0
2032	11.0	1	0.00	3880	4600	0	8480
2033	0.0	0	0.00	0	0	0	0
2034	11.0	0	0.00	3880	0	0	3880
2035	0.0	4	0.00	0	18400	0	18400
2036	11.0	1	0.00	3880	4600	0	8480
2037	11.0	1	0.00	3880	4600	0	8480
2038	0.0	0	0.00	0	0	0	0
2039	11.0	1	0.00	3880	4600	0	8480
2040	0.0	0	484.41	0	0	69090	69090
2041	0.0	0	0.00	0	0	0	0
2042	0.0	1	0.00	0	4600	0	4600
2043	0.0	0	0.00	0	0	0	0
2044	0.0	0	0.00	0	0	0	0
2045	0.0	4	0.00	0	18400	0	18400
2046	11.0	1	0.00	3880	4600	0	8480
2047	0.0	1	0.00	0	4600	0	4600
2048	11.0	1	0.00	3880	4600	0	8480
2049	11.0	1	0.00	3880	4600	0	8480

Table 7.5: Annual additions for the 5% unmet demand scenario, with SOC $\in$ [10%, 90%].

Year	Total PV (kWp)	Effective PV (kWp)	Battery Effective (kWh)	SOC Min (%)	Demand Not Met (%)
2025	88.0	85.8	409.6	10.0	4.5
2026	88.0	85.8	404.1	10.0	4.9
2027	99.0	96.0	398.7	10.0	4.2
2028	99.0	95.5	393.2	10.0	4.6
2029	99.0	94.9	387.8	10.0	4.9
2030	110.0	105.0	382.3	10.0	4.3
2031	110.0	104.4	376.8	10.0	4.7
2032	121.0	114.5	371.4	10.0	4.3
2033	121.0	113.8	365.9	10.0	4.7
2034	132.0	123.8	360.4	10.0	4.4
2035	132.0	123.1	355.0	10.0	4.8
2036	143.0	133.0	349.5	10.0	4.6
2037	154.0	142.9	344.1	10.0	4.5
2038	154.0	142.1	338.6	10.0	4.9
2039	165.0	151.9	333.1	10.0	4.9
2040	165.0	151.0	484.4	10.0	3.0
2041	165.0	150.0	478.0	10.0	3.3
2042	165.0	149.0	471.5	10.0	3.6
2043	165.0	148.0	465.0	10.0	3.9
2044	165.0	147.0	458.6	10.0	4.3
2045	165.0	146.0	452.1	10.0	4.7
2046	176.0	155.7	445.7	10.0	4.6
2047	176.0	154.7	439.2	10.0	5.0
2048	187.0	164.4	432.7	10.0	4.9
2049	198.0	174.1	426.3	10.0	4.9

Table 7.6: System characteristics with minimum SOC and percentage of demand not met.

The annual investment profile associated with this roll-out is displayed in Figure 7.16. Relative to the all-demand-met case (Figure 7.11), two differences stand out. First, the overall expenditure level is markedly lower. The initial investment in 2025 is reduced, and subsequent yearly costs remain modest, owing to the acceptance that 5% of total demand will not be satisfied. Second, the composition of expenditure shifts: PV modules and inverters account for a larger share of total costs, whereas battery investment is

107

considerably reduced. This outcome reflects a structural change in system design priorities: instead of dimensioning storage to cover rare extended low-irradiance events, the system allows limited demand curtailment, thus placing greater emphasis on generation and conversion capacity.
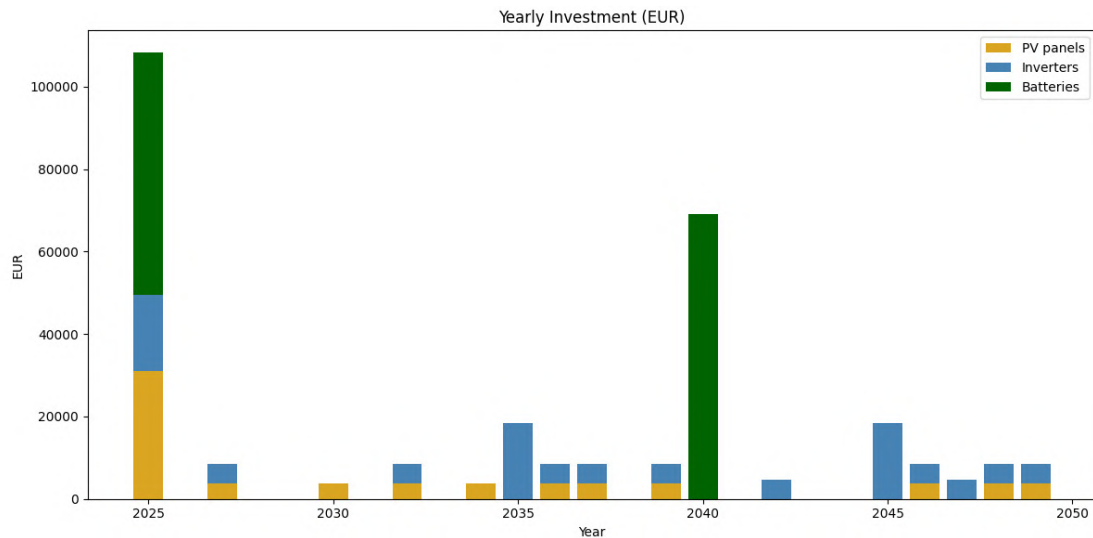
Figure 7.16: Annual investment for the progressive PV roll-out, for the 5% unmet demand scenario, SOC $\in [10\%, 90\%]$.

Overall, the roll-out strategy demonstrates how allowing a limited share of unmet demand substantially reduces capital requirements, while preserving operational reliability through targeted capacity additions. This highlights the central trade-off between investment intensity and service quality that will be further examined in the comparative analysis of scenarios.

7.4 Optimization of PV and Battery Capacity with a Generator

The objective of this section is to examine how the integration of a generator affects the optimal sizing of PV and battery capacity. To this end, two generator dispatch strategies are tested:

1. The generator turns on whenever the battery SOC falls below 20%.

2. The generator turns on whenever the SOC falls below 20% *and* the system is operating during night hours (18:00–06:00).

7.4.1 Generator dispatch at SOC below 20%

In this configuration, the generator is triggered once the SOC reaches 20% and remains active until the SOC climbs back to 30%. To preserve lifetime, the generator operates at 80% of its rated load, exceeding this threshold only when strictly necessary. Any surplus electricity is directed to battery charging.

The optimization algorithm evaluates multiple PV–battery combinations and selects the one that minimizes the annualized cost. The cost components include PV modules, batteries, inverters, generator capital expenditure, and diesel fuel. Generator capital cost is annualized over a rated service life of 20,000 hours; consequently, higher utilization directly increases its equivalent yearly cost.

Simulations are performed for the target years 2039 and 2049. Figures 7.17 and 7.18 show the configuration space explored by the algorithm. Unlike the PV-only scenario (Figure 7.6), no infeasible region emerges: the generator guarantees system viability across all tested PV–battery configurations, provided that at least one battery unit is included.

Figure 7.17: High-level view of tested configurations for generator dispatch at SOC 20% in 2039.

Figure 7.18: High-level view of tested configurations for generator dispatch at SOC 20% in 2049.

The optimal configurations are summarized in Table 7.7. Results indicate generator operation of 339 hours in 2039 and 417 hours in 2049. Actual operation hours are expected to vary with the chosen rollout strategy: a gradual expansion of PV capacity, as in the PV-only case, would increase generator reliance, while upfront installation of larger PV capacity would reduce generator usage at the expense of higher initial investment.

Year	Required useful PV capacity (Wp)	Required useful battery capacity (Wh)	Diesel usage (L)	Operating hours (h)
2039	110,000	317,440	3541	339
2049	132,000	389,120	4353	417

Table 7.7: Optimal PV–battery sizing with generator activation at SOC 20%.

An illustrative example is shown in Figure 7.19. On days with high irradiance, PV generation fully covers demand and recharges the batteries. During the cloudy second day, the SOC drops to 20% in the evening, triggering generator activation (orange). The generator continues until SOC reaches 30%, thereby restoring stability.

110
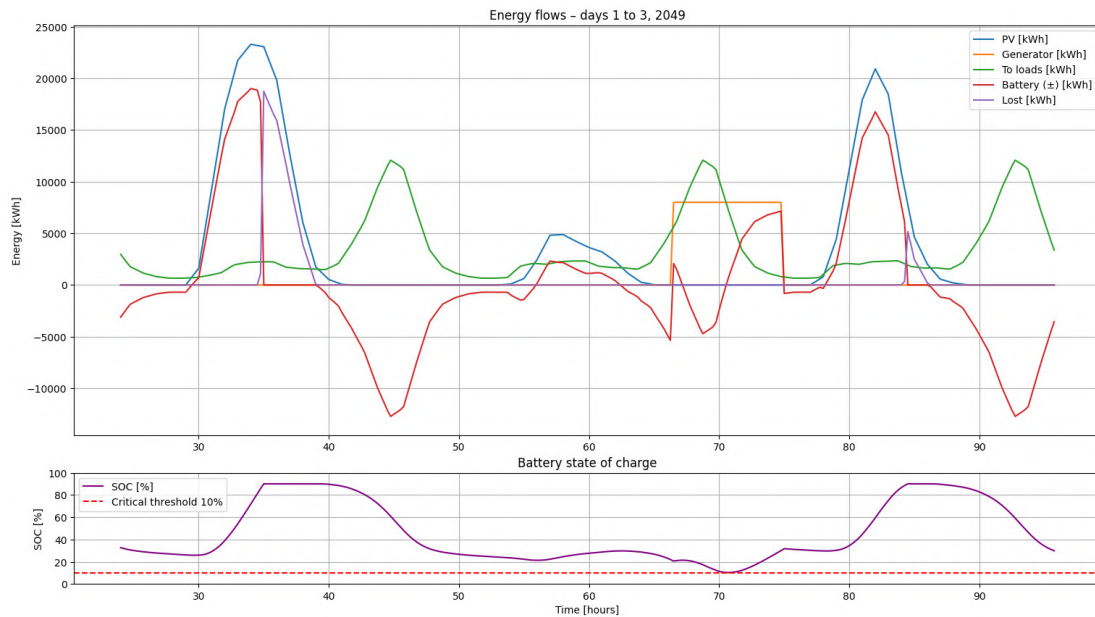
Figure 7.19: Estimated energy flows and SOC during three days in 2049, with generator activation at SOC 20%.

A phased rollout strategy, analogous to the PV-only scenario, could also be implemented under this dispatch rule.

7.4.2 Generator dispatch at SOC below 20% during night-time

In this variant, the generator is constrained to operate exclusively during night-time hours. It is activated whenever the SOC falls below 20% between 18:00 and 06:00, and remains on until the SOC reaches 30% or daylight begins. As in the previous scenario, the generator operates at 80% of its rated capacity whenever possible, with surplus power directed to battery charging.

The rationale for this strategy is to concentrate generator usage on periods when it provides the greatest value, namely during the evening and night. These hours are characterized by elevated demand and the absence of PV generation, making the generator a critical back-up resource.

The optimization procedure mirrors that of the previous scenario, with annualized system cost minimized across a range of PV–battery configurations. The configuration spaces for 2039 and 2049 are illustrated in Figures 7.20 and 7.21. As in the unrestricted case, all tested systems remain feasible, since the generator prevents SOC from dropping below the minimum 10% threshold.
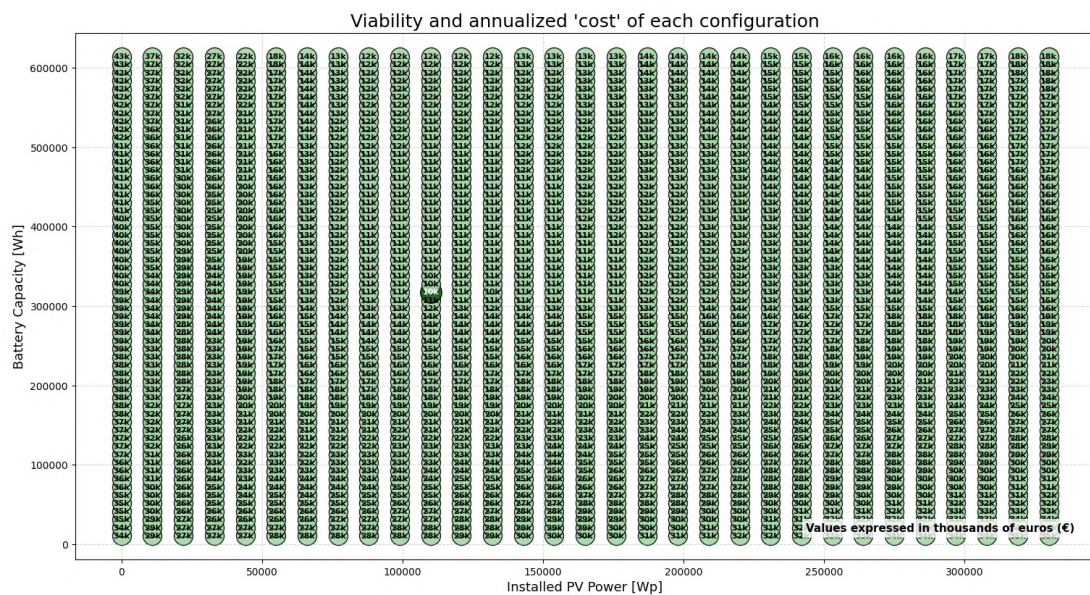
111
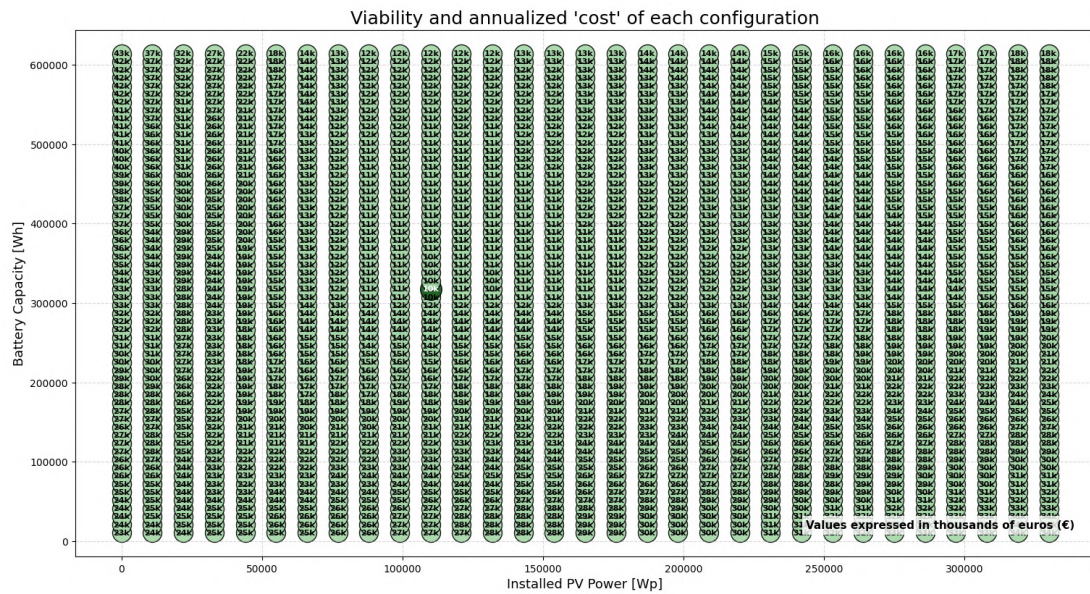
Figure 7.20: High-level view of tested configurations for generator dispatch at SOC 20% during night-time, 2039.
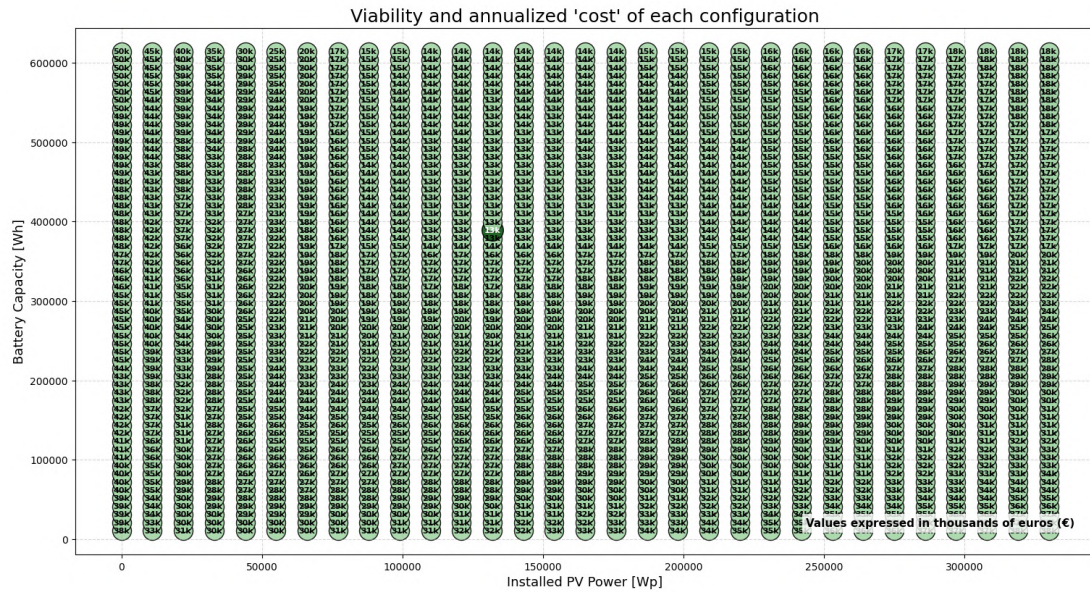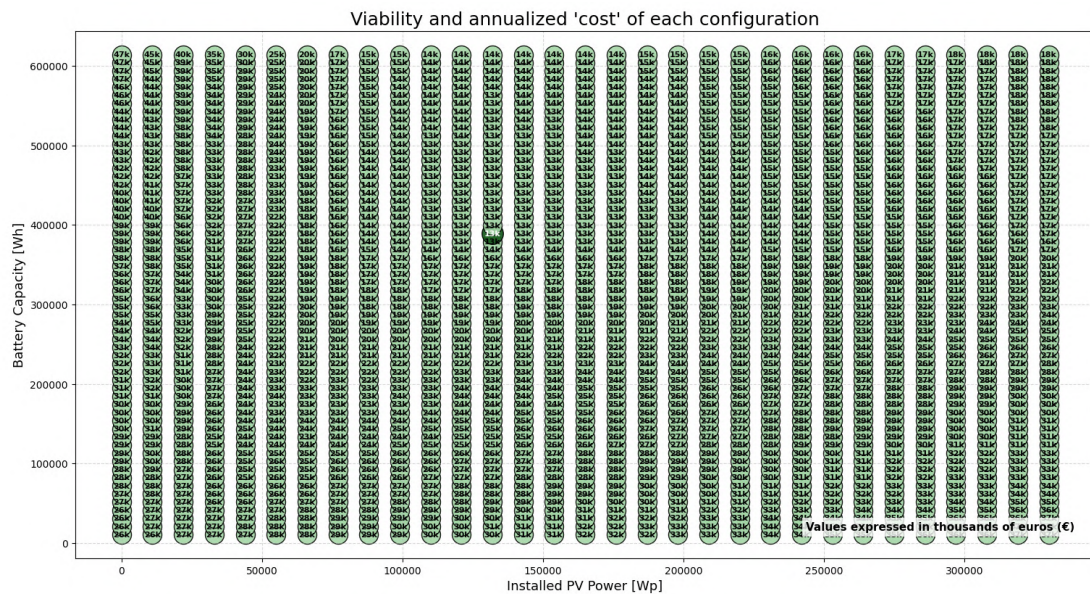

Figure 7.21: High-level view of tested configurations for generator dispatch at SOC 20% during night-time, 2049.

The optimal configurations are summarized in Table 7.8. The required PV and bat-

tery capacities are identical to those obtained under the unrestricted dispatch strategy (Table 7.7). Generator usage, however, is slightly reduced: operating hours decrease by about 3%, with a corresponding reduction in diesel consumption. This outcome indicates that, even in the absence of explicit temporal restrictions, the cost-minimizing strategy naturally concentrates generator operation during evening and night-time hours.

Year	Required useful PV capacity (Wp)	Required useful battery capacity (Wh)	Diesel usage (L)	Operating hours (h)
2039	110,000	317,440	3445	330
2049	132,000	389,120	4218	404

Table 7.8: Optimal PV–battery sizing with generator dispatch restricted to night-time operation at SOC 20%.

Having examined the two generator dispatch strategies individually, the following section compares their performance in order to highlight the trade-offs between system cost, generator reliance, and renewable integration.

7.5 Comparison

The previous sections presented results for four distinct scenarios, yet no systematic comparison has been undertaken. To enable such an evaluation, the annualized investment cost is adopted as the principal metric. While not a perfect indicator, it provides a consistent and transparent benchmark for relative comparison across scenarios. This metric consolidates the costs of batteries, photovoltaic panels, inverters, and—where applicable—diesel fuel consumption and generator investment. Effects of degradation and component efficiencies are already incorporated in the calculations. The formulation is expressed as:

$$C_{\text{annual}} = \frac{C_{\text{bat}}}{\text{Battery lifespan}} + \frac{C_{\text{PV}}}{\text{PV lifespan}} + \frac{C_{\text{inv}}}{\text{Inverter lifespan}} + C_{\text{fuel}} + C_{\text{gen}}. \quad (7.9)$$

Here, C_{bat}, C_{PV}, and C_{inv} denote the investment costs of batteries, photovoltaic panels, and inverters, with assumed lifetimes of 15, 30, and 10 years, respectively. The annual fuel cost is given by

$$C_{\text{fuel}} = V_{\text{diesel}} \cdot p_{\text{diesel}}, \quad (7.10)$$

where V_{diesel} is yearly diesel consumption (litres) and p_{diesel} the unit price (0.95 €/L). The generator cost is annualized according to its actual usage:

113

$$C_{\text{gen}} = \frac{C_{\text{GEN}}}{\frac{\text{Lifespan (h)}}{\text{Operating hours per year}}}, \tag{7.11}$$

where C_{GEN} is the purchase cost of the generator. The denominator reflects the effective lifetime in years, ensuring that higher utilization directly increases the equivalent annual cost.

It should be emphasized that this comparison metric has limitations. First, the *all-demand-met, no-generator* scenario operates with a shallower depth of discharge (DoD), which could extend battery lifetime or allow the use of less expensive batteries, thereby reducing costs in practice. Second, the *5% unmet-demand, no-generator* scenario is structurally advantaged, as it is the only case in which full demand satisfaction is not required. Third, generator-based scenarios are somewhat favoured: maintenance costs, requirements for technical expertise, and exposure to fuel price volatility or supply risks are not included. Finally, the annualized metric does not capture the dynamics of staged roll-outs, where different deployment strategies could lead to non-linear cost trajectories over time.

Scenario	Year	PV (kWp)	Batt. (kWh)	Diesel (L/yr)	Annualized investment cost (€)
All demand met, no gen.	2039	264	881	0	19,772
	2049	330	1014	0	22,649
5% unmet demand, no gen.	2039	154	328	0	8,760
	2049	176	420	0	10,718
Gen. when SOC $< 20\%$	2039	110	317	3541	10,942
	2049	132	389	4353	13,329
Gen. when SOC $< 20\%$ & night	2039	110	317	3445	10,843
	2049	132	389	4218	13,190

Table 7.9: Comparison of scenarios with required capacities and annualized investment cost.

To extend the comparison beyond purely economic terms, the analysis incorporates the environmental dimension through life-cycle CO_2-equivalent emissions. The objective is not to provide an exact carbon footprint but to approximate the relative magnitude

of emissions across scenarios. Methodological details and emission factors for each component were established in Chapter 6. In brief, the adopted values are 810 kgCO$_2$-eq/kWp for photovoltaic modules, 540–908 kgCO$_2$-eq per 10 kWh for LiFePO$_4$ batteries, and 3.16 kgCO$_2$/L for diesel fuel (well-to-wheel).

Since scenarios differ in their deployment profiles, a consistent method is required to estimate cumulative capacities and fuel use. For PV capacity, the 2049 installed value is divided by 0.8, which approximates the cumulative installed stock over time while accounting for reduced efficiency. The real value, will depend on the roll-out plan. Battery capacity is estimated by adjusting the 2039 and 2049 installed values (each divided by 0.8) and then summing them, representing the total installations over the project horizon. Diesel consumption is approximated by multiplying the annual use in 2039 by 30, which reflects long-term cumulative consumption; the 2049 value is not used, as it may represent an extremum rather than average operation.

This procedure yields a consolidated estimate of embodied emissions for each scenario, disaggregated into PV, battery, and diesel contributions. While simplified, it ensures comparability across cases and provides an upper–lower bound range where battery emissions are concerned.

Scenario	PV (kWp)	Batt. (kWh)	Diesel (L)	CO$_2$ emissions (tCO$_2$)
All demand met, no gen.	412.50	2368.75	0	462.04 – 549.22
5% unmet demand, no gen.	220.00	935.00	0	228.69 – 263.11
Gen. when SOC < 20%	165.00	882.50	106230	517.06 – 549.56
Gen. when SOC < 20% & night	165.00	882.50	103350	507.94 – 540.44

Table 7.10: Comparison of scenarios with required capacities and CO$_2$ emissions.

Figure 7.22 complements the table by showing the breakdown of emissions by source (PV, batteries, diesel).
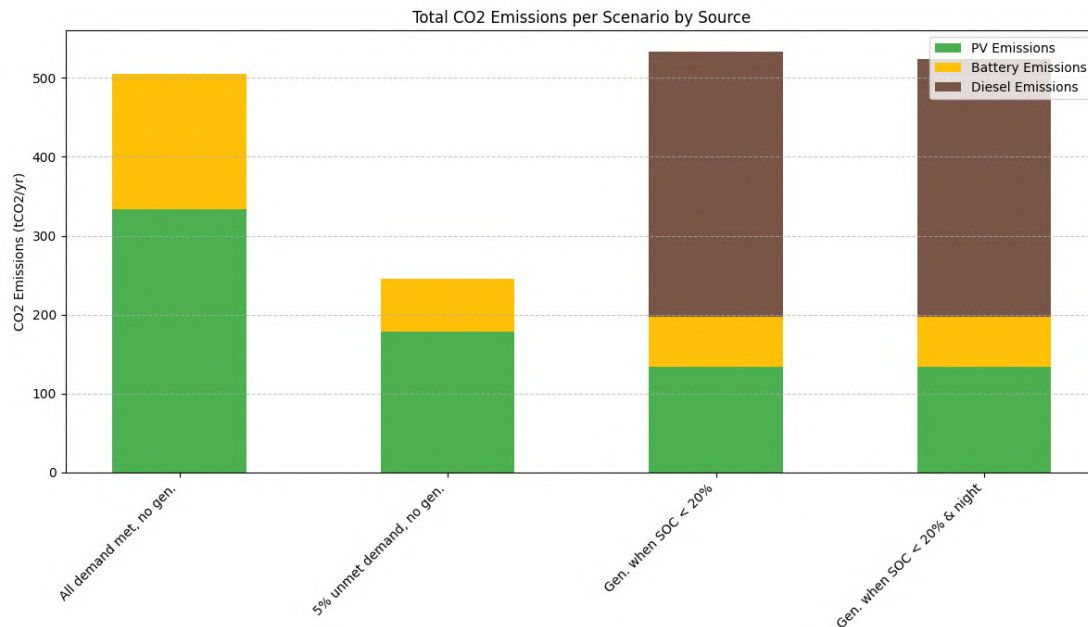
Figure 7.22: Breakdown of CO_2 emissions per scenario by source.

As indicated in Table 7.10 and Figure 7.22, the *5% unmet demand, no generator* scenario achieves the lowest overall emissions, largely due to its smaller infrastructure requirements and the absence of diesel. Across all cases, PV manufacturing dominates embodied emissions relative to batteries, underscoring the carbon intensity of solar panel production. In generator-based scenarios, however, diesel overwhelmingly dominates the footprint, with annual fuel consumption exceeding the combined impact of PV and batteries. This highlights the severe environmental trade-off of introducing fossil backup, even if it reduces renewable investment needs.

Overall, total emissions in generator scenarios exceed those of purely renewable configurations, confirming that diesel use is the key determinant of sustainability. These results conclude the technical dimensioning analysis. The next and final chapter synthesizes the main findings, discusses their implications for rural electrification in Madagascar, and formulates recommendations for implementation and future work.

Chapter 8

Conclusions and Recommendations

8.1 Summary of the Study

This thesis set out to design and evaluate a solar microgrid for the rural village of Antana-
malaza, Madagascar. The objective was to identify a technically feasible and econom-
ically viable system that could ensure long-term access to electricity while minimizing
both financial and environmental costs.

The research progressed in several stages. First, the broader energy context was
presented, showing that despite abundant solar potential, Madagascar still faces one of
the lowest electrification rates worldwide, particularly in rural areas. National policies
promote electrification, but implementation is constrained by financial, technical, and
institutional challenges. This provides a strong rationale for decentralized renewable
solutions such as microgrids.

Second, the local case of Antanamalaza was studied in detail. The village's set-
tlement pattern, modest economic activity (agriculture centered around rice, carpentry,
local services), and lack of reliable energy access make it a representative site for ru-
ral electrification projects. A methodology was developed to estimate population and
household demand in the absence of official statistics, combining building counts with
data at the national level.

Third, a comparative review of other microgrids was undertaken, with a particular fo-
cus on projects that disclosed not only installed capacities but also operational data such
as load profiles, tariff structures, and user behavior. These case studies revealed that
designing a microgrid requires careful consideration of technical, economic, and social
dimensions, including system sizing, affordability, governance, and long-term mainte-
nance. The lessons learned from these experiences provided critical benchmarks and
contextual evidence, strengthening the methodological framework and ensuring that the
proposed design for Antanamalaza is both realistic and informed by proven practice.

Fourth, demand estimation revealed that electricity needs are not limited to basic

household consumption but also extend to schools, health services, and productive activities such as rice processing. The projected demand curve therefore reflects both social infrastructure and economic development potential. A long-term horizon of 25 years was considered, with growth rates that account for gradual adoption of appliances and population growth.

Fifth, individual components were analyzed. Lithium iron phosphate ($LiFePO_4$) batteries were identified as the most suitable storage technology due to their high cycle life and resilience to deep discharges. Photovoltaic panels were selected as the sole primary energy source, given the site's high solar resource. Inverters and system topology were dimensioned to accommodate three-phase AC distribution, which, although slightly more expensive than single-phase AC systems, is necessary to support productive loads and future growth. Environmental impacts of each component were also reviewed, underlining the embodied emissions of PV and batteries, and the ecological risks of diesel backup.

Finally, technical simulations and optimization were carried out. Different system configurations were tested under multiple scenarios, with and without a generator, and with different constraints on unmet demand. An annualized cost metric was used as the optimization criterion, complemented by an analysis of CO_2 emissions.

8.2 Main Findings

The study produced several key results across its different stages:

- **Contextual analysis**: The electrification gap in Madagascar is large, and centralized grid extension is not realistic in the medium term. Microgrids are among the few practical solutions to bridge this gap in remote villages such as Antanamalaza.

- **Demand estimation**: Projected electricity needs grow significantly over 25 years, with productive uses accounting for a major share of demand. Household demand alone would underestimate system size and lead to designs unable to support local economic development.

- **Component analysis**: The choice of $LiFePO_4$ batteries balances durability and safety, though costs remain high. PV dominates investment costs but benefits from long lifespans. Diesel backup, while reducing renewable capacity requirements, introduces fuel dependency, price volatility, and large emissions.

- **System without generator**: Meeting all demand exclusively with PV and batteries is feasible but requires strong overdimensioning. Allowing up to 5% unmet demand reduces system size and annualized cost significantly, while maintaining high reliability.

118

- **System with generator**: Incorporating a diesel generator reduces the required PV and battery capacities by providing backup supply when the state of charge falls below a critical threshold. This ensures reliability at lower upfront investment, but introduces fuel dependency, price volatility, higher long-term costs, and additional maintenance requirements.

- **Cost comparison**: Based on the simplified annualized cost metric, the most cost-effective option is the *5% unmet demand, no generator* scenario. While generator-assisted systems appear competitive, they do not reflect hidden costs such as maintenance, fuel price volatility, and technical expertise requirements.

- **Environmental perspective**: The embodied emissions of PV and batteries are significant, but still small compared to the emissions of diesel combustion in generator-based scenarios. Among all cases, the *5% unmet demand, no generator* scenario achieves the lowest total CO_2 emissions.

8.3 Recommendations

Based on these findings, the following recommendations are proposed:

1. **System design**: For Antanamalaza, the optimal balance between cost, reliability, and sustainability is achieved by the *5% unmet demand, no generator* configuration.

2. **Demand monitoring**: Actual consumption should be monitored once the system is deployed, to validate assumptions and adjust capacity roll-out as necessary.

3. **Battery management**: Battery State of Health should be periodically monitored, and a clear replacement strategy established. This will prevent premature failures and extend the system's effective life.

4. **Roll-out strategy**: PV and battery capacity should be added gradually, matching real demand growth. This staged investment approach lowers initial capital needs and improves cost efficiency.

5. **Environmental management**: Recycling and end-of-life management of batteries must be addressed early, ideally through partnerships with national or regional programs. Avoiding accumulation of non-recyclable waste is essential for long-term sustainability.

8.4   Limitations and Outlook

Despite the comprehensive analysis, several limitations remain. Demand growth was based on analogies and assumptions that may not fully reflect local dynamics. Component costs and lifespans were taken from current data, but real-world values could diverge, particularly due to supply chain or logistical issues in rural Madagascar. Maintenance costs, training needs, and institutional barriers were not incorporated into the optimization, though they play a decisive role in practice.

Future work should expand in three directions. First, incorporating stochastic simulations of demand growth, solar variability, and fuel prices would provide more resilient system designs. Second, field data from pilot projects in Madagascar could refine assumptions on appliance uptake and productive demand. Third, a broader socioeconomic analysis should assess the impacts of electrification on education, healthcare, and income, complementing the technical results presented here.

8.5   Final Remarks

The electrification of rural Madagascar is both a technical challenge and a social necessity. This thesis demonstrates that solar microgrids, carefully dimensioned and optimized, can provide sustainable electricity access without reliance on fossil fuels. The case of Antanamalaza shows that even under modest assumptions, renewable systems can meet growing demand reliably and affordably.

Ultimately, this work highlights that microgrids are not only engineering solutions, but also instruments of social and economic development. With appropriate support, they can become a cornerstone of rural electrification, contributing to sustainable development in Madagascar and serving as a model for other regions facing similar challenges.

Appendix A

Python Code Appendix

This appendix presents selected excerpts of the Python code developed for the design and optimization of the solar microgrid. The scripts implement the simulation of energy flows at 15-minute resolution, the handling of photovoltaic generation, battery state of charge evolution, and the optional use of a diesel generator. A brute-force search procedure was coded to evaluate all possible combinations of photovoltaic and battery sizes, subject to the constraint of serving at least 95% of the demand. The simulation outputs were further processed to compute annualized costs, reliability metrics, and to generate the figures shown in the main body of the thesis.

The complete set of scripts (including demand estimation, climatic data gatherer and treatment, roll-out plans, etc.) can be made available upon request to the author.

```python
import numpy as np
import matplotlib.pyplot as plt
import plotly.graph_objects as go

"""
Brute-force optimization of a solar-battery microgrid
    configuration.

For each (PV size, battery size) pair, simulate a full year
    (15-min resolution)
with optional generator behavior. A configuration is valid if
    it serves at least
95% of the total energy demand. Among valid configurations,
    pick the one with
the lowest annualized cost. Produce plots and a performance
    summary.
"""

# --- 1. Parameters (all ASCII) ---
```

```python
battery_cost_per_Wh = 0.147        # EUR per Wh (set to 0.16 if
    desired)
pv_cost_per_Wp       = 0.353       # EUR per Wp
Tn                   = 25 + 273    # K (reference cell
    temperature)
Gn                   = 1000        # W/m^2 (reference irradiance)
gamma                = -0.00039    # 1/K (temperature coefficient
    )
NOCT                 = 43          # degC (Nominal Operating Cell
     Temperature)
panel_age_factor     = 1.0         # PV efficiency due to aging
    (1.0 means none)
inverter_efficiency  = 0.91        # Inverter efficiency (e.g.,
    0.91)
battery_efficiency   = 0.95        # Battery round-trip
    efficiency
inverter_cost        = 4600        # EUR per inverter

step_pv  = 11000  # Wp increment per step
step_bat = 10240  # Wh increment per step
lower_bounds = [step_pv * 10, step_bat * 30]
upper_bounds = [step_pv * 20, step_bat * 50]

panels_per_step    = 20
batteries_per_step = 1

parameters = [
    battery_cost_per_Wh, pv_cost_per_Wp, Tn, Gn, gamma, NOCT,
        panel_age_factor,
    inverter_efficiency, battery_efficiency, inverter_cost,
        step_pv, step_bat
]

P_vals = np.arange(lower_bounds[0], upper_bounds[0] + 1,
    step_pv)
C_vals = np.arange(lower_bounds[1], upper_bounds[1] + 1,
    step_bat)
n_combinations = len(P_vals) * len(C_vals)

# Reliability threshold
SOC_min_percent = 10.0                   # Minimum SOC (%) allowed for
    discharge
unsupplied_energy_threshold = 0.05 # Max fraction of energy NOT
```

```python
          served (<= 5%)
46
47  # Kept only for display
48  soc_critical = 10
49  time_threshold = 0.08
50
51  # --- 2. Full-year simulation ---
52  def simulate_configuration(params, P_PV, C_bat,
53                             initial_SOC_percent=80,
54                             generator_mode='default',
55                             soc_start=50):
56      """
57      Simulate one year for a given PV capacity (P_PV, in Wp) and
              battery capacity
58      (C_bat, in Wh). Return cost and performance metrics if
              configuration meets
59      the reliability criterion; otherwise return None.
60
61      generator_mode options:
62          - 'default'      : generator turns on whenever there is a
                  shortfall
63          - 'soc_critical' : generator turns on if SOC < soc_start
64          - 'schedule'     : generator turns on between 18:00 and
                  22:00 if SOC < soc_start
65          - 'none'         : generator never turns on
66      """
67      (battery_cost_per_Wh, pv_cost_per_Wp, Tn, Gn, gamma, NOCT,
              panel_age_factor,
68       inverter_efficiency, battery_efficiency, inverter_cost,
              step_pv, step_bat) = params
69
70      # Inputs: 15-min resolution arrays for one full year
71      Ga     = np.load("data/irradiance_2019.npy")
                              # W/m^2
72      Ta     = np.load("data/temperature_2019.npy")
                              # degC
73      P_load = np.load("data/TFG_consumption2/consumption_2039.
              npy")# W
74
75      # PV energy per 15 min, Wh
76      Tc       = Ta + (NOCT - 20) * Ga / 800.0              # degC
77      Power_PV = (Ga / Gn) * P_PV * (1.0 + gamma * (Tc + 273.0 -
              Tn)) * panel_age_factor * 0.25
```

```python
E_pv      = Power_PV  # Wh per 15 minutes

# Energy arrays (Wh) per 15 minutes
E_to_load  = np.zeros_like(E_pv)
E_batt     = np.zeros_like(E_pv)
E_lost     = np.zeros_like(E_pv)
E_gen      = np.zeros_like(E_pv)
E_unserved = np.zeros_like(E_pv)
diesel_liters = np.zeros_like(E_pv)  # liters per interval

# Battery state (Wh)
E_bat_hist = [initial_SOC_percent / 100.0 * C_bat]
C_bat_max  = 0.9 * C_bat
C_bat_min  = (SOC_min_percent / 100.0) * C_bat

# Generator model
P_generator = 28000.0     # W
diesel_100  = 8.5 * 0.25  # L per 15 min (approx at full
    load)
diesel_75   = 6.1 * 0.25
diesel_50   = 4.3 * 0.25

for i in range(len(E_pv)):
    soc_Wh  = E_bat_hist[-1]      # Wh
    demand  = P_load[i] * 0.25    # Wh (15-min)
    prod_AC = E_pv[i] * inverter_efficiency
    surplus = prod_AC - demand

    if surplus >= 0.0:
        # Demand covered by PV; charge battery with surplus
        E_to_load[i] = demand
        headroom = C_bat_max - soc_Wh
        charge_in = min(surplus, max(0.0, headroom) /
            battery_efficiency)
        E_batt[i] = charge_in
        E_lost[i] = surplus - charge_in
        E_bat_hist.append(soc_Wh + charge_in *
            battery_efficiency)

    else:
        # Shortfall; discharge battery down to minimum SOC
        shortfall = -surplus
        usable_Wh = max(0.0, soc_Wh - C_bat_min)
```

```
118              discharge = min(shortfall / battery_efficiency,
                     usable_Wh)
119              remaining = shortfall - discharge *
                     battery_efficiency
120
121              E_to_load[i] = prod_AC + discharge *
                     battery_efficiency
122              E_batt[i]    = -discharge
123              E_bat_hist.append(soc_Wh - discharge)
124
125              # Generator logic
126              turn_on_gen = False
127              hour_of_day = (i % 96) // 4   # 0..23
128              soc_pct     = E_bat_hist[-1] / C_bat * 100.0
129
130              if generator_mode == 'default':
131                  if remaining > 0.0:
132                      turn_on_gen = True
133              elif generator_mode == 'soc_critical':
134                  if soc_pct < soc_start:
135                      turn_on_gen = True
136              elif generator_mode == 'schedule':
137                  if 18 <= hour_of_day < 22 and soc_pct <
                         soc_start:
138                      turn_on_gen = True
139              elif generator_mode == 'none':
140                  turn_on_gen = False
141
142              if turn_on_gen:
143                  Wh_to_cover = demand - E_to_load[i]
144                  P_required  = Wh_to_cover / 0.25   # W
145
146                  if P_required <= P_generator * 0.5:
147                      E_gen[i]         = Wh_to_cover
148                      diesel_liters[i] = diesel_50
149                  elif P_required <= P_generator * 0.75:
150                      E_gen[i]         = Wh_to_cover
151                      diesel_liters[i] = diesel_75
152                  else:
153                      E_gen[i]         = min(P_generator * 0.25,
                             Wh_to_cover)
154                      diesel_liters[i] = diesel_100
155
```

```python
                    E_to_load[i] += E_gen[i]

                    # Remaining shortfall after generator
                    remaining_after_gen = demand - E_to_load[i]
                    if remaining_after_gen > 0.0:
                        E_unserved[i] = remaining_after_gen

                    # Use remaining generator capacity to charge
                        battery if any
                    gen_surplus_Wh = P_generator * 0.25 - E_gen[i]
                    if gen_surplus_Wh > 0.0:
                        headroom = C_bat_max - E_bat_hist[-1]
                        gen_charge = min(gen_surplus_Wh, max(0.0,
                            headroom) / battery_efficiency)
                        if gen_charge > 0.0:
                            E_batt[i]        += gen_charge
                            E_bat_hist[-1] += gen_charge *
                                battery_efficiency
                            E_gen[i]         += gen_charge
                else:
                    # No generator: any remaining shortfall is
                        unserved
                    remaining_after_gen = demand - E_to_load[i]
                    if remaining_after_gen > 0.0:
                        E_unserved[i] = remaining_after_gen

    # SOC in percent
    SOC_array = np.array(E_bat_hist[:-1]) / C_bat * 100.0

    # Unserved energy metric
    E_demand_total   = float(np.sum(P_load * 0.25))
    E_unserved_total = float(np.sum(E_unserved))
    pct_unserved     = 0.0 if E_demand_total == 0.0 else (
        E_unserved_total / E_demand_total)

    # Feasibility: at least 95% served
    if pct_unserved > unsupplied_energy_threshold:
        return None

    # Annualized cost model (very simplified)
    diesel_total_l = float(np.sum(diesel_liters))
    diesel_cost    = diesel_total_l * 0.95  # EUR/L estimate
```

```python
    n_inverters = int(np.ceil(P_PV / (2.0 * step_pv)))
    total_inverter_cost = n_inverters * inverter_cost

    capex_ann = (battery_cost_per_Wh * C_bat) / (15.0 * 0.87) \
                + (pv_cost_per_Wp * P_PV) / (30.0 * 0.8968) \
                + total_inverter_cost / 10.0

    total_cost = capex_ann + diesel_cost

    return {
        'cost': total_cost,
        'SOC': SOC_array,
        'SOC_min': float(np.min(SOC_array)),
        'diesel': diesel_liters,
        'E_pv': E_pv,
        'E_gen': E_gen,
        'E_batt': E_batt,
        'E_to_load': E_to_load,
        'E_lost': E_lost,
        'C_bat': C_bat,
        'P_PV': P_PV,
        'E_unserved': E_unserved,
        'pct_unserved': pct_unserved,
    }

# --- 3. Brute-force search ---
best_result = None
counter = 1
all_results = []

# Choose generator mode for the search
generator_mode = 'none'  # 'none' | 'default' | 'soc_critical'
    | 'schedule'
soc_start      = 50

for P in P_vals:
    for C in C_vals:
        result = simulate_configuration(
            parameters, P, C,
            generator_mode=generator_mode,
            soc_start=soc_start
        )
        print(f"{counter} / {n_combinations}")
```

```
236              counter += 1
237
238          if result is not None:
239              all_results.append({
240                  'P_PV': P,
241                  'C_bat': C,
242                  'is_valid': True,
243                  'cost': result['cost'],
244                  'unsup': result['pct_unserved'],
245              })
246              if best_result is None or result['cost'] <
                     best_result['cost']:
247                  best_result = result
248          else:
249              all_results.append({
250                  'P_PV': P,
251                  'C_bat': C,
252                  'is_valid': False,
253                  'cost': np.nan,
254                  'unsup': np.nan
255              })
256
257  # --- 4. Results and plots ---
258  if best_result is None:
259      print("No configuration meets the criterion (served >= 95%)
             .")
260  else:
261      print(f"Best annualized cost (served >= 95%): {best_result
             ['cost']:.2f} EUR")
262      print(f"  P_PV_opt = {int(best_result['P_PV'])} Wp")
263      print(f"  C_bat_opt = {int(best_result['C_bat'])} Wh")
264      print(f"  SOC_min = {best_result['SOC_min']:.1f} %")
265      print(f"  Percent unserved = {best_result['pct_unserved
             ']*100:.3f} %")
266
267      # Plotly: full-year SOC
268      fig = go.Figure()
269      fig.add_trace(go.Scatter(y=best_result['SOC'], mode='lines'
             , name='SOC (%)'))
270      fig.update_layout(
271          title='Battery state of charge (full year)',
272          xaxis_title='Interval (15 min)',
273          yaxis_title='SOC (%)'
```

```
274        )
275        fig.show()
276
277        # Matplotlib: 2-day window
278        day_start = 1
279        day_end   = 3
280        start = day_start * 96
281        end   = (day_end + 1) * 96
282        x = np.arange(start, end) / 4.0   # hours
283
284        fig = plt.figure(figsize=(15, 10))
285
286        ax1 = plt.subplot2grid((4, 1), (0, 0), rowspan=3)
287        ax1.plot(x, best_result['E_pv'][start:end], label="PV [Wh]"
               )
288        ax1.plot(x, best_result['E_gen'][start:end], label="
               Generator [Wh]")
289        ax1.plot(x, best_result['E_to_load'][start:end], label="To
                loads [Wh]")
290        ax1.plot(x, best_result['E_batt'][start:end], label="
               Battery (+/-) [Wh]")
291        ax1.plot(x, best_result['E_lost'][start:end], label="Lost [
               Wh]")
292        ax1.set_ylabel("Energy [Wh]")
293        ax1.set_title(f"Energy flows - days {day_start} to {day_end
               }, 2039")
294        ax1.legend()
295        ax1.grid(True)
296
297        ax2 = plt.subplot2grid((4, 1), (3, 0), rowspan=1, sharex=
               ax1)
298        ax2.plot(x, best_result['SOC'][start:end], label="SOC [%]")
299        ax2.axhline(SOC_min_percent, linestyle='--', label=f'
               Critical threshold {SOC_min_percent:.0f}%')
300        ax2.set_ylim(0, 100)
301        ax2.set_ylabel("SOC [%]")
302        ax2.set_xlabel("Time [hours]")
303        ax2.set_title("Battery state of charge")
304        ax2.legend()
305        ax2.grid(True)
306
307        plt.tight_layout()
308        plt.show()
```

129

```python
    # --- 5. Global performance summary ---
    E_gen_total   = float(np.sum(best_result['E_gen']))
                # Wh
    diesel_total  = float(np.sum(best_result['diesel']))
                # liters

    gen_active_intervals = int(np.count_nonzero(best_result['
        E_gen'] > 0.0))
    gen_hours_total = gen_active_intervals * 0.25
    total_days = len(best_result['SOC']) / 96.0
    gen_hours_per_day = gen_hours_total / max(1.0, total_days)
    gen_hours_by_day = np.array([
        np.count_nonzero(best_result['E_gen'][i*96:(i+1)*96]) *
            0.25
        for i in range(int(total_days))
    ])
    gen_hours_max_day = float(np.max(gen_hours_by_day)) if len(
        gen_hours_by_day) else 0.0

    co2_kg = diesel_total * 2.68  # kg CO2 per liter diesel (
        approx)

    P_load = np.load("data/TFG_consumption2/consumption_2039.
        npy")
    E_demand_total   = float(np.sum(P_load * 0.25))
    E_unserved_total = float(np.sum(best_result['E_unserved']))
    pct_unserved = 0.0 if E_demand_total == 0.0 else (100.0 *
        E_unserved_total / E_demand_total)

    pv_margin = ""
    if best_result['P_PV'] == lower_bounds[0]:
        pv_margin = "(at LOWER bound)"
    elif best_result['P_PV'] == upper_bounds[0]:
        pv_margin = "(at UPPER bound)"

    bat_margin = ""
    if best_result['C_bat'] == lower_bounds[1]:
        bat_margin = "(at LOWER bound)"
    elif best_result['C_bat'] == (upper_bounds[1] - step_bat):
        bat_margin = "(at UPPER bound)"
    elif best_result['C_bat'] == upper_bounds[1]:
        bat_margin = "(at UPPER bound)"
```

130

```
344
345     print("\nGlobal performance summary:")
346     print(f"  Generator energy supplied: {E_gen_total/1000.0:.1
            f} kWh")
347     print(f"  Diesel consumed: {diesel_total:.1f} liters")
348     print(f"  Generator operating hours: {gen_hours_total:.1f}
            h/year")
349     print(f"  Average per day: {gen_hours_per_day:.2f} h/day")
350     print(f"  Maximum in a single day: {gen_hours_max_day:.2f}
            h")
351     print(f"  Estimated CO2 emissions: {co2_kg:.1f} kg")
352     print(f"  Time below {soc_critical}% SOC: "
353           f"{100.0*np.sum(np.array(best_result['SOC']) <
                soc_critical)/len(best_result['SOC']):.2f}%")
354     print(f"  Unserved demand: {pct_unserved:.2f}%")
355     print(f"  Battery capacity: {int(best_result['C_bat'])} Wh
            {bat_margin}")
356     print(f"  Number of batteries: {int(best_result['C_bat']/
            step_bat * batteries_per_step)}")
357     print(f"  PV power: {int(best_result['P_PV'])} Wp {
            pv_margin}")
358     print(f"  Number of PV modules: {int(best_result['P_PV']/
            step_pv * panels_per_step)}")
359
360     # --- 6. Scatter of all results (validity and cost) ---
361     P_PV_list  = [r['P_PV'] for r in all_results]
362     C_bat_list = [r['C_bat'] for r in all_results]
363     valid_list = [r['is_valid'] for r in all_results]
364     cost_list  = [r['cost'] for r in all_results]
365
366     valid_results = [r for r in all_results if r['is_valid']]
367     best_result_overall = min(valid_results, key=lambda r: r['
            cost']) if valid_results else None
368
369     color_valid = "#A5D6A7"
370     color_best  = "#1B5E20"
371     size_valid  = 350
372     size_best   = 450
373
374     fig, ax = plt.subplots(figsize=(14, 9))
375
376     for i in range(len(all_results)):
377         x = P_PV_list[i]
```

131

```python
        y = C_bat_list[i]
        is_valid = valid_list[i]
        cost = cost_list[i]

        if is_valid:
            label = f"{int(cost / 1000.0)}k"
            if best_result_overall and cost ==
                best_result_overall['cost']:
                ax.scatter(x, y, color=color_best, s=size_best,
                    edgecolor='black', alpha=0.95)
                ax.text(x, y, label, fontsize=8, ha='center',
                    va='center', color='white', weight='bold')
            else:
                ax.scatter(x, y, color=color_valid, s=
                    size_valid, edgecolor='black', alpha=0.9)
                ax.text(x, y, label, fontsize=8, ha='center',
                    va='center', color='black', weight='bold')
        else:
            ax.scatter(x, y, color='red', s=160, edgecolor='
                black', alpha=0.3)

    ax.set_title("Viability and annualized cost of each
        configuration")
    ax.set_xlabel("Installed PV power [Wp]")
    ax.set_ylabel("Battery capacity [Wh]")
    ax.ticklabel_format(style='plain')
    ax.grid(True, linestyle='--', alpha=0.5)
    ax.text(
        0.98, 0.05,
        "Values inside markers are thousands of euros (EUR)",
        transform=ax.transAxes,
        fontsize=11,
        ha='right',
        va='bottom',
        color='black',
        fontweight='bold',
        bbox=dict(facecolor='white', alpha=0.8, edgecolor='none
            ')
    )

    plt.tight_layout(rect=[0, 0.03, 1, 1])
    plt.show()
```

Bibliography

[1] United Nations. *Transforming our world: the 2030 Agenda for Sustainable Development*. 2015. https://sdgs.un.org/2030agenda.

[2] United Nations. *Sustainable Development Goals icons and infographics*. 2015. https://www.un.org/sustainabledevelopment/news/communications-material.

[3] IEA et al. *Tracking SDG 7: The Energy Progress Report 2024*. Some data retrieved from https://data.worldbank.org/indicator/EG.ELC.ACCS.ZS, and EG.ELC.ACCS.UR.ZS and and EG.ELC.ACCS.RU.ZS; Accessed: May 2025. 2024. https://trackingsdg7.esmap.org/downloads.

[4] Mikul Bhatia and Nicolina Angelou. *Beyond Connections: Energy Access Redefined*. Tech. rep. The World Bank, 2015. https://openknowledge.worldbank.org/server/api/core/bitstreams/248a7205-e926-5946-9025-605b8035ad95/content.

[5] Hannah Ritchie, Pablo Rosado, and Max Roser. *Access to Energy*. Accessed: May 5, 2025. 2024. https://ourworldindata.org/energy-access.

[6] World Bank. *Madagascar Set to Expand Access to Renewable Energy and Digital Services Thanks to $400 Million Credit*. Press release, April 2023. 2023. https://www.worldbank.org/en/news/press-release/2023/04/07/madagascar-afe-set-to-expand-access-to-renewable-energy-and-digital-services-thanks-to-400-million-credit.

[7] Sustainable Energy for All, NRECA, and Government of Madagascar. *RAPPORT D'ÉLECTRIFICATION DU PEI DE MADAGASCAR*. Accessed: May 2025. 2024. https://www.seforall.org/Madagascar_IEP-Electrification-Technical_Report-FR.

[8] SEforALL and Government of Madagascar. *Madagascar SDG7 Energy Planning Dashboard*. Accessed: May 2025. 2021. https://madagascar.sdg7energyplanning.org/dashboard/mdg-iep.

[9] Lucas Richard et al. "A New Electrification Model to End Energy Poverty: An example from a novel rural electrification approach in Madagascar". In: *IEEE Electrification Magazine* 11.2 (2023). https://read.nxtbook.com/ieee/electrification/electrification_june_2023/a_new_electrification_model_t.html.

[10]   Nikolas Schöne et al. "Matchmaking in Off-Grid Energy System Planning: A Novel Approach for Integrating Residential Electricity Demands and Productive Use of Electricity". In: *Sustainability* 16.8 (2024), p. 3442. DOI: 10.3390/su1608 3442. https://doi.org/10.3390/su16083442.

[11]   Experts-Solidaires and Mad'Eole. *Rapport Semestriel Juin 2015 – Projet d'amélioration des conditions de développement local via l'accès à l'électricité en zone rurale*. Tech. rep. Experts-Solidaires, 2015. https://experts-solidaires.org /projets/madagascar-ampasindava-electrification-rurale.

[12]   Experts-Solidaires. *Rapport Final Septembre 2017- Projet d'amélioration des conditions de développement local via l'accès à l'électricité dans le village d'Ampasindava*. Tech. rep. Experts-Solidaires, 2017. https://experts-solidaires.or g/projets/madagascar-ampasindava-electrification-rurale.

[13]   Nigel Scott and William Coley. "Understanding Load Profiles of Mini-Grid Customers in Tanzania". In: *Energies* 14.14 (2021). https://doi.org/10.3390/en14144 207.

[14]   Andante Hadi Pandyaswargo et al. "Estimating the Energy Demand and Growth in Off-Grid Villages: Case Studies from Myanmar, Indonesia, and Laos". In: *Energies* 13.20 (2020). https://doi.org/10.3390/en13205313.

[15]   Électriciens sans frontières. *Rapport annuel 2022*. https://electriciens-sans-front ieres.org/actualites/rapport-annuel-2022/. Accessed: August 20, 2025. 2022.

[16]   Mapsofindia.com. *Vakinankaratra Location Map, Madagascar*. Accessed: May 10, 2025. 2023. https://www.mapsofindia.com/world-map/madagascar/vakinank aratra/location-map.html.

[17]   Région Vakinankaratra. *Découpage administratif de la région Vakinankaratra*. Accessed: May 10, 2025. 2016. https://region-vakinankaratra.mg/historique/.

[18]   Romaric Luc. *Mba manao ahoana ny lalana any aminareo?* Accessed: May 24, 2025. 2024. https://www.facebook.com/groups/584428033871972/permalink/68 4884770492964/.

[19]   NASA POWER Project. *POWER Data Access Viewer*. https://power.larc.nasa.go v/data-access-viewer/. Accessed: May 10, 2025. 2023. https://power.larc.nasa.g ov/data-access-viewer/.

[20]   Ilo Program, Cornell University, FOFIFA, and INSTAT. *Commune Census of Madagascar*. Accessed: May 10, 2025. 2001. https://www.ilo.cornell.edu/ilo/dat a.html.

[21]   Centre de Recherches, d'Études et d'Appui à l'Analyse Économique à Madagascar (CREAM). *Monographie de la Région VAKINANKARATRA*. Accessed: May 10, 2025. 2013. https://www.instat.mg/p/cream-monographie-region-vakinankaratra-fevrier-2013.

[22]   World Bank. *Rural population - Madagascar*. Accessed: May 10, 2025. 2024. https://data.worldbank.org/indicator/SP.RUR.TOTL?locations=MG.

[23]   Institut National de la Statistique (INSTAT) and ICF. *Enquête Démographique et de Santé à Madagascar 2021*. Tech. rep. Accessed: June 7, 2025. Antananarivo, Madagascar: INSTAT and ICF, 2022. https://dhsprogram.com/publications/publication-FR376-DHS-Final-Reports.cfm.

[24]   Google Research. *Open Buildings Dataset*. Accessed: May 8, 2025. 2021. https://sites.research.google/open-buildings/.

[25]   Institut National de la Statistique (INSTAT). *Troisième Recensement Général de la Population et de l'Habitation (RGPH-3)*. Accessed: June 7, 2025. 2018. https://www.instat.mg/autres/rgph-3.

[26]   Xiangkun Li, James Salasovich, and Tim Reber. *Microgrid Load and LCOE Modelling Results*. https://data.nrel.gov/submissions/79. NREL Data Catalog. Golden, CO. Last updated: December 18, 2024. 2018.

[27]   World Bank. *Madagascar Poverty Assessment: Navigating Two Decades of High Poverty and Charting a Course for Change*. Tech. rep. Accessed: June 7, 2025. Washington, D.C.: World Bank, 2024. http://documents.worldbank.org/curated/en/099021424172020915.

[28]   Macrotrends LLC. *Madagascar Poverty Rate 1991-2024*. Accessed: June 7, 2025. 2025. https://www.macrotrends.net/global-metrics/countries/mdg/madagascar/poverty-rate.

[29]   Max Aklin et al. "Economics of household technology adoption in developing countries: Evidence from solar technology adoption in rural India". In: *Energy Economics* 72 (2018). Accessed: June 7, 2025, pp. 35–46. DOI: 10.1016/j.eneco.2018.02.011. https://doi.org/10.1016/j.eneco.2018.02.011.

[30]   Elise Harrington, Ameya Athavankar, and David Hsu. "Variation in rural household energy transitions for basic lighting in India". In: *Renewable and Sustainable Energy Reviews* 119 (2020). Accessed: June 7, 2025, p. 109568. DOI: 10.1016/j.rser.2019.109568. https://www.sciencedirect.com/science/article/pii/S1364032119307762.

[31]   CountryEconomy.com. *Madagascar - Electricity consumption*. https://countryeconomy.com/energy-and-environment/electricity-consumption/madagascar. Accessed: July 20, 2025.

[32] Azimut360. *Micro-réseaux PV hybrides: Guide de conception et calcul*. Accessed: June 7, 2025. 2017. https://azimut360.coop/wp-content/uploads/2023/11/Micro-reseaux-PV-hybrides-Guide-de-conception-et-calcul-ECOWAS_compressed.pdf.

[33] City of Cape Town. *Smart Office Toolkit – Energy Cheat Sheet*. Accessed: June 7, 2025. https://resource.capetown.gov.za/documentcentre/Documents/Procedures,%20guidelines%20and%20regulations/SOH_Audit_Energy_cheat_sheet.pdf.

[34] Samuel Booth et al. *Productive Use of Energy in African Micro-Grids: Technical and Business Considerations*. Tech. rep. Accessed: July 6, 2025. National Renewable Energy Laboratory (NREL) and Energy 4 Impact, 2018. https://docs.nrel.gov/docs/fy18osti/71663.pdf#page=38.72.

[35] Ahmad H. Sabry and Pin Jern Ker. "DC Environment for a Refrigerator with Variable Speed Compressor: Power Consumption Profile and Performance Comparison". In: *International Journal of Refrigeration* (2020). Accessed: July 6, 2025. https://www.researchgate.net/publication/343560360_DC_Environment_for_a_Refrigerator_With_Variable_Speed_Compressor_Power_Consumption_Profile_and_Performance_Comparison.

[36] World Standards. *Madagascar - Power plug, socket and mains voltage in Madagascar*. Accessed: July 26, 2025. 2025. https://www.worldstandards.eu/electricity/plug-voltage-by-country/madagascar/.

[37] Power Technology. *Accueil*. Accessed: July 26, 2025. 2022. https://pwrt.mg/.

[38] ENF Solar. *Solar Installers in Madagascar – ENF Company Directory*. Accessed: July 26, 2025. 2025. https://www.enfsolar.com/directory/installer/Madagascar.

[39] Gaïa Madagascar. *Convertisseurs Phoenix 24/5000*. Accessed: July 27, 2025. 2025. https://gaiamadagascar.com/produit/convertisseurs-phoenix-48-5000/.

[40] Allo Solar. *Inverter 20kW Triphase - 2 MPPT - 20KTLX-G3 - SOFAR*. Accessed: August 3, 2025. 2025. https://allo.solar/onduleur-20kw-triphase-2-mppt-20ktlx-g3-sofar.html.

[41] PwC. *Madagascar – Corporate – Other taxes*. Accessed: August 3, 2025. 2025. https://taxsummaries.pwc.com/madagascar/corporate/other-taxes.

[42] Power Technology Madagascar. *SOLAR TECHNOLOGY CONVERTISSEUR HYBRID TRIPHASE OCH10K-48 avec régulateur solaire MPPT OCH10K / 15K*. Accessed: August 3, 2025. 2024. https://pwrt.mg/produit/solar-technology-convertisseur-hybrid-triphase-och10k-48-avec-regulateur-solaire-mppt-och10k-15k/.

[43] IEA-PVPS Task 9. *Mini-réseaux hybrides PV-diesel pour l'électrification rurale*. Tech. rep. 2013. https://iea-pvps.org/wp-content/uploads/2020/01/PVPS_T9_-_Hybrides_FR_-_updated_Feb_2014.pdf.

[44] Gaïa Madagascar. *Panneau Solaire Amerisolar AS-7M 144-HC – 550Wc – Black-Silver*. Accessed: August 4, 2025. 2025. https://gaiamadagascar.com/produit/panneau-solaire-amerisolar-as-7m-144-hc-550wc-black-silver/.

[45] Emiliano Bellini. *Solar module prices will soon go back to over \$0.12/W*. Accessed: August 4, 2025. PV Magazine. Feb. 26, 2025. https://www.pv-magazine.com/2025/02/26/solar-module-prices-will-soon-go-back-to-over-0-12-w/.

[46] Christian Reichel et al. "CO_2 emissions of silicon photovoltaic modules – impact of module design and production location". In: *Proceedings of the WCPEC-8, 8th World Conference on Photovoltaic Energy Conversion*. Milan, Italy, 2022. https://www.ise.fraunhofer.de/content/dam/ise/de/documents/publications/conference-paper/wcpec-8/Reichel_5DV234.pdf.

[47] Abraham Alem Kebede et al. "Techno-economic analysis of lithium-ion and lead-acid batteries in stationary energy storage application". In: *Journal of Energy Storage* 41 (2021), p. 102748. DOI: 10.1016/j.est.2021.102748.

[48] Balvender Singh et al. "Role of lithium-ion batteries in microgrid system". In: *Transportation Engineering* 21 (2025), p. 100368. DOI: 10.1016/j.treng.2025.100368.

[49] GSL Energy. *Factory Price Deep Cycles Smart LiFePO4 48V 200ah 10kWh Powerwall Lithium Ion Battery for Home Solar Storage System*. Accessed: August 5, 2025. 2025. https://powerwall.en.made-in-china.com/product/uFfAstrvhHhl/China-Factory-Price-Deep-Cycles-Smart-LiFePO4-48V-200ah-10kwh-Powerwall-Lithium-Ion-Battery-for-Home-Solar-Storage-System.html.

[50] Sino Shipping. *Shipping from China to Madagascar | Sea & Air Freight Rates*. https://sino-shipping.com/shipping-from-china-to-madagascar/. Accessed: August 2025. 2025.

[51] WTO. *Tariffs and imports: Summary and duty ranges - Madagascar*. https://www.wto.org/english/res_e/statis_e/daily_update_e/tariff_profiles/mg_e.pdf. 2024.

[52] PwC. *Madagascar Corporate - Other taxes*. https://taxsummaries.pwc.com/madagascar/corporate/other-taxes. Accessed: August 2025. 2025.

[53] Leopold Peiseler et al. "Carbon footprint distributions of lithium-ion batteries and their materials". In: *Nature Communications* 15 (2024), p. 10301. DOI: 10.1038/s41467-024-54634-y. https://www.nature.com/articles/s41467-024-54634-y.

[54]   Xin Lin et al. "Environmental impact analysis of lithium iron phosphate batteries for energy storage in China". In: *Frontiers in Energy Research* 12 (2024), p. 1361720. DOI: 10.3389/fenrg.2024.1361720. https://doi.org/10.3389/fenrg.2024.1361720.

[55]   Sandy Cheng et al. "A PSO-Optimized Fuzzy Logic Control-Based Charging Method for Individual Household Battery Storage Systems within a Community". In: *Energies* 11.2 (2018), p. 469. DOI: 10.3390/en11020469. https://doi.org/10.3390/en11020469.

[56]   PowerTech Systems. *New high-performance lithium LiFePO4 cells*. https://www.powertechsystems.eu/new-high-performance-lithium-lifepo4-cells/. Accessed: August 10, 2025. 2019.

[57]   Sufyan Alattar and Wassim Saadeh. "Trafficar". MA thesis. Lebanon: Lebanese University, Branch I, 2018. https://www.researchgate.net/publication/331074918_Trafficar.

[58]   Giuliana Vinci et al. "Reuse of Lithium Iron Phosphate (LiFePO4) Batteries from a Life Cycle Assessment Perspective: The Second-Life Case Study". In: *Energies* 17.11 (2024), p. 2544. DOI: 10.3390/en17112544.

[59]   Andrew Weng et al. "Parallel-Connected Battery Current Imbalance Dynamics". In: *arXiv preprint arXiv:2211.04961* (2022). https://arxiv.org/pdf/2211.04961.

[60]   Batimax. *GEI006 Groupe Diesel GREAVES 50kVA / 400V Avec ATS*. Accessed: August 16, 2025. 2025. https://www.batimax-mada.com/shop/product/gei006-groupe-diesel-greaves-50kva-400v-avec-ats-53119011044g-ind-58522?search=diesel.

[61]   Alternative Power Solutions. *50 kVA Greaves Power Diesel Generator*. Accessed: August 16, 2025. https://www.alternativepower.in/50-kva-greaves-power-diesel-generator/.

[62]   React Power Team. *The Life Expectancy of Your Diesel Generator*. Accessed: August 17, 2025. Aug. 2020. https://www.reactpower.com/blog/the-life-expectancy-of-your-diesel-generator/.

[63]   Total Generators. *The Life Expectancy of a Diesel Generator*. Accessed: August 17, 2025. July 2024. https://totalgenerators.com/the-life-expectancy-of-a-diesel-generator/.

[64]   Turnkey Industries. *What is the Life Expectancy of Industrial Generators?* Accessed: August 17, 2025. July 2022. https://turnkey-industries.com/what-is-the-life-expectancy-of-industrial-generators.

[65]   Kelly Benton. "A Life Cycle Assessment of a Diesel Generator Set". MA thesis. Montana Tech of the University of Montana, 2016. http://digitalcommons.mtech .edu/grad_rsch/63.

[66]   ADEME. *Information GES – Méthodologie de calcul des émissions de gaz à effet de serre des produits énergétiques*. https://www.ecologie.gouv.fr/sites/default/fil es/documents/Information_GES%20-%202019.pdf. 2019.

[67]   Vat Sun et al. "A new method for evaluating nominal operating cell temperature (NOCT) of unglazed photovoltaic thermal module". In: *Energy Reports* 6 (2020), pp. 1029–1042. DOI: 10.1016/j.egyr.2020.04.003. https://www.researchgate.net /publication/340879228_A_new_method_for_evaluating_nominal_operating_c ell_temperature_NOCT_of_unglazed_photovoltaic_thermal_module.

[68]   Iain Staffell and Stefan Pfenninger. *Renewables.ninja*. https://www.renewables.n inja. Accessed: August 7, 2025. 2016.

[69]   European Commission, Joint Research Centre. *Photovoltaic Geographical Information System (PVGIS)*. Accessed: August 7, 2025. 2024. https://re.jrc.ec.europa .eu/pvg_tools/en/.